UC San Diego
Research Theses and Dissertations

Title
Hydrodynamic Pressure and Added Mass for Axisymmetric Bodies

Permalink
https://escholarship.org/uc/item/1ck8r5z3

Author
Nilrat, Fukij

Publication Date
1980-06-14

eScholarship.org Powered by the California Digital Library
University of California

INFORMATION TO USERS

This was produced from a copy of a document sent to us for microfilming. While the most advanced technological means to photograph and reproduce this document have been used, the quality is heavily dependent upon the quality of the material submitted.

The following explanation of techniques is provided to help you understand markings or notations which may appear on this reproduction.

1. The sign or "target" for pages apparently lacking from the document photographed is "Missing Page(s)". If it was possible to obtain the missing page(s) or section, they are spliced into the film along with adjacent pages. This may have necessitated cutting through an image and duplicating adjacent pages to assure you of complete continuity.

2. When an image on the film is obliterated with a round black mark it is an indication that the film inspector noticed either blurred copy because of movement during exposure, or duplicate copy. Unless we meant to delete copyrighted materials that should not have been filmed, you will find a good image of the page in the adjacent frame.

3. When a map, drawing or chart, etc., is part of the material being photographed the photographer has followed a definite method in "sectioning" the material. It is customary to begin filming at the upper left hand corner of a large sheet and to continue from left to right in equal sections with small overlaps. If necessary, sectioning is continued again—beginning below the first row and continuing on until complete.

4. For any illustrations that cannot be reproduced satisfactorily by xerography, photographic prints can be purchased at additional cost and tipped into your xerographic copy. Requests can be made to our Dissertations Customer Services Department.

5. Some pages in any document may have indistinct print. In all cases we have filmed the best available copy.

University
Microfilms
International

300 N. ZEEB ROAD, ANN ARBOR, MI 48106
18 BEDFORD ROW, LONDON WC1R 4EJ, ENGLAND

Reproduced with permission of the copyright owner. Further reproduction prohibited without permission.

8029524

NILRAT, FUKIJ

HYDRODYNAMIC PRESSURE AND ADDED MASS FOR AXISYMMETRIC BODIES

University of California, Berkeley PH.D. 1980

University
Microfilms
International 300 N. Zeeb Road, Ann Arbor, MI 48106

Reproduced with permission of the copyright owner. Further reproduction prohibited without permission.

PLEASE NOTE:

In all cases this material has been filmed in the best possible way from the available copy. Problems encountered with this document have been identified here with a check mark ✓.

1. Glossy photographs _____
2. Colored illustrations _____
3. Photographs with dark background _____
4. Illustrations are poor copy _____
5. Print shows through as there is text on both sides of page _____
6. Indistinct, broken or small print on several pages ✓
7. Tightly bound copy with print lost in spine _____
8. Computer printout pages with indistinct print ✓
9. Page(s) _____ lacking when material received, and not available from school or author
10. Page(s) _____ seem to be missing in numbering only as text follows
11. Poor carbon copy _____
12. Not original copy, several pages with blurred type _____
13. Appendix pages are poor copy ✓
14. Original copy with light type _____
15. Curling and wrinkled pages _____
16. Other _____

University Microfilms International
300 N. ZEEB RD. ANN ARBOR MI 48106 (313) 761-4700

Reproduced with permission of the copyright owner. Further reproduction prohibited without permission.

Hydrodynamic Pressure and Added Mass for Axisymmetric Bodies

By

Fukij Nilrat

B.Eng. (Chulalongkorn University, Thailand) 1971
M.S. (University of California, Los Angeles) 1974

DISSERTATION

Submitted in partial satisfaction of the requirements for the degree of

DOCTOR OF PHILOSOPHY

in

Engineering

in the

GRADUATE DIVISION

OF THE

UNIVERSITY OF CALIFORNIA, BERKELEY

Approved:

Joseph Penzien — May 9, 80
Chairman — Date

Robert W. Clough — 12 May 1980

William C. Webster — 12 May 1980

DOCTORAL DEGREE CONFERRED
JUNE 14, 1980

Reproduced with permission of the copyright owner. Further reproduction prohibited without permission.

ACKNOWLEDGEMENTS

This work is a result of research sponsored by NOAA, Office of Sea Grant, Department of Commerce under Project R/E-14, by the State Resources Agency of California, and by Standard Oil Company of California (Chevron Oil Field Research Company). The author sincerely appreciates their support.

This work also constitutes the author's doctoral dissertation submitted to the University of California, Berkeley. The dissertation committee consisted of Professors Joseph Penzien (Chairman), Robert L. Wiegel, and William C. Webster. The author is grateful to the professors in the committee and to Professor Ben C. Gerwick, Jr. for providing advice and invaluable suggestions.

Special thanks are extended to Professor Joseph Penzien who served as dissertation committee chairman and advisor throughout the author's doctoral program.

The author is also thankful to Dr. Robert C. Byrd for his helpful suggestions, to Mr. John F. Hall for providing discussions, and to Ms. Ellen A. McCutcheon for typing the manuscript.

Reproduced with permission of the copyright owner. Further reproduction prohibited without permission.

TABLE OF CONTENTS

Page

ACKNOWLEDGEMENTS i

TABLE OF CONTENTS ii

LIST OF FIGURES iv

LIST OF NOTATIONS vii

1. INTRODUCTION 1

2. DYNAMICS OF A RIGID AXISYMMETRIC BODY 3

2.1 Equations of Motion 3

2.2 Added Mass and Hydrodynamic Damping Representation . . . 5

3. CONTINUUM SOLUTIONS OF HYDRODYNAMIC PRESSURE FOR PIERCING CIRCULAR CYLINDRICAL BODIES 9

3.1 Scope and Introduction 9

3.2 Assumptions and Governing Equations 9

3.3 Expressions for Complex Frequency Solutions 12

3.3.1 Excitation of the Form of $\cos\theta$ 13

3.3.2 Axisymmetric Excitation 15

3.4 Inverse Representation 16

3.4.1 Excitation of the Form of $\cos\theta$ 16

3.4.2 Axisymmetric Excitation 17

4. FINITE ELEMENT ANALYSIS OF HYDRODYNAMIC PRESSURE FOR RIGID AXISYMMETRIC BODIES 19

4.1 Scope 19

4.2 Governing Equations 19

4.3 Finite Element Discretization of Fluid and Formulation 21

4.4 Transmitting Boundary Representation 26

Reproduced with permission of the copyright owner. Further reproduction prohibited without permission.

Page

4.4.1 Horizontal and Rotational Excitations 30

4.4.2 Vertical Excitation 33

4.5 Added Mass and Hydrodynamic Damping Representation . . . 34

5. COMPARISON WITH EXPERIMENTAL RESULTS 39

5.1 Added Mass and Hydrodynamic Damping 39

5.2 Hydrodynamic Pressures 43

5.2.1 Horizontal Harmonic Oscillations 44

5.2.2 Vertical Harmonic Oscillations 45

5.3 Analytical Errors 50

6. CONCLUSIONS 87

REFERENCES 89

APPENDIX A - FINITE ELEMENT FORMULATION OF MATRICES 91

APPENDIX B - COMPUTER PROGRAM USER'S GUIDE 107

APPENDIX C - COMPUTER PROGRAM LISTING 115

Reproduced with permission of the copyright owner. Further reproduction prohibited without permission.

LIST OF FIGURES

Figure		Page
2.1	Idealized System of a Rigid Structure in Fluid	8
3.1	Types of Excitations	18
3.2	Circular Cylindrical Tower in Water	18
4.1	Finite Element Discretization of Fluid Domain	37
4.2	Fluid Domain Outside Transmitting Boundary	38
4.3	Structure in Fluid	38
5.1	Finite Element Mesh	51
5.2a	Typical Amplitude of Hydrodynamic Pressure (Real Part) at $\theta = 0°$ Due to Horizontal Excitation $\ddot{x} = \ddot{\bar{x}} e^{i\omega t}$	52
5.2b	Typical Amplitude of Hydrodynamic Pressure (Real Part) at Any θ Due to Vertical Excitation $\ddot{z} = \ddot{\bar{z}} e^{i\omega t}$	53
5.2c	Typical Amplitude of Hydrodynamic Pressure (Real Part) at $\theta = 0°$ Due to Rotational Excitation $\ddot{\phi} = \ddot{\bar{\phi}} e^{i\omega t}$	54
5.3	Horizontal Added Mass Coefficients for Model	55
5.4	Horizontal Added Mass Coefficients for Model	56
5.5	Vertical Added Mass Coefficients for Model	57
5.6	Vertical Added Mass Coefficients for Model	58
5.7	Rotational Added Mass Coefficients for Model	59
5.8	Rotational Added Mass Coefficients for Model	60
5.9	Coupled Added Mass Coefficients for Model	61
5.10	Coupled Added Mass Coefficients for Model	62
5.11	Hydrodynamic Damping Coefficients for Model	63
5.12	Hydrodynamic Damping Coefficients for Model	64
5.13	Horizontal Added Mass Coefficients for Prototype	65
5.14	Horizontal Added Mass Coefficients for Prototype	66

Reproduced with permission of the copyright owner. Further reproduction prohibited without permission.

Figure		Page
5.15	Vertical Added Mass Coefficients for Prototype	67
5.16	Vertical Added Mass Coefficients for Prototype	78
5.17	Rotational Added Mass Coefficients for Prototype	69
5.18	Rotational Added Mass Coefficients for Prototype	70
5.19	Coupled Added Mass Coefficients for Prototype	71
5.20	Coupled Added Mass Coefficients for Prototype	72
5.21	Hydrodynamic Damping Coefficients for Prototype	73
5.22	Hydrodynamic Damping Coefficients for Prototype	74
5.23	Locations of Pressure Gauges	75
5.24	Model on Shaking Table	75
5.25	Hydrodynamic Pressure Amplitudes of Gauges S1 - S8 Due to Horizontal Harmonic Excitations, $H/H_S = 2.5$	76
5.26	Hydrodynamic Pressure Amplitudes of Gauges S1 - S8 Due to Horizontal Harmonic Excitations, $H/H_S = 2.0$	77
5.27	Hydrodynamic Pressure Amplitudes of Gauges S1 - S8 Due to Horizontal Harmonic Excitations, $H/H_S = 1.5$	78
5.28	Hydrodynamic Pressure Amplitudes of Gauges S1 - S8 Due to Horizontal Harmonic Excitations, $H/H_S = 1.0$	79
5.29	Hydrodynamic Pressure Amplitudes of Gauges T3, T5, T6 and T8 Due to Horizontal Harmonic Excitations	80
5.30	Superposition of Model Motion	81
5.31	Superposition of Ground Motion	81
5.32	Superposition of Ground Motion Outside r_b	82
5.33	Discretized Truncated Domain	82
5.34	Hydrodynamic Pressure Amplitudes of Gauges T1 - T8 Due to Vertical Harmonic Excitations, $H/H_S = 2.5$	83
5.35	Hydrodynamic Pressure Amplitudes of Gauges T1 - T8 Due to Vertical Harmonic Excitations, $H/H_S = 2.0$	84
5.36	Hydrodynamic Pressure Amplitudes of Gauges T1 - T8 Due to Vertical Harmonic Excitations, $H/H_S = 1.5$	85

Reproduced with permission of the copyright owner. Further reproduction prohibited without permission.

Figure Page

5.37 Hydrodynamic Pressure Amplitudes of Gauges S1 - S8 Due to Vertical Harmonic Excitations 86

Reproduced with permission of the copyright owner. Further reproduction prohibited without permission.

LIST OF NOTATIONS

a = $a(z,t)$, acceleration of body surface in horizontal direction

$\bar{a}$ = $\bar{a}(z,\omega)$, harmonic amplitude of acceleration $a(z,t)$

a_i = $a_i(r,\theta,z,t)$, accelerations of fluid particles in direction i , $i = r,\theta,z,n$ (where n here is an outward normal of fluid surface)

$\tilde{a}_i$ = $\tilde{a}_i(r,z,t) = a_i(r,\theta,z,t)\big|_{\theta=0}$

$\bar{a}_i$ = $\bar{a}_i(r,\theta,z,\omega)$, Fourier transforms of a_i

$[C]$ = damping matrix containing elements C_{ij}

c = velocity of sound in fluid

$[C^a]$ = hydrodynamic damping matrix

C_{ij} = elements of damping matrix $[C]$

C^D_{ij} = dimensionless damping coefficients

C^M_{ij} = dimensionless added mass coefficients

D = fluid domain inside transmitting boundary or diameter of circular cylindrical body, depending on context

$\{D\}$ = time dependent loading vector containing $D_i(t)$

$\{\bar{D}\}$ = frequency dependent loading vector containing $\bar{D}_i(\omega)$

D_i = $D_i(t)$, elements of $\{D\}$, $i=1,2,.....n$

$\bar{D}_i$ = $\bar{D}_i(\omega)$, elements of $\{\bar{D}\}$, $i=1,2,.....n$

$[E]$ = matrix containing vectors $\{Z\}_i$, $i=1,2,.....n_{TB}$

$[F]$ = matrix containing elements F_{ij}

Reproduced with permission of the copyright owner. Further reproduction prohibited without permission.

$\{f\}$ = complex hydrodynamic force vector containing time dependent elements $f_i(t)$

$\{\bar{f}\}$ = complex hydrodynamic force vector containing frequency dependent elements $f_i(\omega)$

f_i = $f_i(t)$, complex time dependent force components in direction i

$[F^B]$ = matrix associated with transmitting boundary

$[F^C]$ = matrix associated with compressibility of fluid

$[F^S]$ = matrix associated with surface waves

$\bar{f}_i$ = $f_i(\omega)$, complex frequency dependent force components in direction i

F_{ij} = elements of [F] , defined by Eq. 4.13

$\bar{f}_{ij}$ = $\bar{f}_{ij}(\omega)$, complex frequency dependent forces in direction i due to unit amplitude of relative acceleration (with respect to foundation) in direction j

F^B_{ij} = elements of matrix $[F^B]$, defined by Eq. 4.15

F^C_{ij} = elements of matrix $[F^C]$, defined by Eq. 4.16

F^S_{ij} = elements of matrix $[F^S]$, defined by Eq. 4.17

$\bar{f}^g_{ij}$ = $\bar{f}^g_{ij}(\omega)$, complex frequency dependent forces in directions i due to unit amplitude of ground acceleration in direction j

$\bar{f}^I_{ij}$ = $\bar{f}^I_{ij}(\omega)$, imaginary part of $\bar{f}_{ij}(\omega)$

$\bar{f}^R_{ij}$ = $\bar{f}^R_{ij}(\omega)$, real part of $\bar{f}_{ij}(\omega)$

FS = free surface

Reproduced with permission of the copyright owner. Further reproduction prohibited without permission.

g = acceleration of gravity

H = depth of fluid

$H_0^{(2)}$ = Hankel function of the second kind of order zero

$H_1^{(2)}$ = Hankel function of the second kind of order one

H_s = height of structure or body

IF = interface between fluid and body

$[K]$ = stiffness matrix containing elements k_{ij}

k = largest integer satisfying condition $\alpha_k^2 < \frac{\omega^2}{c^2}$

K_0 = modified Bessel function of second kind of order zero

K_1 = modified Bessel function of second kind of order one

k_{ij} = elements of stiffness matrix

$[M]$ = mass matrix

$[M^a]$ = added mass matrix

$[M^g]$ = complex added mass matrix associated with ground acceleration

$\langle N \rangle$ = row matrix containing interpolation functions $N_i(r,z)$

n = total number of fluid nodes

$\langle \bar{N} \rangle$ = row matrix containing interpolation functions $\bar{N}_i(r)$

$\langle \hat{N} \rangle$ = row matrix containing interpolation functions $\hat{N}_i(z)$

$\langle N^G \rangle$ = row matrix containing interpolation functions $N^G(r,\theta,z)$

N_i = $N_i(r,z) = N_i^G(r,\theta,z)\big|_{\theta=0}$

n_i = direction cosines of an outward normal of fluid surface, $i=r,\theta,z$

Reproduced with permission of the copyright owner. Further reproduction prohibited without permission.

$\bar{N}_i$ = $\bar{N}_i(r)$, interpolation functions as a function of r

$\hat{N}_i$ = $\hat{N}_i(z)$, interpolation functions as a function of z

N_i^G = $N_i^G(r,\theta,z)$, interpolation functions as functions of r,θ, and z

n_{TB} = number of fluid nodes on transmitting boundary

[P] = matrix containing elements P_{ij}

p = $p(r,\theta,z,t)$, time dependent hydrodynamic pressure

{p} = time dependent hydrodynamic pressure vector containing elements $p_i(t)$

[P*] = matrix containing elements P^*_{ij}

$\bar{p}$ = $\bar{p}(r,\theta,z,\omega)$, frequency dependent hydrodynamic pressure

p_2 = time dependent hydrodynamic pressure associated with Fig. 5.32 (independent of variables r and θ)

$\{p_2\}$ = discrete counterpart of p_2

$\bar{p}_2$ = Fourier transform of p_2

$\{\bar{p}_2\}$ = Fourier transform of $\{p_2\}$

$\{\bar{p}_B\}$ = vector of hydrodynamic pressures at interlayers of fluid outside transmitting boundary θ=0 (functions of r and ω)

p_i = $p_i(t)$, time dependent hydrodynamic pressures at nodes i, i=1,2,.....n

$\bar{p}_j$ = $\bar{p}_j(r,\theta,z,\omega)$, frequency dependent hydrodynamic pressure distributions due to unit amplitude of harmonic acceleration in direction j, j=x,ϕ,z

$\{\bar{p}_j\}$ = discrete counterparts of $\bar{p}_j$, j=x,ϕ,z

P_{ij} = elements of matrix [P], defined by Eq. 4.30

Reproduced with permission of the copyright owner. Further reproduction prohibited without permission.

P^*_{ij} = elements of matrix [P*], defined by Eq. 4.31

[Q] = matrix containing elements Q_{ij}

Q_{ij} = elements of matrix [Q], defined by Eq. 4.30

R = R(r,ω), frequency dependent function of variable r

[R] = diagonal matrix containing $R_i(r,\omega)$

r = variable in cylindrical coordinates

{r} = time dependent vector of relative displacements of mass center

$\{\bar{r}\}$ = Fourier transform of {r}

r_0 = radius of circular cylindrical body

r_b = radius of transmitting boundary

R_g = radius of gyration of displaced volume of fluid about its center of gravity

$\{r_g\}$ = vector of ground displacements

R_i = $R_i(r,\omega)$, frequency dependent functions of variable r, corresponding to constants of separation β_i or α_i^2

R_i' = first derivative of R with respect to r

$\{r^t\}$ = vector of total displacements

S = surface

<T> = row of complex transformation functions T_i in transmitting boundary representation

t = time variable

T_i = complex transformation functions T_i in transmitting boundary representation

$<T^B>$ = compact form of <T>

Reproduced with permission of the copyright owner. Further reproduction prohibited without permission.

TB = transmitting boundary

V = volume of fluid displaced by the body

w = weight per unit volume of fluid

W_i = linearly independent weight functions

x = x(t), time dependent horizontal displacement of the body, relative to foundation

$\bar{x}$ = $\bar{x}(\omega)$, Fourier transform of x(t)

x_g = $x_g(t)$, time dependent horizontal displacement of foundation

x^t = $x^t(t)$, time dependent total horizontal displacement of the body

Z = Z(r,ω), frequency dependent function of variable z

z = z(t), time dependent vertical displacement of the body, relative to foundation or

= variable in cylindrical coordinates

$\bar{z}$ = $z(\omega)$, Fourier transform of z(t) or

= height of the center of gravity of the body from its base, depending on context

Z_i = $Z_i(z,\omega)$, frequency dependent functions of variable z, corresponding to α_i

$\{Z\}_i$ = discrete counterparts of Z_i

z_g = $z_g(t)$, time dependent vertical displacement of foundation

z^t = $z^t(t)$, time dependent total vertical displacement of the body

α_i^2 = constants of separation in continuum solution

Reproduced with permission of the copyright owner. Further reproduction prohibited without permission.

β_i = constants of separation in discretized solution (obtained by solving eigenvalue problem)

λ_i = constants related to α_i as shown in Eq. 3.15 and related to β_i by the relation $\lambda_i^2 = \beta_i + \frac{\omega^2}{c^2}$

ω = angular frequency

ϕ = $\phi(t)$, time dependent rotational displacement of the body, relative to foundation

$\bar{\phi}$ = $\bar{\phi}(\omega)$, Fourier transform of $\phi(t)$

ϕ_g = $\phi_g(t)$, time dependent rotational displacement of foundation

ϕ^t = $\phi^t(t)$, time dependent total rotational displacement of the body

ρ = mass density of fluid

Θ = function of variable

θ = variable in cylindrical coordinates

Reproduced with permission of the copyright owner. Further reproduction prohibited without permission.

1. INTRODUCTION

Large volume, gravity structures are used as storage tanks in offshore development. To design these gravity structures, the understanding of major environmental loadings are needed. In seismic areas, one of these loadings is due to earthquakes. The pressure distributions associated with hydrodynamic inertia forces acting on large structures during earthquakes are important while the drag forces may be neglected.

A closed form solution of hydrodynamic pressure acting on rigid cylindrical tanks, surrounded by incompressible water and subjected to horizontal ground excitation, was given by Jacobsen[1*] many years ago. Later, Petrauskas[2], Chandrasekaran, et al[3] investigated the influence of response interaction between flexible cylindrical columns or towers and fluid pressures. Chandrasekaran also investigated the effect of water compressibility on hydrodynamic pressure.

These closed form solutions are, however, limited to surface piercing, circular cylindrical structures having vertical outer surfaces. This limitation led to other investigations using methods that apply to more complex structures such as totally submerged structures and floating bodies. Of these methods, the boundary integral method or the method of distributed sources, utilizing Green's functions on the discretized surfaces of bodies, was used by many researchers, e.g. Garrison and Berklite[4], and Garrison[5]. This method is based on Laplace's equation which is valid only for incompressible fluids. In obtaining

---

* Refers to corresponding item under "References".

Reproduced with permission of the copyright owner. Further reproduction prohibited without permission.

solutions, singularities occur at sharp corners causing considerable difficulty.

Another method, which has become increasingly popular, is the finite element method. Investigations using this method have been reported by Bai[6], Zienkiewicz and Newton[7], and by Liaw and Chopra[8]. In these investigations, the infinite boundary was truncated but at a large distance which made the procedure computationally complex and subject to truncation errors.

The objectives of this investigation are (1) to develop an effective finite element procedure for determining fluid forces on rigid axisymmetric bodies, and (2) to verify the procedure by comparing analytical results with experimental results.

Reproduced with permission of the copyright owner. Further reproduction prohibited without permission.

2. DYNAMICS OF A RIGID AXISYMMETRIC BODY

In this chapter, the dynamics of a submerged or partially submerged axisymmetric body supported at the surface of an elastic half-space and subjected to earthquake excitations is presented. The idealized system of such a body is shown in Fig. 2.1 where it is supported by foundation impedances. First, the equations of motion of the body vibrating in the xz-plane are presented; then, the hydrodynamic inertia and damping forces which resist the movement of the body in fluid are formulated.

2.1 Equations of Motion

The equations of planar motion of the idealized body shown in Fig. 2.1 may be written in the matrix form

$$[M]\{\ddot{r}^{t}(t)\} + [C]\{\dot{r}(t)\} + [K]\{r(t)\} = -\{f(t)\} \qquad (2.1)$$

where

$$[M] = \begin{bmatrix} m & 0 & 0 \\ 0 & I & 0 \\ 0 & 0 & m \end{bmatrix}$$

is the mass matrix, m and I are the mass and mass moment of inertia of the body, respectively,

$$[C] = \begin{bmatrix} C_{xx} & C_{x\phi} & 0 \\ C_{\phi x} & C_{\phi\phi} & 0 \\ 0 & 0 & C_{zz} \end{bmatrix}$$

is the damping matrix,

$$[K] = \begin{bmatrix} k_{xx} & k_{x\phi} & 0 \\ k_{\phi x} & k_{\phi\phi} & 0 \\ 0 & 0 & k_{zz} \end{bmatrix}$$

Reproduced with permission of the copyright owner. Further reproduction prohibited without permission.

is the stiffness matrix,

$$\{r(t)\} = \begin{Bmatrix} x(t) \\ \phi(t) \\ z(t) \end{Bmatrix}$$

is the vector of relative displacements of the mass center with respect to the moving foundation in the x, ϕ, and z directions, respectively,

$$\{r^t(t)\} = \begin{Bmatrix} x^t(t) \\ \phi^t(t) \\ z^t(t) \end{Bmatrix}$$

is the corresponding vector of total displacements from a fixed reference, and

$$\{f(t)\} = \begin{Bmatrix} f_x(t) \\ f_\phi(t) \\ f_z(t) \end{Bmatrix}$$

is the external force vector. The single and double dots shown in Eq. 2.1 indicate velocity and acceleration vectors, respectively. It is seen that the vertical degree of freedom is uncoupled the other two degrees of freedom; therefore, it may be treated separately.

In case of earthquake excitation, $\{\ddot{r}^t(t)\}$ may be written in the form

$$\{\ddot{r}^t(t)\} = \{\ddot{r}_g(t)\} + \{\ddot{r}(t)\} \tag{2.2}$$

where

$$\{\ddot{r}_g(t)\} = \begin{Bmatrix} \ddot{x}_g(t) \\ \ddot{\phi}_g(t) \\ \ddot{z}_g(t) \end{Bmatrix}$$

is the vector of ground accelerations in the x, ϕ, and z directions, respectively. Substituting Eq. 2.2 into Eq. 2.1, one obtains

Reproduced with permission of the copyright owner. Further reproduction prohibited without permission.

$$[M]\{\ddot{r}(t)\} + [C]\{\dot{r}(t)\} + [K]\{r(t)\} = -\{f(t)\} - [M]\{\ddot{r}_g(t)\} \qquad (2.3)$$

which includes fluid effects caused by the earthquake motions. Since the hydrodynamic forces and the foundation impedances are frequency dependent, solutions of Eq. 2.3 must be obtained in the frequency domain. To convert from the time domain to the frequency domain, Eq. 2.3 can be transformed to

$$[M]\{\bar{\ddot{r}}(\omega)\} + [C]\{\bar{\dot{r}}(\omega)\} + [K]\{\bar{r}(\omega)\} = -\{\bar{f}(\omega)\} - [M]\{\bar{\ddot{r}}_g(\omega)\} \qquad (2.4)$$

where $\{\bar{\ddot{r}}(\omega)\}$, $\{\bar{\dot{r}}(\omega)\}$, $\{\bar{r}(\omega)\}$, $\{\bar{f}(\omega)\}$, and $\{\bar{\ddot{r}}_g(\omega)\}$ are the Fourier transforms of $\{\ddot{r}(t)\}$, $\{\dot{r}(t)\}$, $\{r(t)\}$, $\{f(t)\}$, and $\{\ddot{r}_g(t)\}$, respectively, expressed in terms of angular velocity ω. Using the known relationships

$$\{\bar{\dot{r}}(\omega)\} = i\omega\{\bar{r}(\omega)\}$$

and

$$\{\bar{\ddot{r}}(\omega)\} = -\omega^2\{\bar{r}(\omega)\},$$

Eq. 2.4 can be rewritten as

$$(-\omega^2[M] + i\omega[C] + [K])\{\bar{r}(\omega)\} = -\{\bar{f}(\omega)\} - [M]\{\bar{\ddot{r}}_g(\omega)\} \qquad (2.5)$$

2.2 Added Mass and Damping Representation

At this point, it is assumed that the physical properties of the body [M], the foundation impedances [K] and [C], and the foundation accelerations $\{\bar{\ddot{r}}_g(\omega)\}$ are known. Equation 2.5 can then be solved for $\{\bar{r}(\omega)\}$ provided $\{\bar{f}(\omega)\}$ and $\{\bar{\ddot{r}}_g(\omega)\}$ are known. The hydrodynamic forces $\{\bar{f}(\omega)\}$ are however dependent upon $\{\bar{r}(\omega)\}$ and $\{\bar{\ddot{r}}_g(\omega)\}$; thus, there is interaction between the body and its surrounding fluid.

The hydrodynamic forces in the linear formulation vary as the acceleration of the moving surface of the body (velocity dependent damping forces can be neglected due to the large size of the rigid

Reproduced with permission of the copyright owner. Further reproduction prohibited without permission.

body considered). Hence, these forces can be represented in the frequency domain by the relations

$$\bar{f}_x(\omega) = \bar{f}_{xx}(\omega)\ddot{\bar{x}} + \bar{f}^g_{xx}(\omega)\ddot{\bar{x}}_g + \bar{f}_{x\phi}(\omega)\ddot{\bar{\phi}} + \bar{f}^g_{x\phi}(\omega)\ddot{\bar{\phi}}_g \qquad (2.6a)$$

$$\bar{f}_\phi(\omega) = \bar{f}_{\phi x}(\omega)\ddot{\bar{x}} + \bar{f}^g_{\phi x}(\omega)\ddot{\bar{x}}_g + \bar{f}_{\phi\phi}(\omega)\ddot{\bar{\phi}} + \bar{f}^g_{\phi\phi}(\omega)\ddot{\bar{\phi}}_g \qquad (2.6b)$$

$$\bar{f}_z(\omega) = \bar{f}_{zz}(\omega)\ddot{\bar{z}} + \bar{f}^g_{zz}(\omega)\ddot{\bar{z}}_g \qquad (2.6c)$$

where $\bar{f}_{ij}(\omega)$ are the hydrodynamic forces in the i-direction due to a unit amplitude relative acceleration in the j-direction with respect to the moving foundation, and $\bar{f}^g_{ij}(\omega)$ are the hydrodynamic forces in the i-direction due to a unit amplitude ground acceleration in the j-direction. It is important to distinguish forces $\bar{f}_{ij}$ from $\bar{f}^g_{ij}$ due to the fact that the fluid flow patterns causing $\bar{f}_{ij}$ are different from those causing $\bar{f}^g_{ij}$. Forces $\bar{f}_{ix}$ and $\bar{f}^g_{ix}$ can however be assumed equal if the fluid depth is constant and the fluid viscosity is neglected. In the case of incompressible fluid with surface wave effects neglected, the hydrodynamic force coefficient $\bar{f}^g_{zz}$ is independent of the angular velocity ω and it has the same value as that of the hydrostatic force.

Equations 2.6 can be written in the matrix form

$$\begin{Bmatrix} \bar{f}_x(\omega) \\ \bar{f}_\phi(\omega) \\ \bar{f}_z(\omega) \end{Bmatrix} = \begin{bmatrix} \bar{f}_{xx}(\omega) & \bar{f}_{x\phi}(\omega) & 0 \\ \bar{f}_{\phi x}(\omega) & \bar{f}_{\phi\phi}(\omega) & 0 \\ 0 & 0 & \bar{f}_{zz}(\omega) \end{bmatrix} \begin{Bmatrix} \ddot{\bar{x}} \\ \ddot{\bar{\phi}} \\ \ddot{\bar{z}} \end{Bmatrix} + \begin{bmatrix} \bar{f}^g_{xx}(\omega) & \bar{f}^g_{x\phi}(\omega) & 0 \\ \bar{f}^g_{\phi x}(\omega) & \bar{f}^g_{\phi\phi}(\omega) & 0 \\ 0 & 0 & \bar{f}^g_{zz}(\omega) \end{bmatrix} \begin{Bmatrix} \ddot{\bar{x}}_g \\ \ddot{\bar{\phi}}_g \\ \ddot{\bar{z}}_g \end{Bmatrix} \qquad (2.7)$$

containing hydrodynamic forces which are complex frequency dependent functions. They are complex due to radiation of energy from the body into far field. Substituting the relation

$$\bar{f}_{ij}(\omega) = \bar{f}^R_{ij}(\omega) + i\bar{f}^I_{ij}(\omega) \qquad i,j = x, \phi, z$$

Reproduced with permission of the copyright owner. Further reproduction prohibited without permission.

where $\bar{f}^R_{ij}(\omega)$ and $\bar{f}^I_{ij}(\omega)$ are the real and imaginary parts of $\bar{f}_{ij}(\omega)$, respectively, into the first term on the right hand side of Eq. 2.7, recalling that $\{\ddot{\bar{r}}(\omega)\} = -\omega^2\{\bar{r}(\omega)\}$, and then in turn substituting Eq. 2.7 into Eq. 2.5, one obtains

$$(-\omega^2([M]+[M^a])+i\omega([C]+[C^a])+[K])\{\bar{r}(\omega)\} = -([M]+[M^g])\{\ddot{\bar{r}}_g(\omega)\} \tag{2.8}$$

where

$$[M^a] = \begin{bmatrix} \bar{f}^R_{xx}(\omega) & \bar{f}^R_{x\phi}(\omega) & 0 \\ \bar{f}^R_{\phi x}(\omega) & \bar{f}^R_{\phi\phi}(\omega) & 0 \\ 0 & 0 & \bar{f}^R_{zz}(\omega) \end{bmatrix} \tag{2.9}$$

is the added mass matrix,

$$[C^a] = -\omega \begin{bmatrix} \bar{f}^I_{xx}(\omega) & \bar{f}^I_{x\phi}(\omega) & 0 \\ \bar{f}^I_{\phi x}(\omega) & \bar{f}^I_{\phi\phi}(\omega) & 0 \\ 0 & 0 & \bar{f}^I_{zz}(\omega) \end{bmatrix} \tag{2.10}$$

is the hydrodynamic damping matrix, and

$$[M^g] = \begin{bmatrix} \bar{f}^g_{xx}(\omega) & \bar{f}^g_{x\phi}(\omega) & 0 \\ \bar{f}^g_{\phi x}(\omega) & \bar{f}^g_{\phi\phi}(\omega) & 0 \\ 0 & 0 & \bar{f}^g_{zz}(\omega) \end{bmatrix} \tag{2.11}$$

is the complex added mass matrix associated with ground acceleration. Elements of matrices $[M^a]$ and $[C^a]$ are real while those of $[M^g]$ are complex.

Reproduced with permission of the copyright owner. Further reproduction prohibited without permission.

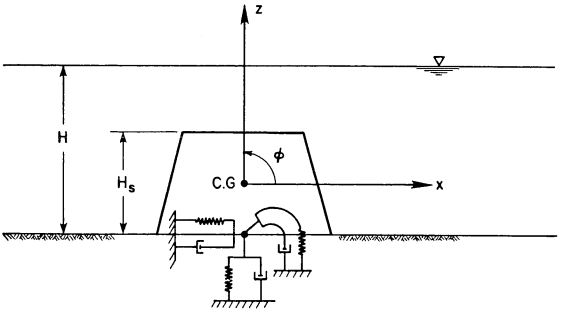

FIG. 2.1 IDEALIZED SYSTEM OF A RIGID STRUCTURE IN FLUID

Reproduced with permission of the copyright owner. Further reproduction prohibited without permission.

3. CONTINUUM SOLUTIONS OF HYDRODYNAMIC PRESSURE FOR PIERCING CIRCULAR CYLINDRICAL BODIES

3.1 Scope and Introduction

In this chapter, the continuum solutions of the hydrodynamic pressure for a piercing cylindrical flexible body of constant circular cross-section subjected to two types of excitations are presented. The first type of excitation is produced by radial accelerations of the vertical outer surface of the body having the form $\cos\theta$ in the circumferential direction, but varying arbitrarily along the height as shown in Fig. 3.1a. This case corresponds to a flexible cylindrical body subjected to a single component horizontal excitation. The second type of excitation is produced by axisymmetrical radial accelerations of the body surface about the vertical axis as shown in Fig. 3.1b.

These solutions are needed to develop the transmitting boundary representation presented later in Chapter 4. The transmitting boundary enables one to reduce the domain of a certain problem that extends to infinity to a finite one; thus, the number of unknowns can be greatly reduced in the discretized formulation. Consequently, the computational effort can be greatly reduced. The solution for the first type of excitation provides a basis for the transmitting boundary representation in the case of horizontal or rotational motion while the solution for the second type of excitation can be used for the case of vertical motion.

3.2 Assumptions and Governing Equations

The constant circular cross-section cylindrical body in fluid is shown in Fig. 3.2. The fluid domain is extended to infinity in the

Reproduced with permission of the copyright owner. Further reproduction prohibited without permission.

horizontal directions but it has constant finite depth H in the vertical direction. By assuming the water to be linearly compressible and inviscid, the small amplitude irrotational motion is governed by the wave equation in cylindrical coordinates as given by[8]

$$\frac{\partial^2 p}{\partial r^2} + \frac{1}{r}\frac{\partial p}{\partial r} + \frac{1}{r^2}\frac{\partial^2 p}{\partial \theta^2} + \frac{\partial^2 p}{\partial z^2} = \frac{1}{c^2}\frac{\partial^2 p}{\partial t^2} \tag{3.1}$$

In this equation, $p(r,\theta,z,t)$ is the hydrodynamic pressure in excess of hydrostatic pressure and c is the speed of sound in the undisturbed fluid. Shock waves either do not exist or are so weak as to justify the small perturbation approximation[18] in Eq. 3.1.

To obtain the boundary conditions which must be applied to Eq. 3.1, the normal accelerations of the outer surface of the cylindrical body must be prescribed. These accelerations are the same as those of fluid particles in contact with the surface. Using Newton's second law of linear momentum, the acceleration of any particle can be expressed in terms of derivatives of the hydrodynamic pressure as follows:

$$-\frac{\partial p}{\partial r} = \frac{w}{g} a_r \tag{3.2a}$$

$$-\frac{1}{r}\frac{\partial p}{\partial \theta} = \frac{w}{g} a_\theta \tag{3.2b}$$

$$-\frac{\partial p}{\partial z} = \frac{w}{g} a_z \tag{3.2c}$$

In these relations, quantities of a_r, a_θ, and a_z are the accelerations of the fluid particle in directions r, θ, and z respectively, w is the unit weight of fluid, and g is the acceleration of gravity.

Corresponding to the two types of excitations shown in Fig. 3.1, there are two different sets of boundary conditions. For the type 1 excitation, Fig. 3.1a, the boundary conditions can be represented as follows:

Reproduced with permission of the copyright owner. Further reproduction prohibited without permission.

a) The radial component of acceleration at the interface boundary $r=r_0$ is governed by

$$-\frac{\partial p}{\partial r}(r_0,\theta,z,t) = \frac{w}{g}a(z,t)\cos\theta \tag{3.3a}$$

where $a(z,t)$ is the acceleration along the z-axis of the body at $\theta=0$, as shown in Fig. 3.1a.

b) The condition of symmetry about the $\theta=0$ vertical plane (i.e., there are no tangential accelerations of particles across that plane) is given by

$$\frac{\partial p}{\partial \theta}(r,0,z,t) = \frac{\partial p}{\partial \theta}(r,\pi,z,t) = 0 \tag{3.3b}$$

c) No vertical motion is presented at the boundary $z=0$; thus,

$$\frac{\partial p}{\partial z}(r,\theta,0,t) = 0 \tag{3.3c}$$

d) The wave condition at the free surface is controlled by

$$-\frac{\partial p}{\partial z}(r,\theta,H,t) = \frac{1}{g}\frac{\partial^2 p}{\partial t^2}(r,\theta,H,t) \tag{3.3d}$$

e) Pressure $p(r,\theta,z,t)$ decays with increasing values of r and the pressure wave moves away from the cylinder.

Similarly, the boundary conditions for the Type 2 excitation can be represented as follows:

a) $$-\frac{\partial p}{\partial r}(r_0,\theta,z,t) = \frac{w}{g}a(z,t) \tag{3.4a}$$

b) Because of the condition of axisymmetry, no tangential accelerations of fluid particles exist at any θ; thus,

$$\frac{\partial p}{\partial \theta}(r,\theta,z,t) = 0 \tag{3.4b}$$

Reproduced with permission of the copyright owner. Further reproduction prohibited without permission.

c) $$\frac{\partial p}{\partial z}(r,\theta,0,t) = 0 \tag{3.4c}$$

d) $$-\frac{\partial p}{\partial z}(r,\theta,H,t) = \frac{1}{g}\frac{\partial^2 p}{\partial t^2}(r,\theta,H,t) \tag{3.4d}$$

e) Same radiation condition as for Type 1 excitation.

The first two boundary conditions for Type 1 and Type 2 accelerations are different but the remaining three conditions are the same.

3.3 Expressions for Complex Frequency Solutions

Equation 3.1 may be rewritten in the equivalent form

$$\nabla^2 p = \frac{1}{c^2}\frac{\partial^2 p}{\partial t^2} \tag{3.5}$$

where

$$\nabla^2 = \frac{\partial^2}{\partial r^2} + \frac{1}{r}\frac{\partial}{\partial r} + \frac{1}{r^2}\frac{\partial^2}{\partial \theta^2} + \frac{\partial^2}{\partial \theta^2}$$

To enforce the above boundary conditions, it is convenient and appropriate first to consider harmonic excitation and then to obtain the complex solution in the frequency domain. Following this approach, the acceleration function of the cylinder surface can be written in the form

$$a(z,t) = \bar{a}(z,\omega)e^{i\omega t} \tag{3.6}$$

where $\bar{a}(z,\omega)$ is the amplitude of the harmonic acceleration at frequency ω. Since the governing equation and the associated boundary conditions are linear, the steady-state response is also harmonic at the same frequency ω. Hence, the solution $p(r,\theta,z,t)$ may be written in the form

$$p(r,\theta,z,t) = \bar{p}(r,\theta,z,\omega)e^{i\omega t} \tag{3.7}$$

Reproduced with permission of the copyright owner. Further reproduction prohibited without permission.

where $\bar{p}(r,\theta,z,\omega)$ is the complex frequency response.

Substituting Eq. 3.7 into Eq. 3.5 gives

$$\nabla^2 \bar{p} = -\frac{\omega^2}{c^2} \bar{p} \tag{3.8}$$

The boundary conditions can similarly be expressed in terms of the complex frequency function $\bar{p}(r,\theta,z,\omega)$.

3.3.1 Excitation of the Form of Cosθ (Type 1)

Substituting Eqs. 3.6 and 3.7 into the boundary condition equations, Eqs. 3.3, one obtains

$$\begin{aligned}
\frac{\partial \bar{p}}{\partial r}(r_o,\theta,z,\omega) &= -\frac{w}{g} \bar{a}(z,\omega) \cos\theta \\
\frac{\partial \bar{p}}{\partial \theta}(r,0,z,\omega) &= \frac{\partial \bar{p}}{\partial \theta}(r,\pi,z,\omega) = 0 \\
\frac{\partial \bar{p}}{\partial z}(r,\theta,0,\omega) &= 0 \\
\frac{\partial \bar{p}}{\partial z}(r,\theta,H,\omega) &= \frac{\omega^2}{g} \bar{p}(r,\theta,H,\omega)
\end{aligned} \tag{3.9}$$

Using the standard method of separation of variables, the solution to Eq. 3.8 which satisfies the boundary conditions of Eq. 3.9 and the radiation condition is

$$\bar{p}(r,\theta,z,\omega) = \sum_{m=0}^{\infty} b_m R_m(r,\omega) Z_m(z,\omega) \cos\theta \tag{3.10}$$

in which b_m are constants to be determined and

$$\left.\begin{aligned}
Z_o(z,\omega) &= \cosh(\alpha_o z) \\
Z_m(z,\omega) &= \cos(\alpha_m z) \quad , \quad m=1,2,.....\infty
\end{aligned}\right\} \tag{3.11}$$

Reproduced with permission of the copyright owner. Further reproduction prohibited without permission.

$$R_m(r,\omega) = H_1^{(2)}(\lambda_m r) \quad , \quad m=0,1,2,.....k$$
$$R_m(r,\omega) = K_1(\lambda_m r) \quad , \quad m=k+1,.....\infty \tag{3.12}$$

$H_1^{(2)}$ is the Hankel function of the second kind of order one and K_1 is the modified Bessel function of the second kind of order one. In these expressions, α_o, α_m, λ_m, and k are defined as follows:

α_o is a solution of

$$\alpha_o \tanh(\alpha_o H) = \frac{\omega^2}{g} \tag{3.13}$$

α_m are the solutions of

$$\alpha_m \tan(\alpha_m H) = -\frac{\omega^2}{g} \quad , \quad m=1,2,.....\infty \tag{3.14}$$

$$\left.\begin{aligned} \lambda_o &= \sqrt{\frac{\omega^2}{c^2} + \alpha_o^2} \\ \lambda_m &= \sqrt{\frac{\omega^2}{c^2} - \alpha_m^2} \quad , \quad m=1,2,.....k \\ \lambda_m &= \sqrt{\alpha_m^2 - \frac{\omega^2}{c^2}} \quad , \quad m=k+1,.....\infty \end{aligned}\right\} \tag{3.15}$$

where k is the largest integer satisfying the condition $\alpha_k^2 < \frac{\omega^2}{c^2}$.

To determine coefficients b_m and $\bar{p}$, Eq. 3.10 is substituted into the first boundary condition relation of Eqs. 3.9, then the orthogonality property of functions Z_m is applied; thus, giving

$$b_m = -\frac{w}{g} \frac{\int_o^H \bar{a}(z,\omega) Z_m(z,\omega)\,dz}{R_m'(r_o,\omega)\int_o^H Z_m^2(z,\omega)\,dz} \quad , \quad m=0,1,2,.....\infty \tag{3.16}$$

Reproduced with permission of the copyright owner. Further reproduction prohibited without permission.

where $R_m'(r_o,\omega)$ is the first derivative of $R_m(r,\omega)$ with respect to r, evaluated at $r=r_o$.

It can be seen that if $\bar{a}(z,\omega)$ is given, coefficients b_m can be obtained. Then, the complex frequency, hydrodynamic pressure is obtained from Eq. 3.10.

3.3.2 Axisymmetric Excitation (Type 2)

Similarly, the boundary conditions of Eqs. 3.4 can be expressed in the frequency domain by the relations

$$\begin{aligned} \frac{\partial \bar{p}}{\partial r}(r_o,\theta,r,\omega) &= -\frac{w}{g}\bar{a}(z,\omega) \\ \frac{\partial \bar{p}}{\partial \theta}(r,\theta,z,\omega) &= 0 \\ \frac{\partial \bar{p}}{\partial z}(r,\theta,0,\omega) &= 0 \\ \frac{\partial \bar{p}}{\partial z}(r,\theta,H,\omega) &= \frac{\omega^2}{g}\bar{p}(r,\theta,H,\omega) \end{aligned} \tag{3.17}$$

Using these relations and the radiation condition, the hydrodynamic pressure is given by

$$\bar{p}(r,\theta,z,\omega) = \sum_{m=0}^{\infty} b_m R_m(r,\omega) Z_m(z,\omega) \tag{3.18}$$

where

$$\begin{aligned} R_m(r,\omega) &= H_o^{(2)}(\lambda_m r) \quad , \quad m=0,1,.....k \\ R_m(r,\omega) &= K_o(\lambda_m r) \quad , \quad m=k+1,.....\infty \end{aligned} \tag{3.19}$$

and Z_m,λ_m,k are the same quantities defined in Section 3.3.1. $H_o^{(2)}$ is the Hankel function of the second kind of order zero and K_o is the modified Bessel function of the second kind of order zero. It should

Reproduced with permission of the copyright owner. Further reproduction prohibited without permission.

be noted that pressure $\bar{p}$ in Eq. 3.18 is independent of θ.

Using the first equation of the boundary conditions given by Eqs. 3.17 and the orthogonality property of Z_m, b_m can be expressed as

$$b_m = -\frac{w}{g}\frac{\int_0^H \bar{a}(z,\omega) Z_m(z,\omega)\, dz}{R_m'(r_o,\omega)\int_0^H Z_m^2(z,\omega)\, dz} \tag{3.20}$$

3.4 Inverse Representation

In the previous sections, the hydrodynamic pressure is obtained in series form containing coefficients b_m which can be determined if the acceleration of the cylinder is known. In this section, the inverse relation is sought, i.e., the acceleration function $\bar{a}(z,\omega)$ expressed in terms of the hydrodynamic pressure. This relation is needed in the transmitting boundary representation as stated earlier. At this boundary, the accelerations of fluid particles are expressed in terms of the unknown hydrodynamic pressures at the boundary.

3.4.1 Excitation of the Form of $\cos\theta$ (Type 1)

Differentiating Eq. 3.10 with respect to r, setting $r=r_o$, and then substituting the resulting relation into the first of Eqs. 3.9 gives

$$-\frac{w}{g}\bar{a}(z,\omega)\cos\theta = \sum_{m=0}^{\infty} b_m R_m'(r_o,\omega) Z_m(z,\omega)\cos\theta \tag{3.21}$$

Coefficients b_m in this equation can be expressed in terms of the hydrodynamic pressure at $r=r_o$, i.e. $\bar{p}(r_o,\theta,z,\omega)$, by substituting $r=r_o$ into Eq. 3.10 and applying the orthogonality property of Z_m. Consequently,

$$b_m = \frac{\int_0^H \bar{p}(r_o,\theta,z,\omega) Z_m(z,\omega)\, dz}{R_m(r_o,\omega)\cos\theta \int_0^H Z_m^2(z,\omega)\, dz} \tag{3.22}$$

Reproduced with permission of the copyright owner. Further reproduction prohibited without permission.

where quantities R_m are given in Eq. 3.12.

Substituting b_m as given by Eq. 3.22 into Eq. 3.21, the acceleration $\bar{a}(z,\omega)$ is obtained as a function of $\bar{p}(r_o,\theta,z,\omega)$.

3.4.2 Axisymmetric Excitation (Type 2)

Similarly for the axisymmetric excitation case, the acceleration function $\bar{a}(z,\omega)$ can be expressed as a function of $\bar{p}(r_o,\theta,z,\omega)$ through the relation

$$-\frac{w}{g}\bar{a}(z,\omega) = \sum_{m=0}^{\infty} b_m R_m'(r_o,\omega) Z_m(z,\omega) \tag{3.23}$$

where

$$b_m = \frac{\int_o^H \bar{p}(r_o,\theta,z,\omega) Z_m(z,\omega)\,dz}{R_m(r_o,\omega)\int_o^H Z_m^2(z,\omega)\,dz} \tag{3.24}$$

Functions R_m are again defined by Eqs. 3.19.

Reproduced with permission of the copyright owner. Further reproduction prohibited without permission.

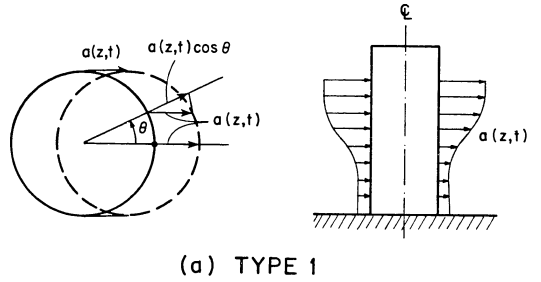

(a) TYPE 1

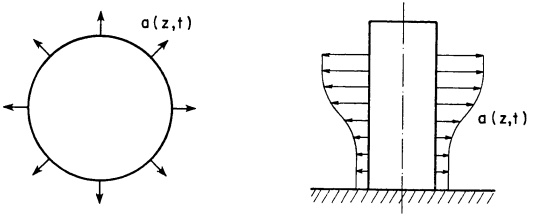

(b) TYPE 2

FIG. 3.1 TYPES OF EXCITATIONS

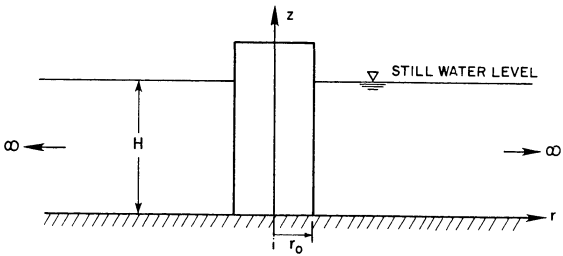

FIG. 3.2 CIRCULAR CYLINDRICAL TOWER IN WATER

Reproduced with permission of the copyright owner. Further reproduction prohibited without permission.

4. FINITE ELEMENT ANALYSIS OF HYDRODYNAMIC PRESSURE FOR RIGID AXISYMMETRIC BODIES

4.1 Scope

In this chapter, the axisymmetric problem of Fig. 2.1 is analyzed by the finite element method. As stated earlier in Chapter 2, the body may be of the surface piercing type. The purpose of this analysis is to determine the hydrodynamic pressure distributions on the interface between the structure and the fluid. Once the distributions are known, the added mass coefficients can be determined.

To determine the pressure distributions, the body is assumed to be excited in the horizontal, vertical, and rotational directions while the foundation remains at rest. Thus, the coefficients obtained are the coefficients of matrices $[M^a]$ and $[C^a]$ of Eqs. 2.9 and 2.10, respectively. It is also possible to find the coefficients of matrix $[M^g]$ given by Eq. 2.11. However, in this treatment we are primarily interested in the added mass matrix $[M^a]$ and the hydrodynamic damping matrix $[C^a]$.

4.2 Governing Equations

The assumptions regarding fluid properties are the same here as those given in Chapter 3. The governing wave equation of the fluid domain shown in Fig. 4.1 is the same as Eq. 3.1 or Eq. 3.5, i.e.

$$\nabla^2 p - \frac{1}{c^2} \ddot{p} = 0 \tag{4.1}$$

While the boundary conditions for each case of the three excitations are not the same, they can be expressed by the following general conditions:

Reproduced with permission of the copyright owner. Further reproduction prohibited without permission.

a) At the interface between the structure and fluid,

$$\left.\frac{\partial p}{\partial n}\right|_{IF} = -\frac{w}{g}\, a_n(r,\theta,z,t)\Big|_{IF} \tag{4.2a}$$

b) At the free surface,

$$\left.\frac{\partial p}{\partial z}\right|_{FS} = -\frac{1}{g}\,\ddot{p}(r,\theta,H,t) \tag{4.2b}$$

c) At the base of the body,

$$\left.\frac{\partial p}{\partial n}\right|_{BF} = 0 \tag{4.2c}$$

d) At the transmitting boundary (TB),

$$\left.\frac{\partial p}{\partial r}\right|_{TB} = -\frac{w}{g}\, a_r(r_b,\theta,z,t) \tag{4.2d}$$

In the above relations, $\frac{\partial p}{\partial n}$ is the hydrodynamic pressure gradient in the outward normal direction of the surface of the fluid domain, a_n is the acceleration function of fluid particles in the outward normal direction of the fluid surface, and a_r is the acceleration function of fluid particles in the r direction. Note that in Eq. 4.2d only the radial component of the particle acceleration is present. This is due to the fact that the transmitting boundary is a vertical surface. At this point, $a_r(r_b,\theta,z,t)$ at the transmitting boundary is assumed to be known. It will be shown later in Section 4.4 that this acceleration function can be expressed in terms of unknown nodal pressures on the boundary.

The acceleration function of inviscid fluid particles on the interface, as mentioned earlier, is the same as the normal component

Reproduced with permission of the copyright owner. Further reproduction prohibited without permission.

of the acceleration of the structure. Thus, in those cases where the body is excited purely in the horizontal and rotational directions, this acceleration as given by Eq. 4.2a can be written in the form

$$a_n(r,\theta,z,t)\Big|_{IF} = \tilde{a}_n(r,z,t)\cos\theta \tag{4.3}$$

For the vertically excited axisymmetric case,

$$a_n(r,\theta,z,t)\Big|_{IF} = \tilde{a}_n(r,z,t) \tag{4.4}$$

where $\tilde{a}_n(r,z,t) = a_n(r,0,z,t)$.

Since the distributions of the excitations in the θ-direction are known as shown above, the distributions of pressures in that same direction are also known since they vary in the θ-direction exactly the same as their corresponding excitations[12]. Hence, $a_r(r_b,\theta,z,t)$ in Eq. 4.2d can be written as

$$a_r(r_b,\theta,z,t) = \tilde{a}_r(r_b,z,t)\cos\theta \tag{4.5}$$

for the horizontal or rotational case. In the vertical case, it is given by

$$a_r(r_b,\theta,z,t) = \tilde{a}_r(r_b,z,t) \tag{4.6}$$

It should be noted here that the original three-dimensional problem is essentially reduced to the two-dimensional case.

4.3 Finite Element Discretization and Formulation

In the finite element discretization, the fluid domain is divided into a finite number of subdomains or elements. As shown in Fig. 4.1, the fluid domain inside the transmitting boundary is discretized into axisymmetric ring elements of quadrilateral and

Reproduced with permission of the copyright owner. Further reproduction prohibited without permission.

triangular cross-sections. The ring elements are interconnected by the circles that are called nodes or nodal circles. In the discretization, the boundary surface of the fluid domain is also divided into subsurfaces.

The next step in the finite element approximation is to assume interpolation functions such that

$$p = \sum_{i=1}^{n} N_i^G p_i = \langle N^G \rangle \{p\} \tag{4.7}$$

where

$$N_i^G = N_i^G(r,\theta,z)$$

are the global interpolation functions,

$$p_i = p_i(t)$$

are nodal values of p at nodes i, and n is the total number of nodes. In this same equation, $\langle N^G \rangle$ is a row vector whose elements are N_1^G, N_2^G, ..., N_n^G and $\{p\}$ is a column vector whose elements are p_1, p_2,....., p_n. The interpolation functions N_i^G in the finite element method have the property that they vanish everywhere in the domain except over the subdomains or elements adjacent to nodes i.

At this stage, the finite element equations are ready to be formulated. There are a variety of ways to derive the finite element equations. Here, a general approach that employs the method of weighted residuals or the Galerkin method is used.

When the approximation of p from Eq. 4.7 is substituted to Eq. 4.1, it is unlikely that the right hand side of Eq. 4.1 will be zero. That is, there is an error or a residual that results from the approximation of p. The aim of the method of weighted residuals is to

Reproduced with permission of the copyright owner. Further reproduction prohibited without permission.

determine p_i such that the residual is small in some average sense over the entire domain. This can be accomplished by forcing weighted average errors over the domain to vanish. That is

$$\int_D (\nabla^2 p - \frac{1}{c^2} \ddot{p})\, W_i \, dD = 0 \quad , \quad i=1,2,.....n \tag{4.8}$$

where W_i are the chosen linearly independent weight functions, D is the discretized fluid domain, and p is the approximated function given by Eq. 4.7.

After integrating the first term of Eq. 4.8 by parts and applying the divergence theorem, the weak form of Eq. 4.8 is obtained as

$$\int_D (\nabla W_i \cdot \nabla p + \frac{1}{c^2} \ddot{p} W_i) dD - \int_S W_i \frac{\partial p}{\partial n} dS = 0 \quad , \quad i=1,2,.....n \tag{4.9}$$

where S is the surface of the fluid domain.

In the Galerkin method of the weighted residual approximation, the weight functions are chosen to be the same as the interpolation functions, i.e.

$$W_i = N_i^G \quad , \quad i=1,2,.....n$$

Thus, the Galerkin form of Eq. 4.9 is

$$\int_D (\nabla N_i^G \cdot \nabla p + \frac{1}{c^2} \ddot{p} N_i^G) dD - \int_S N_i^G \frac{\partial p}{\partial n} dS = 0 \quad , \quad i=1,2,.....n \tag{4.10}$$

where

$$\nabla = u_r \frac{\partial}{\partial r} + u_\theta \frac{1}{r} \frac{\partial}{\partial \theta} + u_z \frac{\partial}{\partial z}$$

Quantities u_r, u_θ, u_z are unit vectors in the r, θ, and z directions, respectively.

Upon substituting Eq. 4.7 and the boundary conditions of Eqs. 4.2 into Eq. 4.10, it becomes

Reproduced with permission of the copyright owner. Further reproduction prohibited without permission.

$$\int_D [\sum_{j=1}^{n} (\nabla N_i^G \cdot \nabla N_j^G) p_j + \frac{1}{c^2} \sum_{j=1}^{n} N_i^G N_j^G \ddot{p}_j] \, dD = \int_{IF} N_i^G (-\frac{w}{g} a_n) dS$$

$$+ \int_{FS} N_i^G (-\frac{1}{g} \sum_{j=1}^{n} N_j^G \ddot{p}_j) dS + \int_{TB} N_i^G (-\frac{w}{g} a_r) dS \quad , \quad i=1,2,.....n \tag{4.11}$$

which can be written in the compact matrix form

$$[F]\{p\} + [F^C]\{\ddot{p}\} = \{D\} - [F^L]\{\ddot{p}\} + [F^B]\{p\}$$

or

$$([F] - [F^B])\{p\} + ([F^C] + [F^S])\{\ddot{p}\} = \{D\} \tag{4.12}$$

Matrix [F] is analogous to the stiffness matrix in the finite element formulation of structural mechanics. Elements F_{ij} are given by

$$F_{ij} = \int_D \nabla N_i^G \cdot \nabla N_j^G \, dD \qquad i,j=1,2,.....n \tag{4.13}$$

$[F^B]$ is the matrix that results from the condition at the transmitting boundary. Coefficients F_{ij}^B do not vanish only if both nodes i and j are on the transmitting boundary. As will be shown later, the quantity $-\frac{w}{g} a_r(r_b,\theta,z,t)$ appearing in the last term on the right hand side of Eq. 4.11 can be expressed as

$$-\frac{w}{g} a_r(r_b,\theta,z,t) = \sum_{j=1}^{n} T_j p_j = \langle T \rangle \{p\} \tag{4.14}$$

where $\langle T \rangle$ is a row transformation matrix and elements T_j=0 if j are not the nodes on the transmitting boundary. Hence,

$$F_{ij}^B = \int_{TB} N_i^G T_j \, dS \qquad i,j=1,2,.....n \tag{4.15}$$

It will also be shown later that T_j are complex and frequency dependent. Thus, F_{ij}^B are complex and frequency dependent. This should be expected since some energy is lost due to radiation into the far-field.

Matrix $[F^C] + [F^S]$ in Eq. 4.12 is analogous to the mass matrix in the finite element formulation of structural mechanics. Their elements are

Reproduced with permission of the copyright owner. Further reproduction prohibited without permission.

$$F^C_{ij} = \int_D \frac{1}{c^2} N^G_i N^G_j \, dD \qquad i,j=1,2,.....n \tag{4.16}$$

$$F^S_{ij} = \int_{FS} \frac{1}{g} N^G_i N^G_j \, dS \qquad i,j=1,2,.....n \tag{4.17}$$

Coefficients F^S_{ij} do not vanish only if nodes i and j are on the free surface. It should be noted that for incompressible fluid $[F^C]$ vanishes which is equivalent to stating $\nabla^2 p = 0$. Furthermore, if the surface waves are neglected, $[F^S]$ also vanishes.

Finally, the column vector $\{D\}$ contains components $D_i(t)$ expressed as

$$D_i(t) = \int_{IF} N^G_i \left(-\frac{w}{g} a_n(r,\theta,z,t)\right) dS \tag{4.18}$$

It is easily seen that $[F]$, $[F^C]$, and $[F^S]$ are symmetric matrices and it will be shown later that $[F^B]$ is also a symmetric matrix. These matrices depend not only on the geometry of the problem but also on the types of excitations; see Appendix A. For example, both matrices $[F^C]$ and $[F^S]$ differ by a factor of two when changing from the case of horizontal or rotational excitation to the case of vertical excitation. These result from the difference in the circumferential distribution of the pressure associated with the two excitation cases.

In the finite element procedure, the expressions given by Eqs. 4.13 and 4.15-4.18 are evaluated over each element and then the contributions of all elements are assembled. This integration over individual element allows the interpolation functions to be defined locally for each element instead of for the entire domain. Such interpolation functions in the local coordinates are easier to obtain

Reproduced with permission of the copyright owner. Further reproduction prohibited without permission.

and they are repetitive for the same type of elements. Another advantage of this procedure is that numerical integration may be used.

4.4 Transmitting Boundary Representation

The fluid domain in Fig. 4.1 is truncated and only the fluid inside the transmitting boundary is considered. At the transmitting boundary either the hydrodynamic pressure or its derivative must be specified as a boundary condition. As shown earlier in Chapter 3, the pressure gradients or the accelerations of fluid particles at the boundary can be expressed implicity in terms of the continuous pressure function at that boundary (see Eq. 3.21 or Eq. 3.23). In this section, the explicit relationship is derived; i.e., the acceleration function or the pressure gradient is expressed explicitly in terms of discrete values of the nodal pressures.

Consider now the fluid domain outside the transmitting boundary with constant depth H as shown in Fig. 4.2. The governing wave equation for the fluid domain is the same as that of Eq. 4.1. However, it is more convenient to solve the problem in the frequency domain. Thus, the governing wave equation, as in Eq. 3.8, is

$$\nabla^2 \bar{p} = -\frac{\omega^2}{c^2} \bar{p} \tag{4.19}$$

Using the method of separation of variables, $\bar{p}$ is assumed to be

$$\bar{p}(r,\theta,z,\omega) = R(r,\omega)\Theta(\theta,\omega)Z(z,\omega) \tag{4.20}$$

Substituting $\bar{p}$ as given by this relation into Eq. 4.19, one obtains after rearranging terms

$$\frac{Z''}{Z} = -\left(\frac{R''}{R} + \frac{1}{r}\frac{R'}{R} + \frac{1}{r^2}\frac{\Theta''}{\Theta} + \frac{\omega^2}{c^2}\right) = \beta \tag{4.21}$$

Reproduced with permission of the copyright owner. Further reproduction prohibited without permission.

where

$$Z'' = \frac{d^2Z}{dz^2} \quad , \quad R'' = \frac{d^2R}{dr^2} \quad , \quad R' = \frac{dR}{dr} \quad , \quad \Theta'' = \frac{d^2\Theta}{d\theta^2}$$

Quantity β in this relation is the constant of separation.

Consider now the relation

$$\frac{Z''}{Z} = \beta$$

or

$$Z'' - \beta Z = 0 \tag{4.22}$$

The boundary conditions at z=0, and z=H to be applied to Eq. 4.19 are, respectively,

$$\left.\frac{\partial \bar{p}}{\partial z}\right|_{z=0} = 0$$

and

$$\left.\frac{\partial \bar{p}}{\partial z}\right|_{z=H} = \left.\frac{\omega^2}{g}\bar{p}\right|_{z=H}$$

Applying these boundary conditions to Eq. 4.22 gives

$$Z'(0) = 0 \tag{4.23}$$

$$Z'(H) = \frac{\omega^2}{g} Z(H) \tag{4.24}$$

If the surface waves are neglected, Eq. 4.24 becomes

$$Z(H) = 0 \tag{4.25}$$

Similarly to that procedure presented in Section 4.2, the fluid domain outside the transmitting boundary is discretized into layers as shown in Fig. 4.2. The approximation of Z is then given by

$$Z(z) = \sum_{j=1}^{n_{TB}} \hat{N}_j Z_j = \langle \hat{N} \rangle \{Z\} \tag{4.26}$$

Reproduced with permission of the copyright owner. Further reproduction prohibited without permission.

where $\hat{N}_j = \hat{N}_j(z)$ are the interpolation functions, Z_j are nodal values of $Z(z)$ at nodes j or interlayers j (Fig. 4.2), and n_{TB} equals the total number of nodes on the transmitting boundary.

Using again the Galerkin procedure to solve for $\{Z\}$, the integral form of Eq. 4.22 is

$$\int_0^H (Z''-\beta Z)\hat{N}_i \, dz = 0 \quad , \quad i=1,2,.....n_{TB} \tag{4.27}$$

Integrating the first term in this equation by parts gives

$$\int_0^H (-Z'\hat{N}_i'-\beta Z\hat{N}_i)dz + Z'(H)\hat{N}_i(H) - Z'(0)\hat{N}_i(0) = 0, \; i=1,2,.....n_{TB} \tag{4.28}$$

Substituting Eq. 4.26 and the boundary conditions, Eqs. 4.23-4.24, into Eq. 4.28, yields

$$\int_0^H [\sum_{j=1}^{n_{TB}} (\hat{N}_i'\hat{N}_j' + \beta\hat{N}_i\hat{N}_j)Z_j]dz - \frac{\omega^2}{g}\sum_{j=1}^{n_{TB}} \hat{N}_i(H)\hat{N}_j(H)Z_j = 0, \; i=1,2,..n_{TB} \tag{4.29}$$

In the finite element procedure, the interpolation functions $\hat{N}_j$ vanish everywhere except over the layers adjacent to nodes j and $\hat{N}_j(z=z_j) = 1$. Hence, Eq. 4.29 may be written as

$$\sum_{j=1}^{n_{TB}} (P_{ij} + \beta Q_{ij})Z_j - \frac{\omega^2}{g}\delta_{il}Z_l = 0 \quad , \quad i=1,2,..n_{TB} \tag{4.30}$$

where

$$P_{ij} = \int_0^H \hat{N}_i'\hat{N}_j' \, dz$$

$$Q_{ij} = \int_0^H \hat{N}_i\hat{N}_j \, dz$$

$$\delta_{il} = \begin{cases} 1 & \text{for } i=l \\ 0 & \text{for } i\neq l \end{cases}$$

Equation 4.30 can be written in the matrix form

Reproduced with permission of the copyright owner. Further reproduction prohibited without permission.

$$([P^*] + \beta[Q])\{Z\} = \{0\} \tag{4.31}$$

where

$$P^*_{11} = P_{11} - \frac{\omega^2}{g}$$

$$P^*_{ij} = P_{ij} \quad \text{for } i,j \neq 1.$$

Equation 4.31 represents an eigenvalue problem. It can be solved for eigenvalues β_i and normalized eigenvectors or mode shapes $\{Z\}_i$ for $i=1,2,.....n_{TB}$. The frequency dependent $\{Z\}_i$ are normalized such that

$$\{Z\}_i^T[Q]\{Z\}_j = \delta_{ij} \tag{4.32a}$$

or

$$[E]^T[Q][E] = [I] \tag{4.32b}$$

where δ_{ij} is the Kronecker delta, [E] is an $n_{TB} \times n_{TB}$ square matrix containing columns $\{Z\}_1$, $\{Z\}_2$,....., $\{Z\}_{n_{TB}}$, and [I] is an identity matrix. The superscript T in Eqs. 4.32 indicates transpose of the matrix. Eigenvalues β_i and eigenvectors $\{Z\}_i$ obtained here are analogous to α_i and the continuous functions $Z_i(z,\omega)$ presented in Chapter 3.

If surface waves are neglected, [P*] = [P] and Eq. 4.31 may be solved by disregarding the first row and the first column in each of matrices [P] and [Q]. Thus, the number of eigenvalues or eigenvectors is reduced to n_{TB}-1. Furthermore, the eigenvalues and the eigenvectors are no longer frequency dependent.

With the known values of β_i, the second of Eqs. 4.21 becomes

$$r^2 \frac{R''}{R} + r \frac{R'}{R} + \lambda_i^2 r^2 = -\frac{\Theta''}{\Theta} = \text{constant} \tag{4.33}$$

Reproduced with permission of the copyright owner. Further reproduction prohibited without permission.

where

$$\lambda_i^2 = \beta_i + \frac{\omega^2}{c^2} \quad .$$

As stated earlier, the circumferential distribution of the hydrodynamic pressure is known, i.e. Θ is known; thus, the constant of separation in Eq. 4.33 can be found.

4.4.1 Horizontal and Angular Excitations

In the case of horizontal excitation or angular excitation, the hydrodynamic pressure is

$$\bar{p}(r,\theta,z,\omega) = \bar{p}(r,0,z,\omega)\cos\theta = \tilde{p}(r,z,\omega)\cos\theta \qquad (4.34)$$

where $\tilde{p}(r,z,\omega)$ is the complex frequency dependent pressure at $\theta=0$. Hence, Θ in this case is

$$\Theta(\theta) = \cos\theta \qquad (4.35)$$

Substituting Eq. 4.35 into Eq. 4.33 gives

$$r^2R'' + rR' + (\lambda_i^2 r^2 - 1)R = 0 \qquad (4.36)$$

which is a Bessel equation of order one. Using the radiation condition that $\bar{p}$ decays with increasing values of r and that the pressure wave is outgoing, the solution of Eq. 4.36 is

$$\left.\begin{aligned} R_i &= H_1^{(2)}(\lambda_i r) \quad \text{for } \lambda_i^2>0 \\ R_i &= K_1\left(\sqrt{|\lambda_i^2|}\,r\right) \quad \text{for } \lambda_i^2<0 \end{aligned}\right\} \qquad (4.37)$$

where $H_i^{(2)}$ and K_1 are, respectively, the Hankel and the modified Bessel functions of second kind and of order one.

Equation 4.20 can now be written in the form

Reproduced with permission of the copyright owner. Further reproduction prohibited without permission.

$$\bar{p}(r,\theta,z,\omega) = \sum_{i=1}^{n_{TB}} b_i R_i \cos\theta \langle \hat{N} \rangle \{Z\}_i \tag{4.38}$$

where b_i are constants to be determined. Equation 4.38 can be written in the equivalent form

$$\bar{p}(r,\theta,z,\omega) = \langle \hat{N} \rangle \cos\theta \, [E][R]\{b\} \tag{4.39}$$

where [R] is an $n_{TB} \times n_{TB}$ diagonal matrix whose elements on the i^{th} row are R_i, $\{b\}$ is a column vector whose elements on the i^{th} row are b_1.

It should be emphasized here that $\bar{p}$ in Eq. 4.39 is the pressure outside the transmitting boundary which can be interpolated over the fluid layers. If $\{\bar{p}_B\}$ is used to represent a vector of the pressure values at the interlayers at $\theta=0°$, then, from Eq. 4.39,

$$\{\bar{p}_B\} = [E][R]\{b\} \tag{4.40}$$

In this equation, $\{\bar{p}_B\}$ is a continuous function of r.

By evaluating Eq. 4.40 at $r=r_b$ and then pre-multiply both sides by $[E]^T[Q]$, one obtains

$$[E]^T[Q]\{\bar{p}_B\}_{r=r_b} = [E]^T[Q][E][R]_{r=r_b}\{b\}$$

Recalling that $[E]^T[Q][E] = [I]$, this equation can be written in the form

$$\{b\} = [R]^{-1}_{r=r_b}[E]^T[Q]\{\bar{p}_B\}_{r=r_b} \tag{4.41}$$

Substituting $\{b\}$ from Eq. 4.41 into Eq. 4.39, the pressure outside the transmitting boundary is expressed in terms of discrete values of pressure at nodes on the boundary, $\{\bar{p}_B\}_{r=r_b}$. It is reminded however

Reproduced with permission of the copyright owner. Further reproduction prohibited without permission.

that our goal is to express the acceleration function of fluid particles or the normal derivative of the pressure in terms of nodal pressures at the boundary. With this in mind, differentiate Eq. 4.39 with respect to r and set $r=r_b$ to obtain

$$\left.\frac{\partial \bar{p}}{\partial r}\right|_{r=r_b} = \langle\hat{N}\rangle\cos\theta[E][R]_{r=r_b}[R]^{-1}_{r=r_b}[E]^T[Q]\{\bar{p}_B\}_{r=r_b} \tag{4.42}$$

Using the transmitting boundary condition

$$\left.\frac{\partial \bar{p}}{\partial r}\right|_{r=r_b} = -\frac{w}{g}\bar{a}_r(r_b,\theta,z,\omega) \quad ,$$

yields

$$-\frac{w}{g}\bar{a}_r(r_b,\theta,z,\omega) = \cos\theta\langle\hat{N}\rangle[E][\frac{R'}{R}]_{r=r_b}[E]^T[Q]\{\bar{p}_B\}_{r=r_b}$$

or

$$-\frac{w}{g}\bar{a}_r(r_b,\theta,z,\omega) = \langle T^B\rangle\{\bar{p}_B\}_{r=r_b} \tag{4.43}$$

where

$$\langle T^B\rangle = \cos\theta\langle\hat{N}\rangle[E][\frac{R'}{R}]_{r=r_b}[E]^T[Q] \tag{4.44}$$

As discussed earlier, [E] is independent of the excitation frequency if the surface waves are neglected. However, $[\frac{R'}{R}]_{r=r_b}$ is frequency dependent if the compressibility of fluid is included. Hence, $\langle T^B\rangle$ is generally frequency dependent except when both surface waves and compressibility of fluid are neglected.

Equation 4.43 may be rewritten to include all nodes of Fig. 4.1 giving

$$-\frac{w}{g}\bar{a}_r(r_b,\theta,z,\omega) = \langle T\rangle\{\bar{p}\} \tag{4.45}$$

Reproduced with permission of the copyright owner. Further reproduction prohibited without permission.

where elements T_i of the row matrix $\langle T \rangle$ vanish if i are not the nodes on the transmitting boundary. The other T_m are essentially T_j^B where both correspond to the same nodes on the boundary. That is, $T_m = T_j^B$, if node m in Fig. 4.1 is node j in Fig. 4.2.

4.4.2 Vertical Excitation

In the vertical case, both the excitation and the pressure are axisymmetric. Hence

$$\bar{p}(r,\theta,z,\omega) = \bar{p}(r,0,z,\omega) = \overset{\circ}{\bar{p}}(r,z,\omega) \tag{4.46}$$

and

$$\Theta(\theta) = \text{constant} \tag{4.47}$$

Thus, Eq. 4.33 becomes

$$r^2R'' + rR' + (\lambda_i^2 r^2)R = 0 \tag{4.48}$$

The solution to the above Bessel equation of order zero, after the radiation condition is applied, is

$$\left.\begin{aligned} R_i &= H_o^{(2)}(\lambda_i r) \quad \text{for } \lambda_i^2 > 0 \\ R_i &= K_o\left(\sqrt{|\lambda_i^2|}\, r\right) \quad \text{for } \lambda_i^2 < 0 \end{aligned}\right\} \tag{4.49}$$

where $H_o^{(2)}$ and K_o are, respectively, the Hankel and the modified Bessel functions of order zero.

Similarly, the acceleration function for the vertical excitation case is given by

$$-\frac{w}{g}\bar{a}_r(r_b,\theta,z,\omega) = \langle T^B \rangle \{\bar{p}_B\}_{r=r_b} \tag{4.50}$$

where

Reproduced with permission of the copyright owner. Further reproduction prohibited without permission.

$$\langle T^B \rangle = \langle \hat{N} \rangle [E] [\frac{\hat{R}'}{R}]_{r=r_b} [E]^T [Q] \tag{4.51}$$

The differences between Eqs. 4.51 and 4.44 are that $\cos\theta$ is absent in Eq. 4.51 and $[\frac{R}{R}]_{r=r_b}$ of Eq. 4.51 are expressed in terms of $H_0^{(2)}$ and K_0 instead of $H_1^{(2)}$ and K_1.

Again, Eq. 4.50 may be written as

$$-\frac{w}{g} \bar{a}_r(r_b,\theta,z,\omega) = \langle T \rangle \{\bar{p}\} \tag{4.52}$$

4.5 Added Mass Representation

In Eq. 4.12, $[F^B]$ is, in general, a complex frequency dependent matrix derived from the condition at the transmitting boundary. The complexity comes from the Hankel functions $H_1^{(2)}$ or $H_0^{(2)}$.

Since matrix $[F^B]$ is frequency dependent, it is appropriate and convenient to solve Eq. 4.12 in the frequency domain. Fourier transforming Eq. 4.12 gives

$$([F] - [F^B] - \omega^2([F^C] + [F^S]))\{\bar{p}\} = \{\bar{D}\} \tag{4.53}$$

where $\{\bar{p}(\omega)\}$ is a vector of nodal pressures in the frequency domain and $\{\bar{D}(\omega)\}$ is the Fourier transform of $\{D(t)\}$. The components $\bar{D}_i(\omega)$ and given by

$$\bar{D}_i(\omega) = \int_{IF} -\frac{w}{g} N_i^G(r,\theta,z,) \bar{a}_n(r,\theta,z,\omega)\, dS \tag{4.54}$$

where $\bar{a}_n(r,\theta,z,\omega)$ is the Fourier transform of $a_n(r,\theta,z,t)$. The right hand side of Eq. 4.54 is integrated over the surface area of the interface between the body and the fluid.

Equation 4.53 can be solved for $\{\bar{p}\}$. The continuous function of the pressure $\bar{p}$ can then be obtained as

$$\bar{p}(r,\theta,z,\omega) = \langle N^G(r,\theta,z) \rangle \{\bar{p}\} \tag{4.55}$$

Reproduced with permission of the copyright owner. Further reproduction prohibited without permission.

Thus, the horizontal force, the moment about the center of gravity, and the vertical force acting on the body in their negative directions are

$$\left.\begin{aligned} \bar{f}_x(\omega) &= \int_{IF} \bar{p}\cos\theta\, \bar{n}_r\, dS \\ \bar{f}_\phi(\omega) &= \int_{IF} [-\bar{p}\cos\theta\, \bar{n}_r(z-\bar{z}) + \bar{p}\, \bar{n}_z\, r\cos\theta]\, dS \\ \bar{f}_z(\omega) &= \int \bar{p}\, \bar{n}_z\, dS \end{aligned}\right\} \qquad (4.56)$$

respectively, where $\bar{n}_r$ and $\bar{n}_z$ are the direction cosines of the outward normal unit vector on the body surface in the r and z directions, respectively.

As presented in Chapter 2, the added mass is essentially a force in the opposite direction to the movement of the body due to a unit acceleration. For example, the added mass $\bar{f}_{\phi x}(\omega)$ can be determined by finding a force in the ϕ direction due to a unit acceleration in the x direction, i.e. $\ddot{\bar{x}}(\omega) = 1$, $\ddot{\bar{\phi}}(\omega) = \ddot{\bar{z}}(\omega) = 0$. Hence, if $\bar{p}_x$, $\bar{p}_\phi$ and $\bar{p}_z$, the pressure distributions due to unit of accelerations $\ddot{\bar{x}}(\omega)$, $\ddot{\bar{\phi}}(\omega)$, $\ddot{\bar{z}}(\omega)$, respectively, are known then the added masses $\bar{f}_{ij}(\omega)$ can be found.

Functions $\bar{p}_x$ and $\bar{p}_\phi$ can be written as

$$\bar{p}_i(r,\theta,z,\omega) = \tilde{\bar{p}}_i(r,z,\omega)\cos\theta = \langle N(r,z)\rangle\cos\theta\{\bar{p}_i\},\ i=x,\phi \qquad (4.57)$$

and $\bar{p}_z$ can be written as

$$\bar{p}_z(r,\theta,z,\omega) = \bar{p}_z(r,z,\omega) = \langle N(r,z)\rangle\{\bar{p}_z\} \qquad (4.58)$$

where

$$\langle N(r,z)\rangle = \langle N^G(r,0,z)\rangle.$$

Reproduced with permission of the copyright owner. Further reproduction prohibited without permission.

Using the relationships given by Eqs. 4.56-4.58, functions $\bar{f}_{ij}(\omega)$ can be expressed as

$$\left.\begin{aligned}
\bar{f}_{xx}(\omega) &= \pi\{D_o^H\}^T\{\bar{p}_x\} \\
\bar{f}_{\phi x}(\omega) &= \pi(-\{D_o^z\}^T + \bar{z}\{D_o^H\}^T + \{D_o^r\}^T)\{\bar{p}_x\} \\
\bar{f}_{\phi\phi}(\omega) &= \pi(-\{D_o^z\}^T + \bar{z}\{D_o^H\}^T + \{D_o^r\}^T)\{\bar{p}_\phi\} \\
\bar{f}_{x\phi}(\omega) &= \pi\{D_o^H\}^T\{\bar{p}_\phi\} \\
\bar{f}_{zz}(\omega) &= 2\pi\{D_o^V\}^T\{\bar{p}_z\}
\end{aligned}\right\} \qquad (4.59)$$

where

$$\left.\begin{aligned}
\{D_o^H\}^T &= \int_o^{H_s} \langle N\rangle r\,dz \\
\{D_o^z\}^T &= \int_o^{H_s} \langle N\rangle z r\,dz \\
\{D_o^r\}^T &= \int_o^{r_o} \langle N\rangle r^2\,dr \\
\{D_o^V\}^T &= \int_o^{r_o} \langle N\rangle r\,dr
\end{aligned}\right\} \qquad (4.60)$$

The added masses are the real parts of $\bar{f}_{ij}(\omega)$. The imaginary parts are associated with the hydrodynamic damping terms as shown in Eqs. 2.9-2.10.

Reproduced with permission of the copyright owner. Further reproduction prohibited without permission.

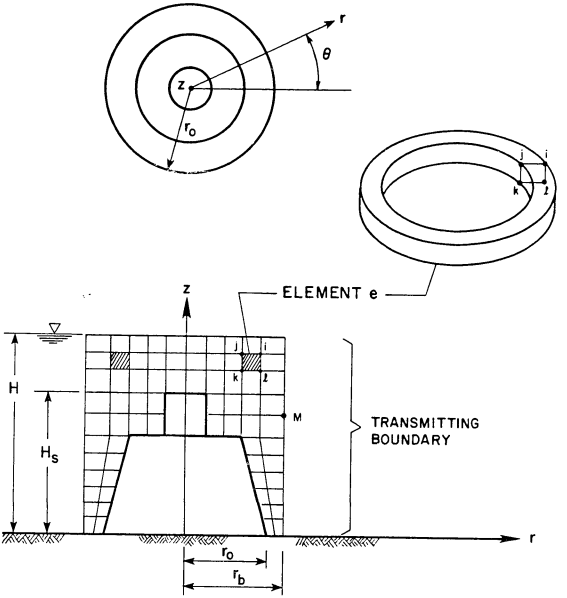

FIG. 4.1 FINITE ELEMENT DISCRETIZATION OF FLUID DOMAIN

Reproduced with permission of the copyright owner. Further reproduction prohibited without permission.

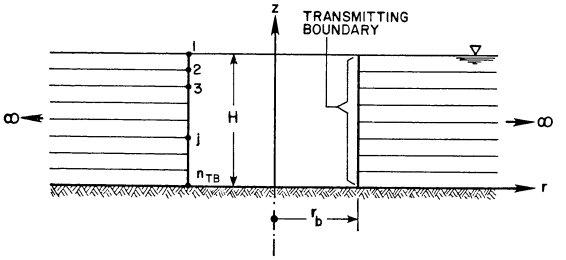

FIG. 4.2 FLUID DOMAIN OUTSIDE TRANSMITTING BOUNDARY

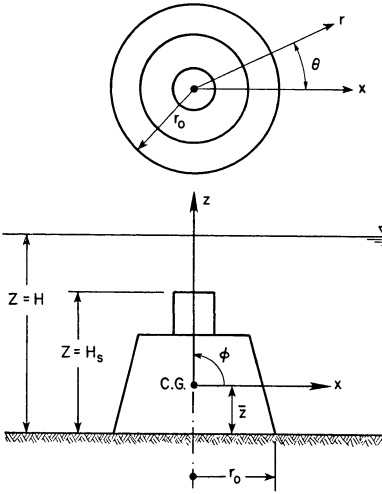

FIG. 4.3 STRUCTURE IN FLUID

Reproduced with permission of the copyright owner. Further reproduction prohibited without permission.

5. COMPARISON WITH EXPERIMENTAL RESULTS

In this chapter, the results of the finite element analysis of the hydrodynamic pressure are compared with those of the experiments by Byrd[14] and with those obtained by Garrison (as presented in the work of Byrd). First, the coefficients of added mass are compared. Then, the hydrodynamic pressure at each pressure gauge is compared. Finally, the errors of the numerical results are discussed.

5.1 Added Mass and Hydrodynamic Damping

In the experimental study, a 1 to 100 scale model of a circular cylindrical body was used. Four levels of water were used in the experimental investigation. The finite element mesh used in the numerical analysis of hydrodynamic pressure against the model is shown in Fig. 5.1.

As stated earlier, the coefficients in Eqs. 2.9-2.10 are of interest. These coefficients can be determined by exciting the body with harmonic motion with the foundation fixed. The body is excited by unit amplitude accelerations in the horizontal, vertical, and rotational directions. Typical pressure distributions on the body obtained by the finite element procedure for all three cases of excitation are shown in Figs. 5.2a-5.2c. Using Eq. 4.59, the real parts on the left hand side are the added masses. The hydrodynamic damping terms are obtained by multiplying the imaginary parts by $-\omega$; see Eqs. 2.10.

The added masses can be normalized to give dimensionless quantities as follows:

Reproduced with permission of the copyright owner. Further reproduction prohibited without permission.

$$
\begin{aligned}
C^M_{xx}(\omega) &= \bar{f}^R_{xx}(\omega)/\rho V \\
C^M_{zz}(\omega) &= \bar{f}^R_{zz}(\omega)/\rho V \\
C^M_{\phi\phi}(\omega) &= \bar{f}^R_{\phi\phi}(\omega)/\rho V R_g^2 \\
C^M_{\phi x}(\omega) &= \bar{f}^R_{\phi x}(\omega)/\rho V R_g \\
C^M_{x\phi}(\omega) &= \bar{f}^R_{x\phi}(\omega)/\rho V R_g
\end{aligned}
\tag{5.1}
$$

where ρ is the mass density of water, V is the volume of water displaced by the body, and R_g is the radius of gyration of the displaced volume of water about its center of gravity.

The hydrodynamic damping terms can also be normalized as follows:

$$
\begin{aligned}
C^D_{xx}(\omega) &= -\bar{f}^I_{xx}(\omega)/\rho V \\
C^D_{zz}(\omega) &= -\bar{f}^I_{zz}(\omega)/\rho V \\
C^D_{\phi\phi}(\omega) &= -\bar{f}^I_{\phi\phi}(\omega)/\rho V R_g^2 \\
C^D_{\phi x}(\omega) &= -\bar{f}^I_{\phi x}(\omega)/\rho V R_g \\
C^D_{x\phi}(\omega) &= -\bar{f}^I_{x\phi}(\omega)/\rho V R_g
\end{aligned}
\tag{5.2}
$$

Since $\bar{f}_{\phi x} = \bar{f}_{x\phi}$, $C^M_{\phi x} = C^M_{x\phi}$ and $C^D_{\phi x} = C^D_{x\phi}$.

It should be noted that $C^M_{\phi\phi}$, $C^M_{\phi x}$, $C^D_{\phi\phi}$, and $C^D_{\phi x}$ are defined the same way as those by Byrd[14]. These coefficients are associated with the center of gravity of the body. They may be defined differently such that they are associated with the overturning moment about the base of the body instead of about the center of gravity.

The dimensionless added mass coefficients C^M_{ij} are compared with

Reproduced with permission of the copyright owner. Further reproduction prohibited without permission.

the average values obtained from experiment for different ratios of depth of water to height of the body (H/H_s) as shown in Figs. 5.3-5.10. These added mass coefficients are plotted versus the dimensionless frequency parameter $\omega^2\sqrt{DH_s}/g$, in which D is the diameter of the cylindrical body, H_s is the height of the body, and g is the acceleration of gravity. The analytical horizontal and vertical added mass coefficients agree well with their experimental values. For the rotational and coupled added mass coefficients, the discrepancies between the analytical and experimental coefficients are larger for small ratios of H/H_s. For $H/H_s = 2.5$, the added mass coefficients are also compared with those obtained by Garrison.

The effects of surface waves generated by the oscillating body and the compressibility of water are also studied. Surface waves show an effect at low frequency only, while the compressibility does not show any significant effects for the small depths of water used and for the frequency range considered. However, as shown later, compressibility is rather important for the larger depths of water which exist for prototype structures.

The dimensionless hydrodynamic damping coefficients C^D_{ij} are also plotted versus the dimensionless frequency parameter as shown in Figs. 5.11-5.12. The experimental values of these coefficients are not available. It should be noted that these coefficients do not vanish in the low frequency range when surface waves are considered. They are primarily positive in value; thus, the coefficients C^a_{ij} of matrix $[C^a]$ in Eq. 2.8 are positive since they are obtained by multiplying $\bar{f}^I_{ij}$ by $-\omega$. The terms $\bar{f}^I_{ij}$ are related to C^D_{ij} as shown in Eqs. 5.2.

Reproduced with permission of the copyright owner. Further reproduction prohibited without permission.

This condition implies that the damping of the dynamic system of Fig. 2.1 is increased. It does not imply that the modal damping ratio of each mode of the three degrees of freedom system is increased. The reason why the modal ratio may or may not be increased is due to the fact that the new mass matrix $[M] + [M^a]$ is also increased. Thus, the mode shapes and their corresponding frequencies are also changed.

As mentioned earlier, the compressibility of water is important for larger depths of water such as in the prototype case. The effects of the compressibility can be seen in both the added mass and hydrodyanmic damping coefficients at high frequency. The analytical results of these coefficients for a prototype of scale 100:1 are shown in Figs. 5.13-5.22.

The reason that compressibility has an effect on the coefficients at some frequencies can be explained by first looking at $R_m'(r_o,\omega)$ in Eq. 3.16. Note that the R_m quantities expressed in terms of $\lambda_m r$ as shown in Eqs. 3.12; thus,

$$R_m' = \frac{dR_m}{dr} = \lambda_m \frac{dR_m}{d(\lambda_m r)} \tag{5.3}$$

When one of the parameters λ_m approaches zero, say $\lambda_i \to 0$, the corresponding b_i as shown in Eq. 3.16 is large. Hence, pressure $\bar{p}$ of Eq. 3.10 is large. When $\lambda_i = 0$, pressure $\bar{p}$ is still bounded because $R_i = \frac{1}{r}$ instead of the quantities R_i given by Eqs. 3.12. From the second or third of Eqs. 3.15, the frequencies corresponding to $\lambda_m = 0$ are

$$\omega_m = \alpha_m c \quad , \quad m=1,2,.....\infty \tag{5.4}$$

The approximate parameters α_m, obtained when surface waves are neglected,

Reproduced with permission of the copyright owner. Further reproduction prohibited without permission.

can be substituted into Eq. 5.4 giving

$$\omega_m = \frac{(2m-1)\pi}{2H} c \quad , \quad m=1,2,.....\infty \tag{5.5}$$

If the excitation frequency ω is greater than ω_1, i.e. $k \geq 1$, hydrodynamic damping due to water compressibility is present. This is due to the fact that the equations

$$R_m = H_1^{(2)}(\lambda_m r) \quad , \quad m=1,2,.....k$$

contain complex functions. The presence of hydrodynamic damping and the presence of peaks in the added mass coefficients for the prototype can be seen at high frequency because the water depth H is 100 times that of the model. This large water depth brings down the first resonant frequency ω_1 to within the frequency range plotted while the velocity of sound in water, c, has the same value for both the prototype and model structures.

The above reasoning can also be applied to the axisymmetric excitation case. In this case, functions R_m are given by Eqs. 3.19. Furthermore, at $\lambda_i=0$, pressure $\bar{p}$ of Eq. 3.18 for the axisymmetric excitation case is unbounded.

5.2 Hydrodynamic Pressures

In the experiment, eight pressure gauges were used to record hydrodynamic pressures at specified locations on the model. Since there were only eight pressure gauges available, they were installed on the side of the model for some tests and on the top of the model for the other tests; see Fig. 5.23. The model was mounted on a system of load cells which were attached to the shaking table as shown in Fig. 5.24. The model in water was then excited through the shaking table.

Reproduced with permission of the copyright owner. Further reproduction prohibited without permission.

In this section, pressure amplitudes of the gauges are compared with the results from the finite element analysis for horizontal and vertical harmonic oscillations.

5.2.1 Horizontal Harmonic Oscillations

The vertical, horizontal, and rotational degrees of freedom of the planar vibration of the model in air were designed to be uncoupled, i.e., the center of gravity of the model was located at its elastic center. In water, however, the horizontal and the rotational degrees of freedom are coupled. This is due to the fact that the horizontal water resistant force does not act on the elastic center. Thus, there is a rotation even though the model is excited purely in the horizontal direction.

The amplitudes of these harmonic rotational accelerations due to horizontal excitations can be obtained from data analysis. These are found to be small compared with the amplitudes of the total horizontal accelerations. Thus, the contribution of these rotations to the hydrodynamic pressures on the model can be neglected.

As discussed earlier in Section 2.2, forces $\bar{f}_{ix}$ due to a unit amplitude of relative horizontal acceleration of the model are considered the same as forces $\bar{f}^{g}_{ix}$ due to a unit amplitude of horizontal ground acceleration when the model is fixed to the table; see Eqs. 2.6 and 2.7. This is due to the fact that the table surface is flat and the viscosity of the water is neglected. Thus, the sum of the pressure distributions due to $\ddot{\bar{x}}$ and $\ddot{\bar{x}}_g$ is essentially the pressure distribution due to the total amplitude $\ddot{\bar{x}}^t$.

The amplitudes of the hydrodynamic pressures of the gauges are normalized, for sake of comparison, by dividing the total amplitudes

Reproduced with permission of the copyright owner. Further reproduction prohibited without permission.

by $\ddot{\bar{x}}^t/g$. The normalized pressures are then compared with the analytical results by plotting them as a function of frequency of excitation. Figures 5.25-5.28 show the comparison for the pressures on the side of the model (Gauges S1-S8) for different ratios of H/H_S. The comparison for pressures on the top of the model are shown in Fig. 5.29. In this latter comparison, only pressures from four gauges (Gauges T3, T5, T6 and T8) are presented because the readings from the other four gauges were too low to be used for comparison purposes.

5.2.2 Vertical Harmonic Oscillations

When excited vertically, the total vertical motion of the model can be considered as a superposition of the relative motion of the model with respect to the table plus the table motion; see Fig. 5.30.

The problems of Figs. 5.30a and 5.30b can be solved for $\bar{f}_{zz}$ and $\bar{f}^g_{zz}$ of Eq. 2.7, respectively. The former can be solved using the finite element procedure previously described; however, some modification of that procedure is required for the latter.

The problem of Fig. 5.30b can be solved by the finite element method using a transmitting boundary that truncates the domain of water within the radius r_b and a modification to the procedure to account for the moving floor outside that boundary. The problem may be separated into two parts. First, only the region inside the transmitting boundary is vertically excited as shown in Fig. 5.31a. The second part is shown in Fig. 5.31b where the floor region outside the transmitting boundary is excited.

The solution of the problem shown in Fig. 5.31a can be obtained by the finite element procedure by treating the floor inside the transmitting boundary as an interface in evaluating loading vector $\{\bar{D}\}$ of

Reproduced with permission of the copyright owner. Further reproduction prohibited without permission.

Eq. 4.53. The problem of Fig. 5.31b may be thought of as a superposition of the problems shown in Figs. 5.32a and 5.32b. In Fig. 5.32a, a fictitious cylindrical wall is assumed to be present at the transmitting boundary, i.e., water particles are not permitted to move across the wall when the floor outside the wall is excited. This fictitious wall is removed in Fig. 5.32b to let water flow across the transmitting boundary.

Let a_1, a_2, and a_3 be the radial accelerations of water particles at the transmitting boundary for the cases shown in Figs. 5.31a, 5.32a, and 5.32b, respectively. Thus, the total radial acceleration at radius $r=r_b$ for the problem shown in Fig. 5.30b is $a_1+a_2+a_3$. If only the water domain inside radius r_b is considered as shown in Fig. 5.33, the boundary condition at the transmitting boundary can be prescribed as $a_1+a_2+a_3$. By including a_2+a_3, the contribution of the floor acceleration outside the transmitting boundary is included.

Let p_1, p_2, and p_3 be the hydrodynamic pressures corresponding to a_1, a_2, and a_3 at the transmitting boundary. Then, as discussed in Chapter 3 and Section 4.4, accelerations a_i can be expressed in terms of pressures p_i as

$$a_i = T(p_i) \quad , \quad i=1,2,3 \tag{5.6}$$

where T is a linear transformation operator. Using this relationship and noting that there is no acceleration across the fictitious wall, i.e. $a_2=0$, the total radial acceleration at the transmitting boundary becomes

$$a_1 + a_3 = T(p_1) + T(p_3) = T(p_1 + p_3) \tag{5.7}$$

Reproduced with permission of the copyright owner. Further reproduction prohibited without permission.

However, if p is the hydrodynamic pressure at radius r=r_b of the problem in Fig. 5.30b, then

$$p = p_1 + p_2 + p_3 \tag{5.8}$$

Using this relation, Eq. 5.7 becomes

$$a_1 + a_3 = T(p - p_2) \tag{5.9}$$

The problem of Fig. 5.30b can now be solved using a truncated water domain and the modified condition of Eq. 5.9 at the transmitting boundary; see Fig. 5.33. Thus, Eq. 4.12 is modified to be

$$[F]\{p\} + [F^C]\{\ddot{p}\} = \{D\} - [F^S]\{\ddot{p}\} + [F^B](\{p\} - \{p_2\})$$

or

$$([F] - [F^B])\{p\} + ([F^C] + [F^S])\{\ddot{p}\} = \{D\} - [F^B]\{p_2\} \tag{5.10}$$

where $\{p_2\}$ is a vector of nodal pressures at the transmitting boundary of the problem in Fig. 5.32a. In the frequency domain, Eq. 5.10 becomes

$$([F] - [F^B] - \omega^2[F^C] - \omega^2[F^S])\{\bar{p}\} = \{\bar{D}\} - [F^B]\{\bar{p}_2\} \tag{5.11}$$

Continuum solution $\bar{p}_2$ corresponding to discrete solution $\{\bar{p}_2\}$ can be obtained by solving the problem of Fig. 5.32a using the standard method of separation of variables. It can be expressed as

$$\bar{p}_2(r_b,\theta,z,\omega) = -\frac{w}{g}\frac{1}{\alpha}\frac{\alpha\cos(H-z) - \frac{\omega^2}{g}\sin(H-z)}{\alpha\sin\alpha H + \frac{\omega^2}{g}\cos\alpha H}\cdot\bar{z}_g \tag{5.12}$$

where $\alpha = \frac{\omega}{c}$.

Reproduced with permission of the copyright owner. Further reproduction prohibited without permission.

It should be noted that function $\bar{p}_2$ is independent of r_b and θ. Actually the pressure distribution outside the wall in Fig. 5.32a is independent of variables r and θ. If the compressibility of water and the surface waves are neglected, the general pressure distribution of Fig. 5.32a becomes

$$\bar{p}_2(r,\theta,z,\omega) = \frac{w}{g}(H-z)\,\ddot{\bar{z}}_g \tag{5.13}$$

In this equation, $\bar{p}_2$ is similar to the hydrostatic pressure except it is multiplied by the ground acceleration amplitude $\ddot{\bar{z}}_g$.

Discrete vector $\{\bar{p}_2\}$ can also be solved directly. Since it is known that $\bar{p}_2(r,\theta,z,\omega)$ is independent of variables r and θ, the governing equation for $\bar{p}_2(r,\theta,z,\omega)$ becomes

$$\frac{d^2\bar{p}_2}{dz^2} = -\frac{\omega^2}{c^2}\bar{p}_2 \tag{5.14}$$

with the boundary conditions

$$\left.\frac{d\bar{p}_2}{dz}\right|_{z=0} = -\frac{w}{g}\ddot{\bar{z}}_g \tag{5.15}$$

and

$$\left.\frac{d\bar{p}_2}{dz}\right|_{z=H} = \frac{\omega^2}{g}\bar{p}_2\Big|_{z=H} \tag{5.16}$$

Again, the water domain outside the wall is discretized into layers and the Galerkin method is applied. The discretized problem becomes

$$([P^*] - \frac{\omega^2}{c^2}[Q])\{\bar{p}_2\} = \{\bar{D}_2\} \tag{5.17}$$

Reproduced with permission of the copyright owner. Further reproduction prohibited without permission.

where

$$\{\bar{D}_2\} = \begin{Bmatrix} 0 \\ 0 \\ \vdots \\ 0 \\ 1 \end{Bmatrix} \frac{w}{g} \ddot{\bar{z}}_g \tag{5.18}$$

Matrices [P*] and [Q] are the same as those of Eq. 4.31.

Vector $\{\bar{p}_2\}$ can be solved from Eq. 5.17 which when substituted into Eq. 5.11 allows the solution of $\{\bar{p}\}$. This vector $\{\bar{p}\}$ is the solution to the problem of Fig. 5.30b.

As shown in Figs. 5.3-5.10, the experimental added masses were obtained in a frequency range for which surface waves and water compressibility have little effect. The solution for the problem in Fig. 5.30b can then be written as

$$\bar{p}(r,\theta,z,\omega) = \frac{w}{g} (H-z) \ddot{\bar{z}}_g \tag{5.19}$$

For simplicity and sake of comparison, this solution is subtracted from the experimental pressure amplitudes of the eight gauges. The remaining amplitudes are then normalized by being divided by $\ddot{\bar{z}}/g$. These normalized amplitudes can now be compared with the analytical results obtained by solving the problem of Fig. 5.30a for $\ddot{\bar{z}} = 1$ g. The comparison of the pressure amplitudes for different ratios of H/H_s are shown in Figs. 5.34-5.37. Figures 5.34-5.36 show pressures on the top of the model (Gauges T1-T8). In this vertical excitation case, pressure gauges that are located at the same radius from the vertical axis of the model are expected to record the same amplitude. Thus, pressure amplitudes of gauges with the same radial distance are summed and averaged.

The comparison for pressures on the side of the model (Gauges S1-S8) are shown in Fig. 5.37. In this comparison the pressure

Reproduced with permission of the copyright owner. Further reproduction prohibited without permission.

amplitudes of gauges at the same level are averaged.

5.3 Analytical Errors

In the finite element analysis of the hydrodynamic pressure, a singularity of solution exists at the reentrant corner of the water domain, i.e., at the top corner of the model. The approximation of the singular solution can be improved using local mesh refinement near the singular point. Strang and Fix[16] have shown that the error due to the singularity may be greatly reduced by adding singular functions into the interpolation functions. These singular functions approximate the solution near the singular point while the conventional finite elements take care of the problem elsewhere. However, it is easier to refine the mesh than to find the singular functions and to incorporate them into the finite element solution.

In comparing the added mass coefficients, it can be seen that the mesh of Fig. 5.1 gives good results for the horizontal and vertical oscillation cases. This shows that the errors of the pressure distributions near the singular corner do not have significant effect on the horizontal and vertical total pressure forces. However, in the cases of the rotational and coupled added mass coefficients, the discrepancies between the experimental and analytical results are greater. This can be explained by the fact that the local errors near the corner are amplified by the moment arm used in the computation of the added masses.

It should also be pointed out that when solving the problem by the finite element method at high frequency, a finer mesh is needed to obtain sufficient accuracy.

Reproduced with permission of the copyright owner. Further reproduction prohibited without permission.

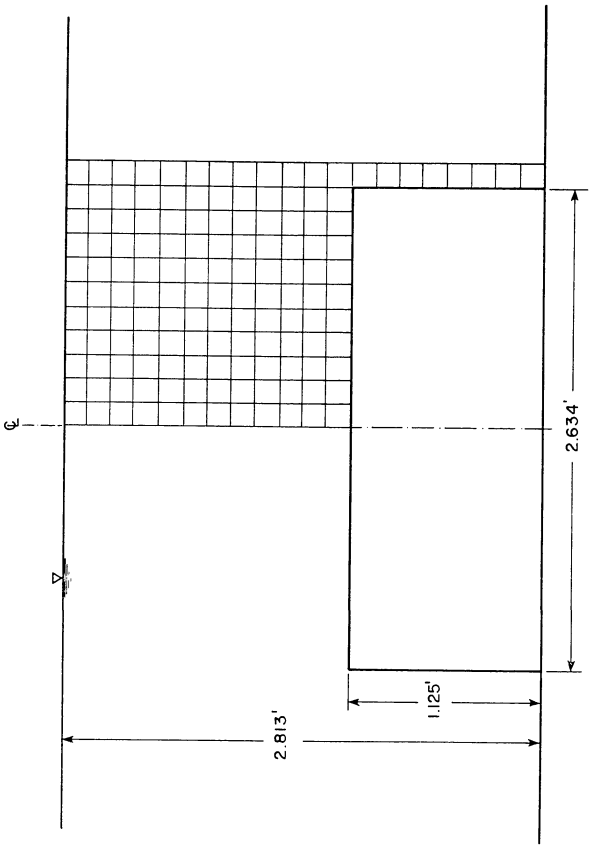

FIG. 5.1 FINITE ELEMENT MESH

Reproduced with permission of the copyright owner. Further reproduction prohibited without permission.

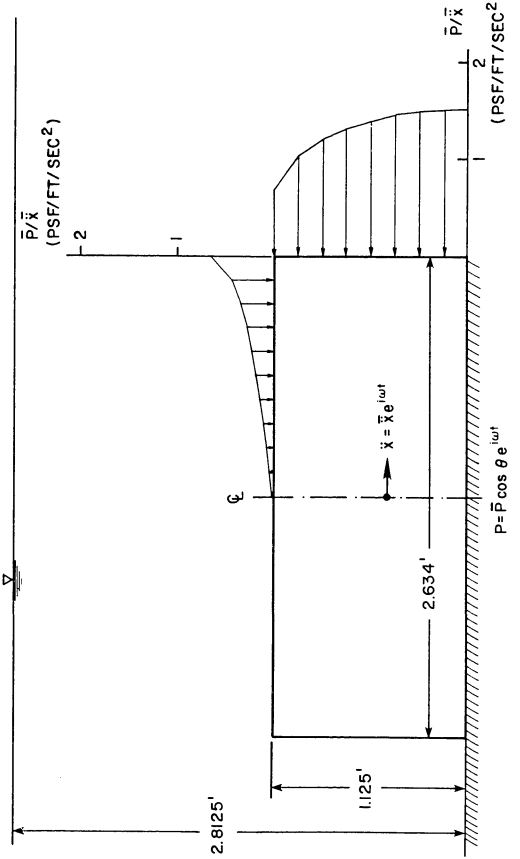

FIG. 5.2a TYPICAL AMPLITUDE OF HYDRODYNAMIC PRESSURE (REAL PART) AT $\theta = 0°$ DUE TO HORIZONTAL EXCITATION $\ddot{x} = \bar{\ddot{x}} e^{i\omega t}$

Reproduced with permission of the copyright owner. Further reproduction prohibited without permission.

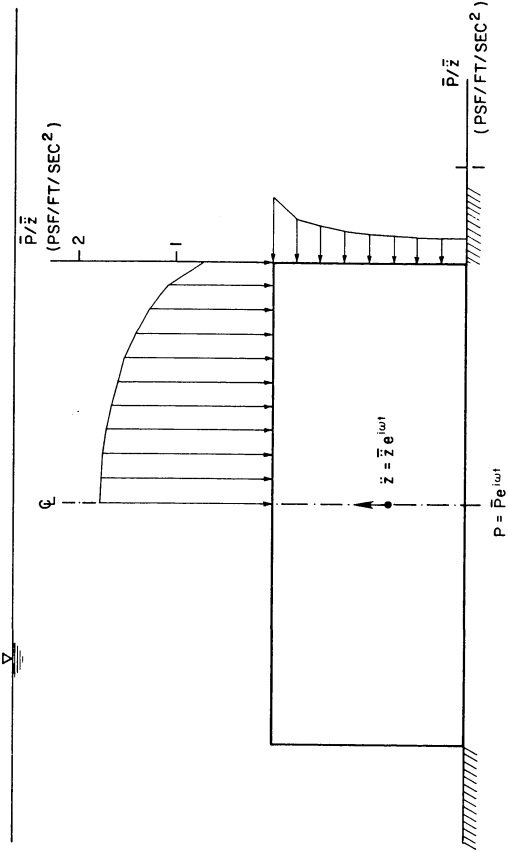

FIG. 5.2b TYPICAL AMPLITUDE OF HYDRODYNAMIC PRESSURE (REAL PART) AT ANY θ DUE TO VERTICAL EXCITATION $\ddot{z} = \ddot{\bar{z}} e^{i\omega t}$

Reproduced with permission of the copyright owner. Further reproduction prohibited without permission.

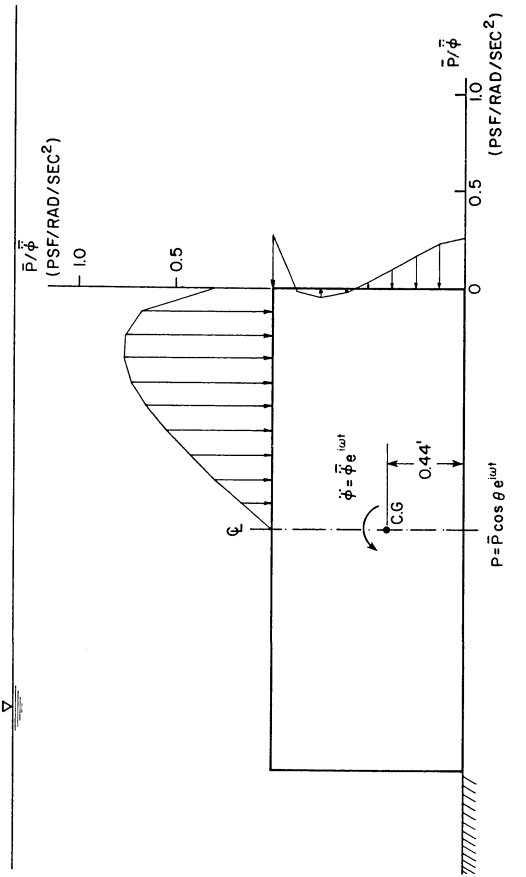

FIG. 5.2c TYPICAL AMPLITUDE OF HYDRODYNAMIC PRESSURE (REAL PART) AT $\theta = 0°$ DUE TO ROTATIONAL EXCITATION $\dot{\phi} = \bar{\phi} e^{i\omega t}$

Reproduced with permission of the copyright owner. Further reproduction prohibited without permission.

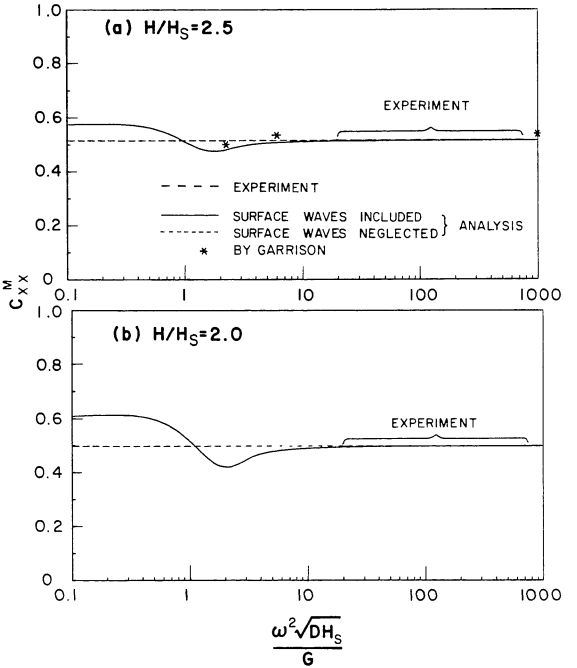

FIG. 5.3 HORIZONTAL ADDED MASS COEFFICIENTS FOR MODEL

Reproduced with permission of the copyright owner. Further reproduction prohibited without permission.

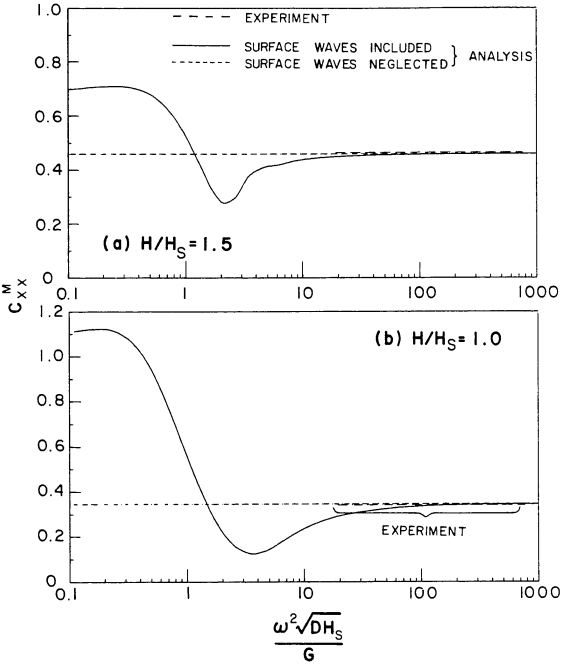

FIG. 5.4 HORIZONTAL ADDED MASS COEFFICIENTS FOR MODEL

Reproduced with permission of the copyright owner. Further reproduction prohibited without permission.

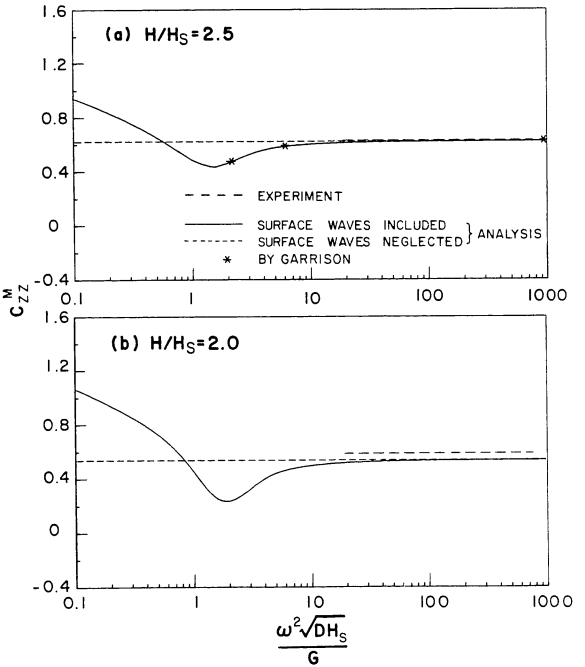

FIG. 5.5 VERTICAL ADDED MASS COEFFICIENTS FOR MODEL

Reproduced with permission of the copyright owner. Further reproduction prohibited without permission.

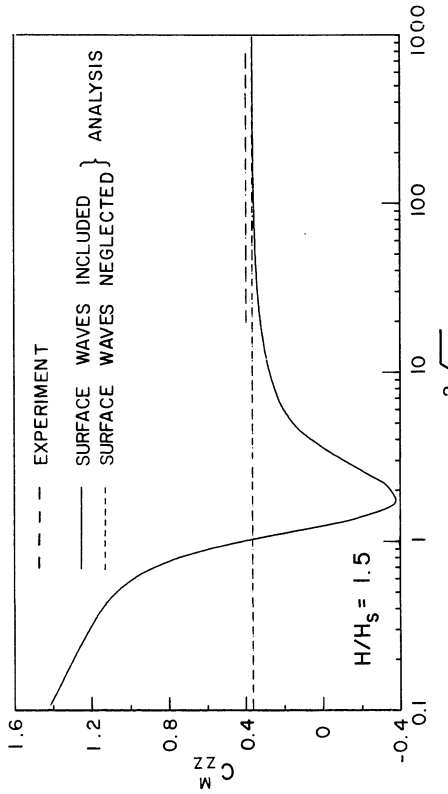

FIG. 5.6 VERTICAL ADDED MASS COEFFICIENT FOR MODEL

Reproduced with permission of the copyright owner. Further reproduction prohibited without permission.

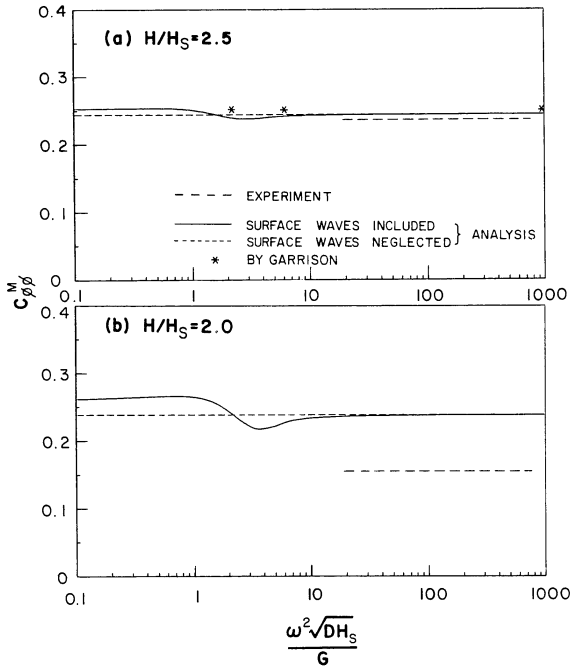

FIG. 5.7 ROTATIONAL ADDED MASS COEFFICIENTS FOR MODEL

Reproduced with permission of the copyright owner. Further reproduction prohibited without permission.

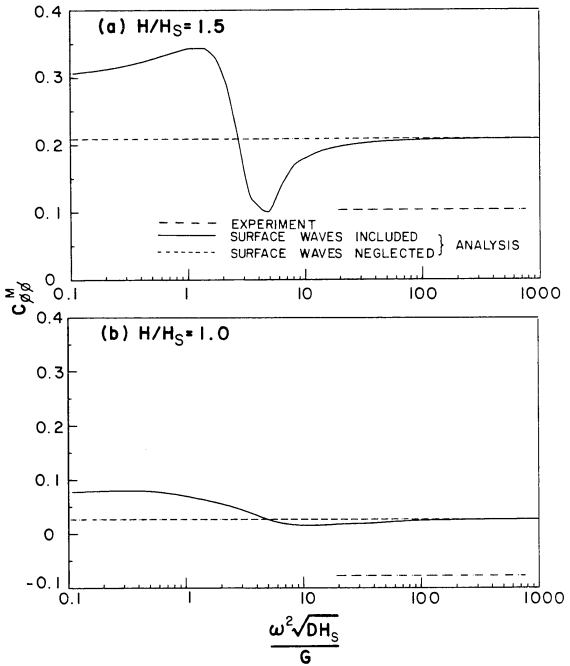

FIG. 5.8 ROTATIONAL ADDED MASS COEFFICIENTS FOR MODEL

Reproduced with permission of the copyright owner. Further reproduction prohibited without permission.

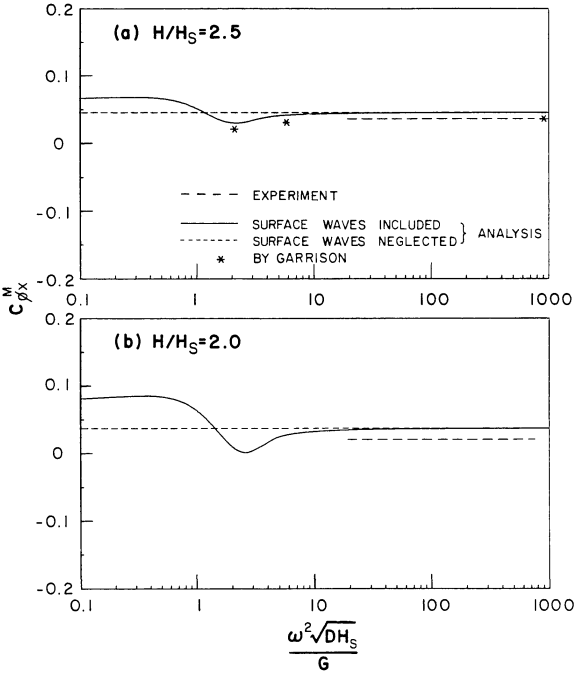

FIG. 5.9 COUPLED ADDED MASS COEFFICIENTS FOR MODEL

Reproduced with permission of the copyright owner. Further reproduction prohibited without permission.

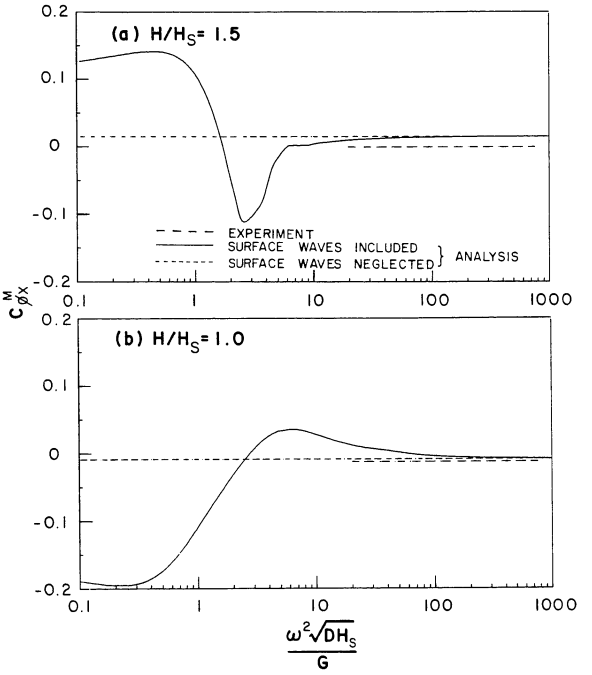

FIG. 5.10 COUPLED ADDED MASS COEFFICIENTS FOR MODEL

Reproduced with permission of the copyright owner. Further reproduction prohibited without permission.

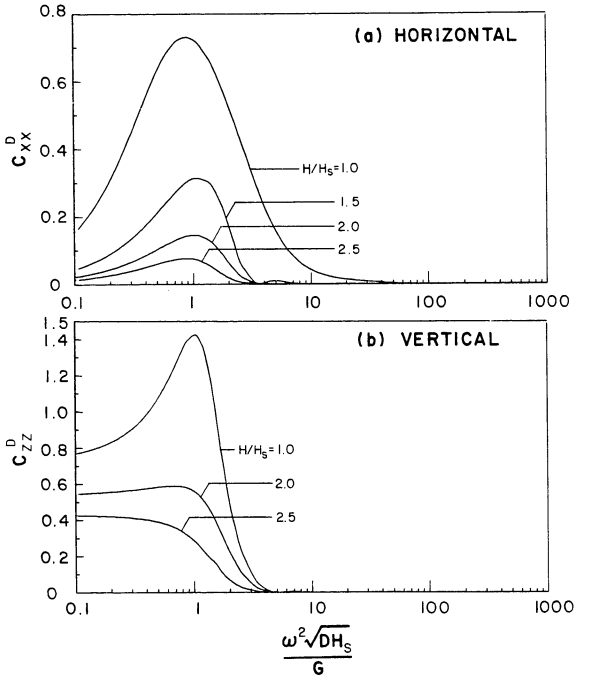

FIG. 5.11 HYDRODYNAMIC DAMPING COEFFICIENTS FOR MODEL

Reproduced with permission of the copyright owner. Further reproduction prohibited without permission.

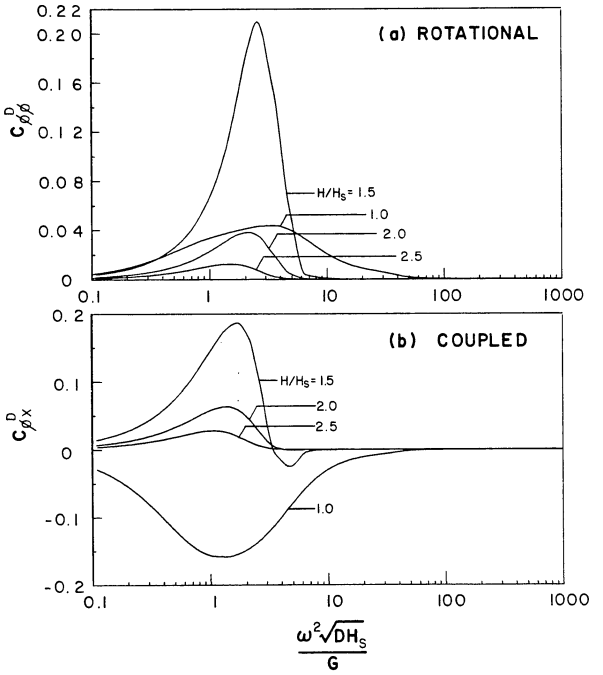

FIG. 5.12 HYDRODYNAMIC DAMPING COEFFICIENTS FOR MODEL

Reproduced with permission of the copyright owner. Further reproduction prohibited without permission.

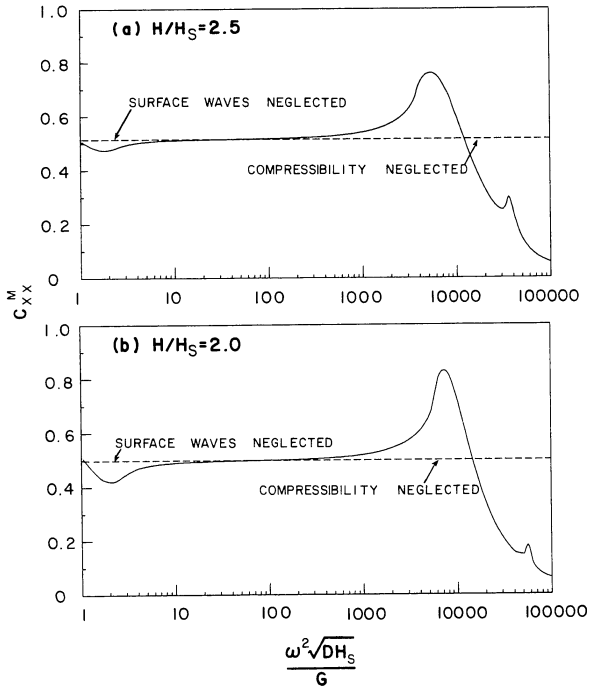

FIG. 5.13 HORIZONTAL ADDED MASS COEFFICIENTS FOR PROTOTYPE

Reproduced with permission of the copyright owner. Further reproduction prohibited without permission.

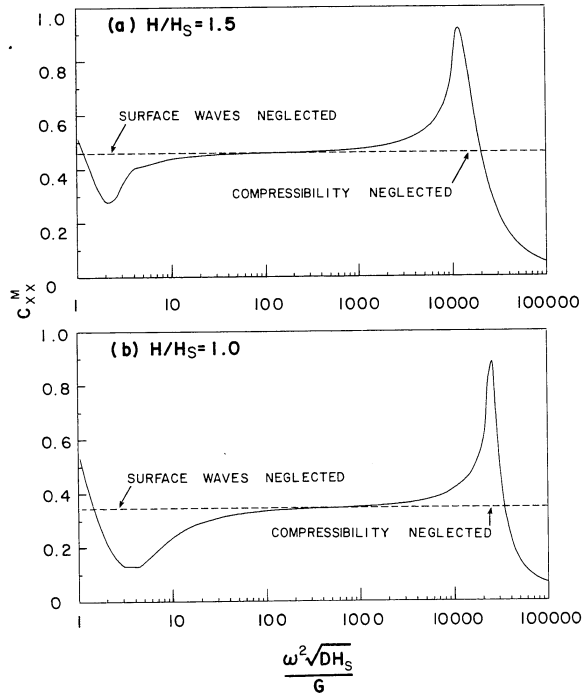

FIG. 5.14 HORIZONTAL ADDED MASS COEFFICIENTS FOR PROTOTYPE

Reproduced with permission of the copyright owner. Further reproduction prohibited without permission.

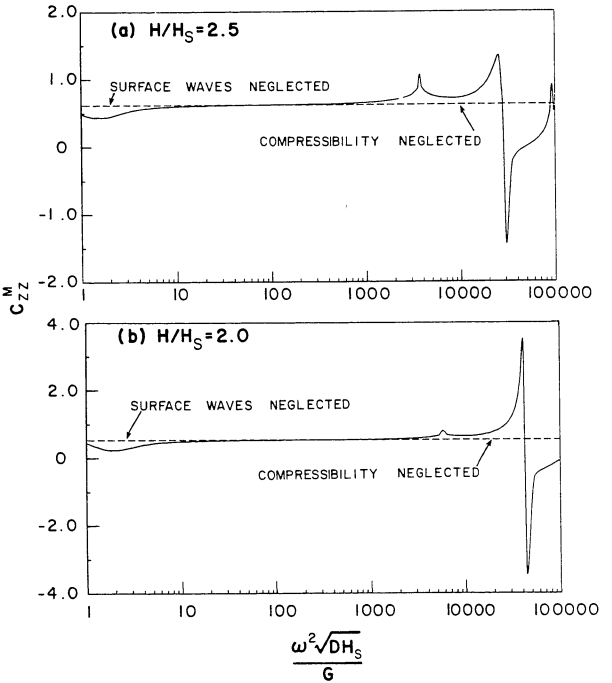

FIG. 5.15 VERTICAL ADDED MASS COEFFICIENTS FOR PROTOTYPE

Reproduced with permission of the copyright owner. Further reproduction prohibited without permission.

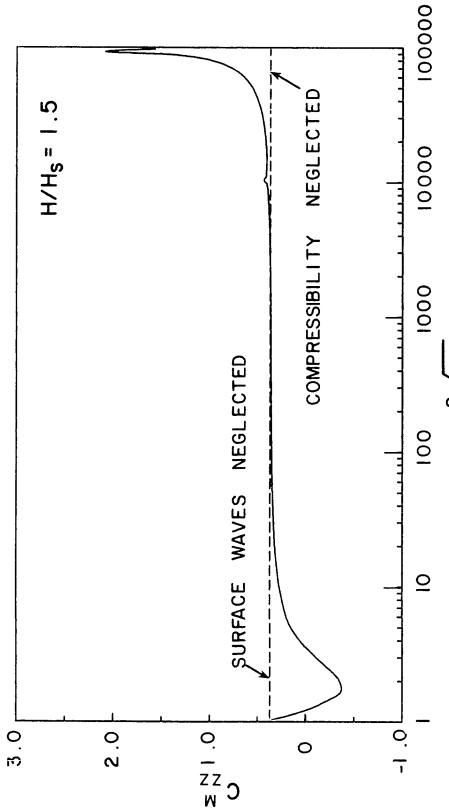

FIG. 5.16 VERTICAL ADDED MASS COEFFICIENT FOR PROTOTYPE

Reproduced with permission of the copyright owner. Further reproduction prohibited without permission.

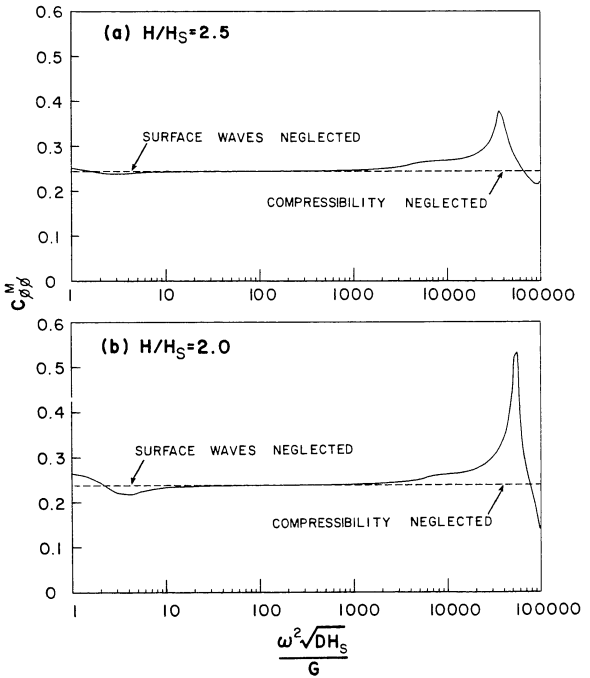

FIG. 5.17 ROTATIONAL ADDED MASS COEFFICIENTS FOR PROTOTYPE

Reproduced with permission of the copyright owner. Further reproduction prohibited without permission.

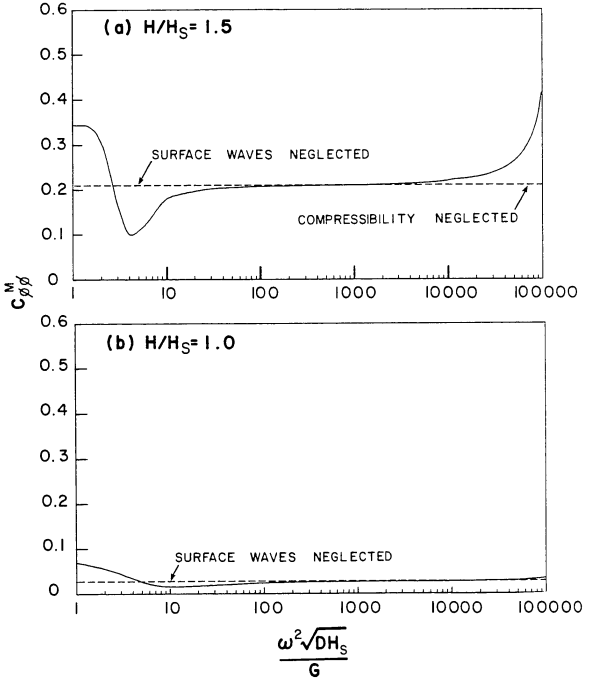

FIG. 5.18 ROTATIONAL ADDED MASS COEFFICIENTS FOR PROTOTYPE

Reproduced with permission of the copyright owner. Further reproduction prohibited without permission.

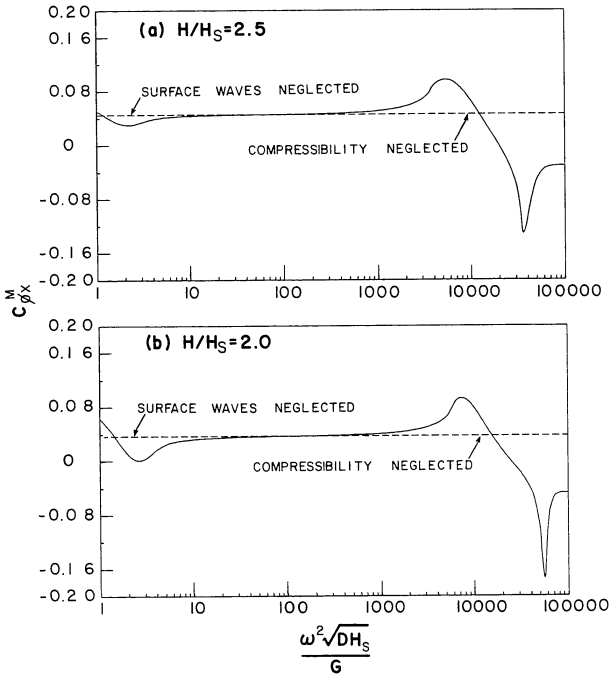

FIG. 5.19 COUPLED ADDED MASS COEFFICIENTS FOR PROTOTYPE

Reproduced with permission of the copyright owner. Further reproduction prohibited without permission.

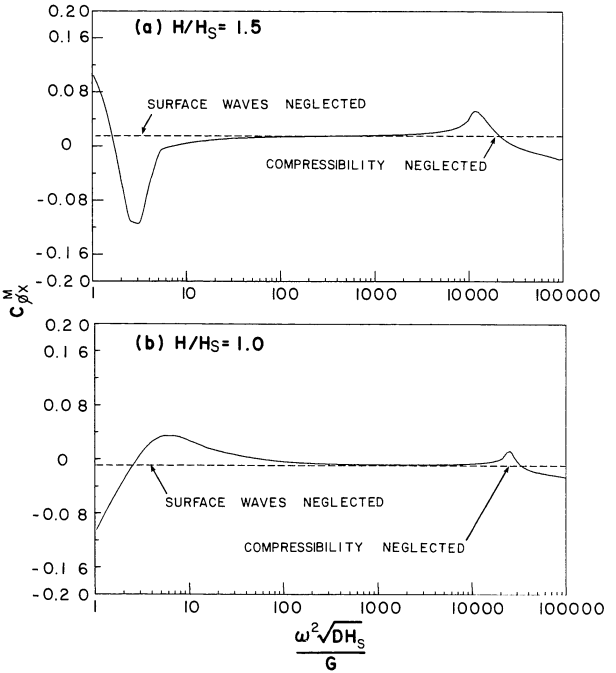

FIG. 5.20 COUPLED ADDED MASS COEFFICIENTS FOR PROTOTYPE

Reproduced with permission of the copyright owner. Further reproduction prohibited without permission.

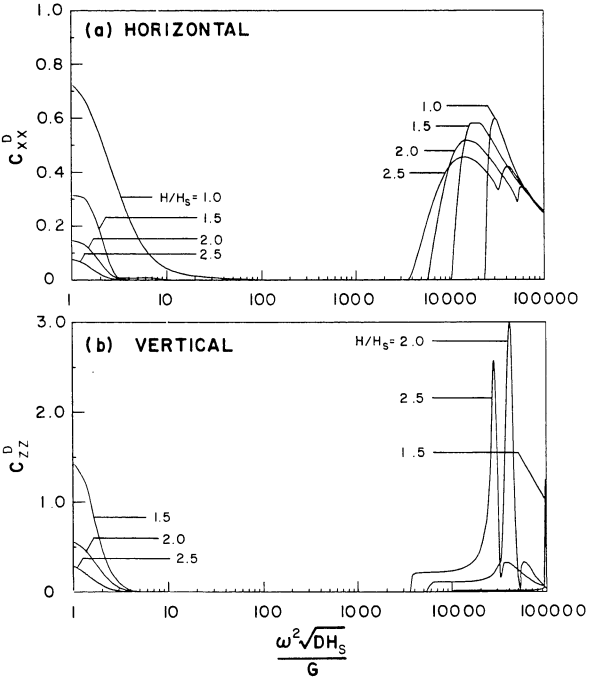

FIG. 5.21 HYDRODYNAMIC DAMPING COEFFICIENTS FOR PROTOTYPE

Reproduced with permission of the copyright owner. Further reproduction prohibited without permission.

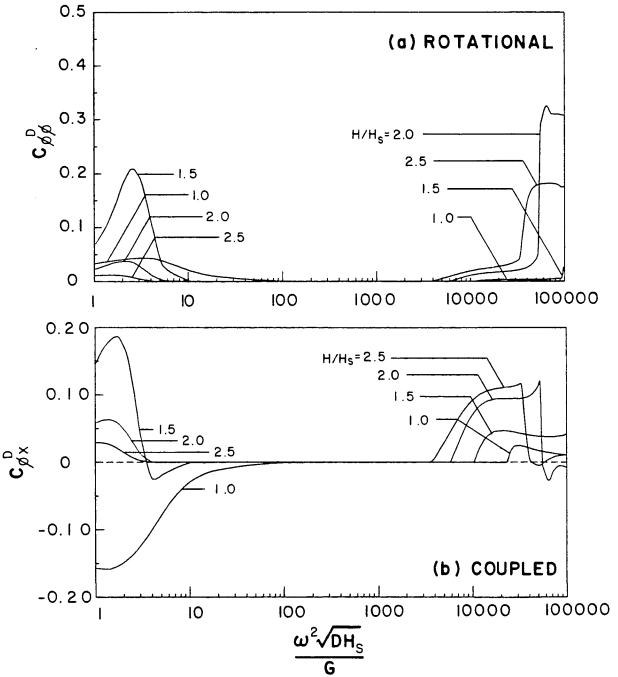

FIG. 5.22 HYDRODYNAMIC DAMPING COEFFICIENTS FOR PROTOTYPE

Reproduced with permission of the copyright owner. Further reproduction prohibited without permission.

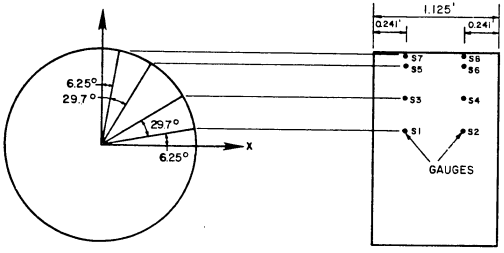

(a) PRESSURE GAGE ON THE SIDE OF THE MODEL

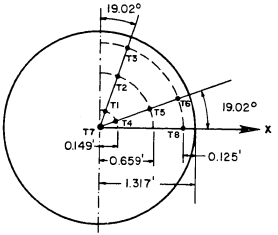

(b) PRESSURE GAGE ON THE TOP OF THE MODEL

FIG. 5.23 LOCATIONS OF PRESSURE GAUGES

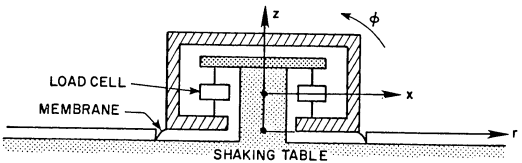

FIG. 5.24 MODEL ON SHAKING TABLE

Reproduced with permission of the copyright owner. Further reproduction prohibited without permission.

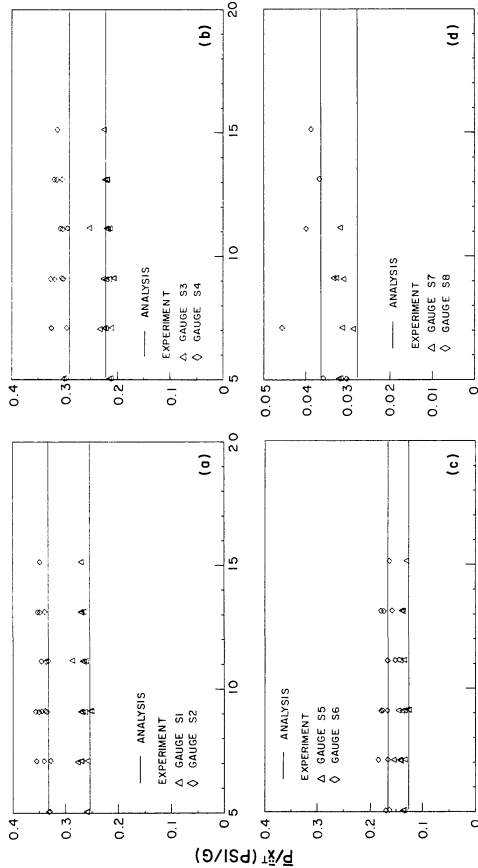

FIG. 5.25 HYDRODYNAMIC PRESSURE AMPLITUDES OF GAUGES S1–S8 DUE TO HORIZONTAL HARMONIC EXCITATIONS, $H/H_S = 2.5$

Reproduced with permission of the copyright owner. Further reproduction prohibited without permission.

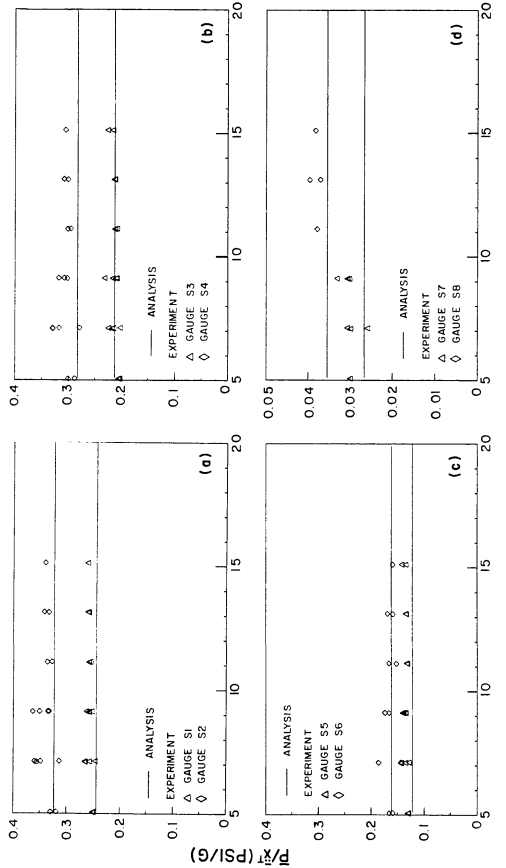

FIG. 5.26 HYDRODYNAMIC PRESSURE AMPLITUDES OF GAUGES S1-S8 DUE TO HORIZONTAL HARMONIC EXCITATIONS, $H/H_S = 2.0$

Reproduced with permission of the copyright owner. Further reproduction prohibited without permission.

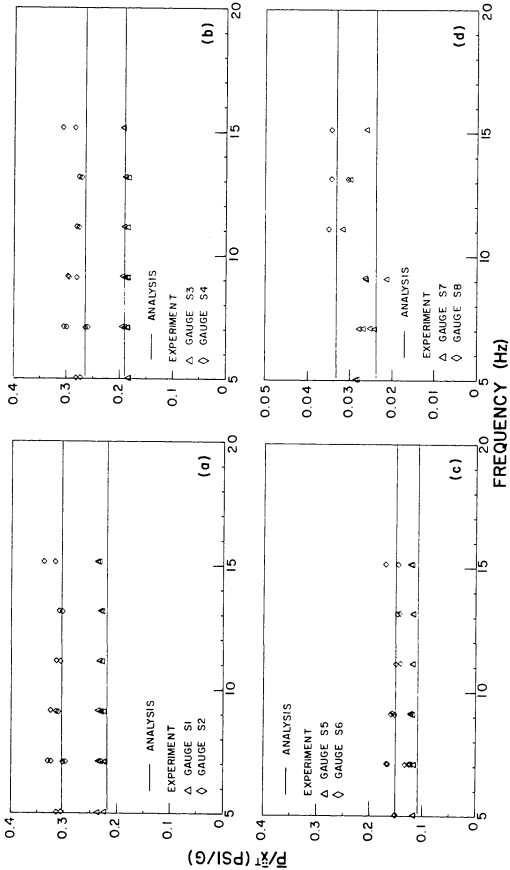

FIG. 5.27 HYDRODYNAMIC PRESSURE AMPLITUDES OF GAUGES S1-S8 DUE TO HORIZONTAL HARMONIC EXCITATIONS, $H/H_S = 1.5$

Reproduced with permission of the copyright owner. Further reproduction prohibited without permission.

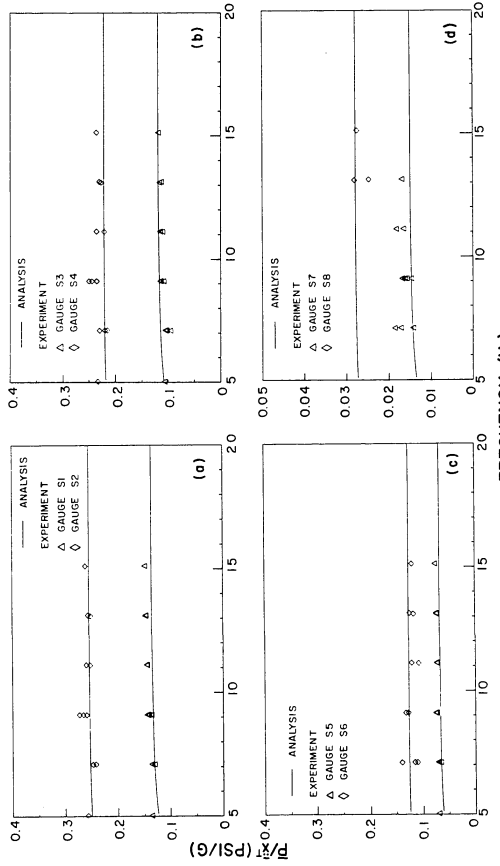

FIG. 5.28 HYDRODYNAMIC PRESSURE AMPLITUDES OF GAUGES S1-S8 DUE TO HORIZONTAL HARMONIC EXCITATIONS, $H/H_S = 1.0$

Reproduced with permission of the copyright owner. Further reproduction prohibited without permission.

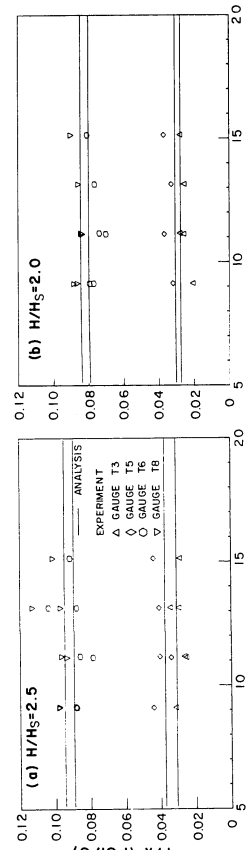

FIG. 5.29 HYDRODYNAMIC PRESSURE AMPLITUDE OF GAUGES T3, T5, T6 AND T8 DUE TO HORIZONTAL HARMONIC EXCITATIONS

Reproduced with permission of the copyright owner. Further reproduction prohibited without permission.

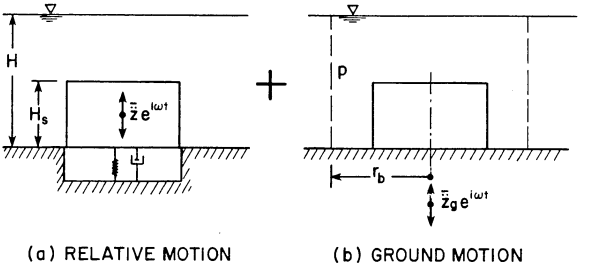

FIG. 5.30 SUPERPOSITION OF MODEL MOTION

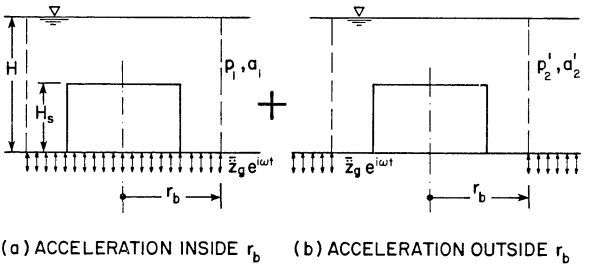

FIG. 5.31 SUPERPOSITION OF GROUND MOTION

Reproduced with permission of the copyright owner. Further reproduction prohibited without permission.

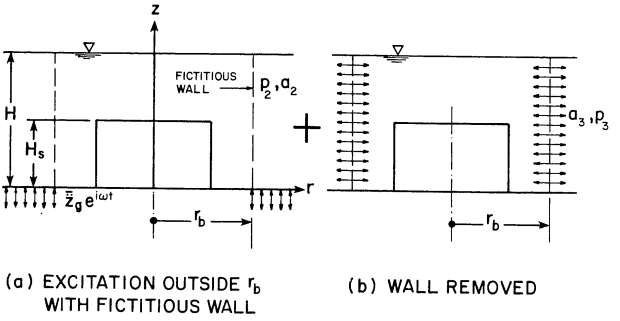

FIG. 5.32 SUPERPOSITION OF GROUND MOTION OUTSIDE r_b

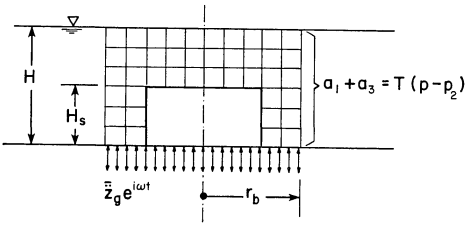

FIG. 5.33 DISCRETIZED TRUNCATED DOMAIN

Reproduced with permission of the copyright owner. Further reproduction prohibited without permission.

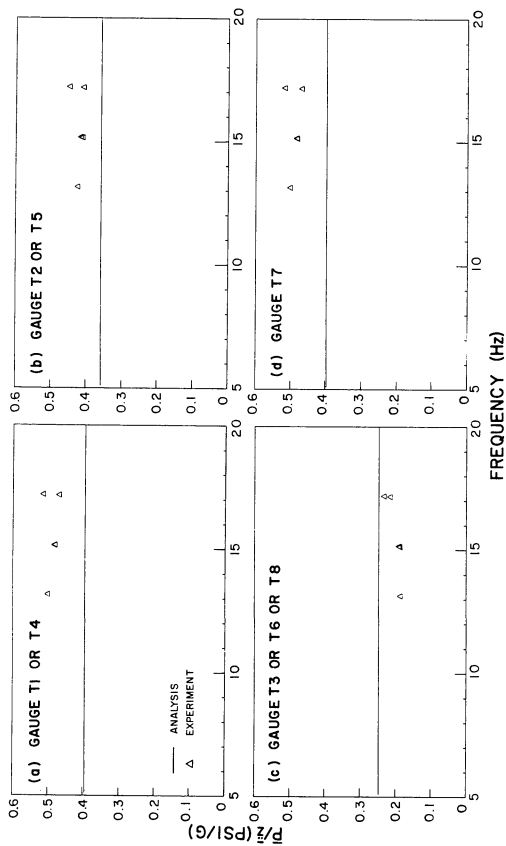

FIG. 5.34 HYDRODYNAMIC PRESSURE AMPLITUDES OF GAUGES T1-T8 DUE TO VERTICAL HARMONIC EXCITATIONS, $H/H_S = 2.5$

Reproduced with permission of the copyright owner. Further reproduction prohibited without permission.

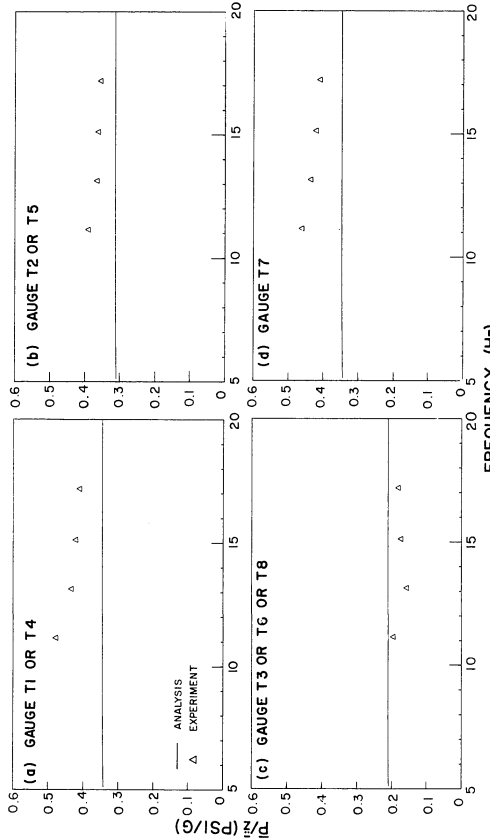

FIG. 5.35 HYDRODYNAMIC PRESSURE AMPLITUDES OF GAUGES T1-T8 DUE TO VERTICAL HARMONIC EXCITATIONS, $H/H_S = 2.0$

Reproduced with permission of the copyright owner. Further reproduction prohibited without permission.

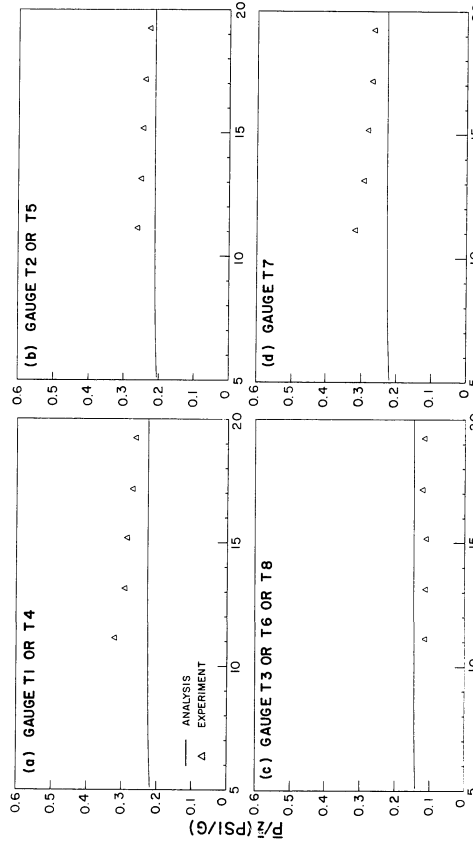

FIG. 5.36 HYDRODYNAMIC PRESSURE AMPLITUDES OF GAUGES T1-T8 DUE TO VERTICAL HARMONIC EXCITATIONS, $H/H_S = 1.5$

Reproduced with permission of the copyright owner. Further reproduction prohibited without permission.

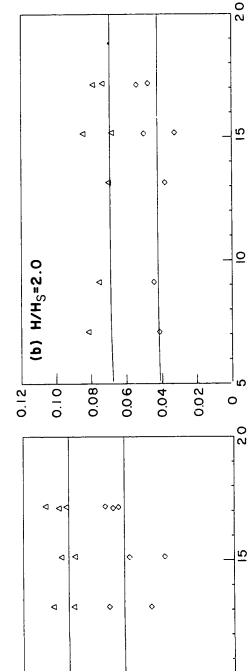

FIG. 5.37 HYDRODYNAMIC PRESSURE AMPLITUDES OF GAUGES S1-S8 DUE TO VERTICAL HARMONIC EXCITATIONS

Reproduced with permission of the copyright owner. Further reproduction prohibited without permission.

6. CONCLUSIONS

The conclusions of this study can be summarized as follows:

1. The finite element method using the transmitting boundary developed herein is proven effective in determining hydrodynamic pressure distributions on rigid axisymmetric bodies oscillating in incompressible and weakly compressible (small perturbation approximation) fluids.

2. The hydrodynamic added mass and damping coefficients are dependent on frequency of oscillation when surface waves (generated by the oscillating bodies) and/or fluid compressibility are included.

3. Fluid compressibility is found to have a significant effect on the hydrodynamic added mass and damping coefficients at high frequencies for cases involving large fluid depths. The added mass coefficients are increased in some frequency range up to 6 times of the values when fluid compressibility is neglected and they are decreased in some frequency range.

4. Surface waves generated by oscillating bodies do not have a significant effect on the hydrodynamic added mass and damping coefficients except at very low frequencies when bodies are near or at the free surface.

5. The hydrodynamic damping coefficients vanish when both fluid compressibility and surface waves generated by oscillating bodies are neglected.

Reproduced with permission of the copyright owner. Further reproduction prohibited without permission.

6. The comparisons of the results of the finite element method with the experimental results and with those obtained by Garrison show good agreement in most cases.

Reproduced with permission of the copyright owner. Further reproduction prohibited without permission.

REFERENCES

1. Jacobsen, L.S., "Impulsive Hydrodynamics of Fluid Inside a Cylindrical Tank and of Fluid Surrounding a Cylindrical Pier," Bulletin, Seismoligical Society of America, Vol. 39, 1949, pp. 189-204.

2. Petrauskas, C., "Hydrodynamic Damping and 'Added Mass' for Flexible Offshore Platforms," Technical Report No. HEL 9-23, Hydraulic Engineering Laboratory, University of California, Berkeley, 1973.

3. Chandrasekaran, A.R., Saini, S.S., and Malhotra, M.M., "Hydrodynamic Pressure on Circular Cylindrical Cantilever Structures Surrounded by Water," Fourth Symposium on Earthquake Engineering, Roorkee, India, November, 1970.

4. Garrison, C.J., and Berklite, R.E., "Impulsive Hydrodynamics of Submerged Rigid Bodies," Journal of the Engineering Mechanics Division, ASCE, Vol. 99, No. EM1, February, 1973.

5. Garrison, C.J., "Hydrodynamic Loading of Large Offshore Structures," International Symposium on Numerical Methods, Offshore Engineering, Swansea, January, 1977.

6. Bai, K.J., "A Variational Method in Potential Flows with a Free Surface," Naval Architecture Report No. NA 72-2, University of California, Berkeley, September, 1972.

7. Zienkiewicz, O.C., and Newton, R.E., "Coupled Vibrations of a Structure Submerged in a Compressible Fluid," Proceedings, International Symposium on Finite Element Techniques, Stuttgart, May, 1969.

8. Liaw, C.-Y., and Chopra, A.K., "Earthquake Response of Axisymmetric Tower Structures Surrounded by Water," Report No. EERC 73-25, Earthquake Engineering Research Center, University of California, Berkeley, October, 1973.

9. Hall, J.F., and Chopra, A.K., "A Transmitting Boundary for Analysis of Hydrodynamic Pressure in Unbounded Domains," Proceedings, Third Engineering Mechanics Division Specialty Conference, ASCE, Austin, Texas, September, 1979.

10. Veletsos, A.S., and Wei, Y.T., "Lateral and Rocking Vibration of Footing," Journal of the Soil Mechanics and Foundation Division, ASCE, Vol. 97, No. SM9, pp. 1277-1249, September, 1971.

11. Vaish, A.K., and Chopra, A.K., "Earthquake Finite Element Analysis of Structure - Foundation Systems," Journal of the Engineering Mechanics Division, ASCE, Vol. 100, No. EM6, pp. 1101-1116, December, 1974.

Reproduced with permission of the copyright owner. Further reproduction prohibited without permission.

12. Zienkiewicz, O.C., The Finite Element Method, Third Edition, McGraw-Hill, London, 1977.

13. Huebner, K.H., The Finite Element Method for Engineers, Wiley, New York, 1975.

14. Byrd, R.C., "A Laboratory Study of the Fluid-Structure Interaction of Submerged Tanks and Caissons in Earthquakes," Report No. UCB/EERC-78/08, Earthquake Engineering Research Center, University of California, Berkeley, October 1978.

15. Byrd, R.C., and Nilrat, F., "Earthquake Excitation of Submerged Tanks and Caissons: A Correlation Study for Physical and Analytic Models," Paper No. OTC 3110, Proceedings, Offshore Technology Conference, Houston, Texas, May 1978.

16. Strang, G., and Fix, G.J., An Analysis of the Finite Element Method, Prentice-Hall, Englewood Cliffs, N.J., 1973.

17. Abramowitz, M., and Stegun, I.A., Handbook of Mathematical Functions, Dover, New York, 1965.

18. Sears, W.R., "Small Perturbation Theory," High Speed Aerodynamics and Jet Propulsion Volume VI, General Theory of High Speed Aerodynamics, Sears, W.R., ed., Princeton University Press, 1954.

Reproduced with permission of the copyright owner. Further reproduction prohibited without permission.

APPENDIX A

FINITE ELEMENT FORMULATION OF MATRICES

A.1 Formulation of [F]

The elements F_{ij} of matrix [F] have been defined as

$$F_{ij} = \int_D \nabla N_i^G \cdot \nabla N_j^G \, dD \tag{A.1}$$

where D is the fluid domain inside the transmitting boundary and

$$\nabla = u_r \frac{\partial}{\partial r} + u_\theta \frac{1}{r} \frac{\partial}{\partial \theta} + u_z \frac{\partial}{\partial z} \tag{A.2}$$

in cylindrical coordinates. Quantities u_r, u_θ, and u_z are unit vectors in the r, θ, and z directions, respectively.

Since the distributions of the hydrodynamic pressure in the circumferential direction are known, the interpolation functions $N_i^G(r,\theta,z)$ can be written as

$$N_i^G(r,\theta,z) = N_i(r,z)\Theta(\theta) \tag{A.3}$$

where $N_i(r,z) = N_i^G(r,0,z)$, $\Theta(\theta) = \cos\theta$ in the horizontal and angular excitation cases, and $\Theta(\theta) = 1$ in the vertical excitation case.

In the finite element approximation, the global interpolation functions $N_i = 1$ at nodes i and vanish everywhere else except over the elements which have i as one of their nodes. Over these elements the interpolation functions are difficult to derive. However, Eq. A.1 can be evaluated for individual elements and the contributions of all elements containing nodes i and j can be summed, i.e.

$$F_{ij} = \sum_e F_{ij}^e \tag{A.4}$$

Reproduced with permission of the copyright owner. Further reproduction prohibited without permission.

These element functions F^e_{ij} can be determined using Eqs. A.1 and A.3; thus, giving

$$F^e_{ij} = \int_{D^e} [N_{i,r} N_{j,r} + N_{i,z} N_{j,z}) \cos^2\theta + \frac{1}{r^2} N_i N_j \sin^2\theta] dD \quad (A.5a)$$

for the horizontal and angular excitation cases, and

$$F^e_{ij} = \int_{D^e} (N_{i,r} N_{j,r} + N_{i,z} N_{j,z}) \, dD \quad (A.5b)$$

for the vertical excitation case, where D^e is the domain of element e. In these relations, a second subscript is used to denote a partial derivative, e.g. $N_{i,r} = \frac{\partial N_i}{\partial r}$.

After evaluating and assembling the element properties, it is convenient to use a local coordinate system to describe the interpolation functions rather than use the global coordinate system. The advantages of the local interpolation functions are that they are simple in form and repetitive. For example, in the four node quadrilateral elements, the element interpolation functions N^e_i in the local s-t coordinate system are

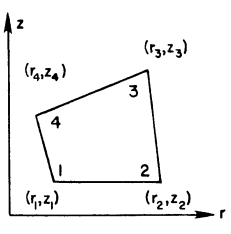

GLOBAL COORDINATE SYSTEM

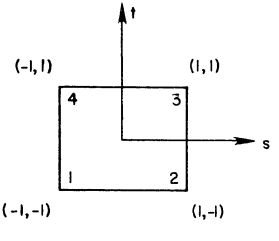

LOCAL COORDINATE SYSTEM

Reproduced with permission of the copyright owner. Further reproduction prohibited without permission.

$$
\begin{aligned}
N_1^e(s,t) &= \tfrac{1}{4}(1-s)(1-t) \\
N_2^e(s,t) &= \tfrac{1}{4}(1+s)(1-t) \\
N_3^e(s,t) &= \tfrac{1}{4}(1+s)(1+t) \\
N_4^e(s,t) &= \tfrac{1}{4}(1-s)(1+t)
\end{aligned}
\tag{A.6}
$$

A coordinate transformation must be established so that the variables r and z can be expressed in terms of the variables s and t. For isoparametric elements, the transformation functions can be taken to be the same as the element interpolation functions, i.e.

$$
\begin{aligned}
r(s,t) &= \sum_{i=1}^{4} N_i^e(s,t) r_i \\
z(s,t) &= \sum_{i=1}^{4} N_i^e(s,t) z_i
\end{aligned}
\tag{A.7}
$$

Now that the element interpolation functions in Eq. A.5 are expressed in the local coordinate system, their partial derivatives with respect to r and z can be determined. Using the chain rule, $N_{i,s}$ and $N_{i,t}$ can be written in the matrix form

$$
\begin{Bmatrix} N_{i,s} \\ N_{i,t} \end{Bmatrix} = \begin{bmatrix} r_{,s} & z_{,s} \\ r_{,t} & z_{,t} \end{bmatrix} \begin{Bmatrix} N_{i,r} \\ N_{i,z} \end{Bmatrix} \tag{A.8}
$$

Equation A.8 may be inverted to obtain

$$
\begin{Bmatrix} N_{i,r} \\ N_{i,z} \end{Bmatrix} = \frac{1}{J} \begin{bmatrix} z_{,t} & -z_{,s} \\ -r_{,t} & r_{,s} \end{bmatrix} \begin{Bmatrix} N_{i,s} \\ N_{i,t} \end{Bmatrix} \tag{A.9}
$$

Reproduced with permission of the copyright owner. Further reproduction prohibited without permission.

where J is the Jacobian of transformation given by

$$J(s,t) = r_{,s} z_{,t} - r_{,t} z_{,s} \qquad (A.10)$$

The terms on the right hand side of Eq. A.9 can be derived from Eqs. A.6 - A.7.

Equations A.5 can now be evaluated in the local coordinate system as

$$F^e_{ij} = \int_0^{2\pi} \int_{-1}^{1} \int_{-1}^{1} [(N_{i,r} N_{j,r} + N_{i,z} N_{j,z}) \cos^2\theta + \frac{1}{r^2} N_i N_j \sin^2\theta] \qquad (A.11a)$$

$$J\ r\ ds\ dt\ d\theta$$

$$F^e_{ij} = \int_0^{2\pi} \int_{-1}^{1} \int_{-1}^{1} (N_{i,r} N_{j,r} + N_{i,z} N_{j,z})\ J\ r\ ds\ dt\ d\theta \qquad (A.11b)$$

Because of the complexity of Eqs. A.11, the Gauss quadrature is used to carry out the integration.

A.2 Formulation of $[F^C]$

The elements F^C_{ij} of matrix $[F^C]$ have been defined as

$$F^C_{ij} = \int_D \frac{1}{c^2} N^G_i N^G_j \, dD \qquad (A.12)$$

Similarly, F^C_{ij} can be expressed as a summation of F^{Ce}_{ij}, contributions of elements containing nodes i and j, i.e.

$$F^C_{ij} = \sum_e F^{Ce}_{ij}$$

where F^{Ce}_{ij} in the local coordinate system are

$$F^{Ce}_{ij} = \int_0^{2\pi} \int_{-1}^{1} \int_{-1}^{1} \frac{1}{c^2} N_i N_j \theta^2(\theta)\ Jr\ ds\ dt\ d\theta \qquad (A.13)$$

Reproduced with permission of the copyright owner. Further reproduction prohibited without permission.

For horizontal and rotational excitation cases, substituting $\Theta(\theta) = \cos\theta$ into this equation, one obtains

$$F_{ij}^{Ce} = \pi \int_{-1}^{1} \int_{-1}^{1} \frac{1}{c^2} N_i N_j J r \, ds \, dt \qquad \text{(A.14a)}$$

For the vertical excitation case, substituting $\Theta(\theta) = 1$ into Eq. A.13 gives

$$F_{ij}^{Ce} = 2\pi \int_{-1}^{1} \int_{-1}^{1} \frac{1}{c^2} N_i N_j J r \, ds \, dt \qquad \text{(A.14b)}$$

where $N_i(s,t)$, $r(s,t)$, and $J(s,t)$ are given by Eqs. A.6, A.7, and A.10, respectively.

The numerical integration is also used to evaluate Eqs. A.14.

A.3 Formulation of $[F^B]$

The elements F_{ij}^B of matrix $[F^B]$ have been defined as

$$F_{ij}^B = \int_{TB} N_i^G T_j \, dS \qquad \text{(A.15)}$$

This equation must be integrated over the surface of the transmitting boundary. Using Eq. A.3, Eq. A.15 can be written in the matrix form

$$[F^B] = \int_{TB} \langle N \rangle^T \langle T \rangle \Theta(\theta) \, dS \qquad \text{(A.16)}$$

Note that $N_i(r,z) = N_i(r_b,z)$ at the transmitting boundary and that functions $N_i(r_b,z) = 0$ if nodes i are not on the transmitting boundary. Thus, Eq. A.16 may be written in a compact form

$$[F^B]_{TB} = \int_{TB} \langle \hat{N} \rangle^T \langle T^B \rangle \Theta(\theta) \, dS \qquad \text{(A.17)}$$

where $[F^B]_{TB}$ is an $n_{TB} \times n_{TB}$ matrix, $\langle \hat{N} \rangle$ is an $1 \times n_{TB}$ row matrix given by Eq. 4.26, and $\langle T^B \rangle$ is an $1 \times n_{TB}$ row matrix given by Eq. 4.44 or 4.51.

Reproduced with permission of the copyright owner. Further reproduction prohibited without permission.

The elements of $[F^B]_{TB}$ are associated only with the nodes on the transmitting boundary.

Substituting Eq. 4.44 or Eq. 4.51 into Eqs. A.17, yields

$$[F^B]_{TB} = r_b \int_0^{2\pi} \int_0^H \langle\hat{N}\rangle^T \langle\hat{N}\rangle [E] [\frac{R'}{R}]_{r=r_b} [E]^T [Q] \cos^2\theta \, dz \, d\theta \qquad \text{(A.18a)}$$

for the horizontal and rotation excitation cases, and

$$[F^B]_{TB} = r_b \int_0^{2\pi} \int_0^H \langle\hat{N}\rangle^T \langle\hat{N}\rangle [E] [\frac{R'}{R}]_{r=r_b} [E]^T [Q] \, dz \, d\theta \qquad \text{(A.18b)}$$

for the vertical excitation case. Recalling that

$$[Q] = \int_0^H \langle\hat{N}\rangle^T \langle\hat{N}\rangle \, dz \ ,$$

Eqs. A.18a and A.18b become

$$[F^B]_{TB} = \pi r_b [Q] [E] [\frac{R'}{R}]_{r=r_b} [E]^T [Q] \qquad \text{(A.19a)}$$

$$[F^B]_{TB} = 2\pi r_b [Q] [E] [\frac{R'}{R}]_{r=r_b} [E]^T [Q] \qquad \text{(A.19b)}$$

respectively, where R_i in Eq. A.19a are functions of $H_1^{(2)}$ and K_1, R_i in Eq. A.19b are functions of $H_0^{(2)}$ and K_0.

Matrix $[F^B]$ can then be assembled from the elements of matrix $[F^B]_{TB}$. It should be noted that $[F^B]_{TB}$ is a symmetric matrix since $[Q]$ is symmetric. Thus, $[F^B]$ is also symmetric and its elements F^B_{ij} vanish if either nodes i or j are not on the transmitting boundary.

A.4 Formulation of $[F^S]$

The elements F^S_{ij} of matrix $[F^S]$ have been defined as

$$F^S_{ij} = \int_{FS} \frac{1}{g} N^G_i N^G_j \, dS \qquad \text{(A.20)}$$

Reproduced with permission of the copyright owner. Further reproduction prohibited without permission.

Using Eq. A.3, $N_i^G(r,\theta,z)$ become $N_i(r,z)\Theta(\theta)$. Since Eq. A.20 is integrated over the free surface, these functions $N_i(r,z)$ become $N_i(r,H)$; thus

$$F_{ij}^S = \int_0^{2\pi}\int_0^{r_b} \frac{1}{g} \bar{N}_i \bar{N}_j \Theta^2(\theta)\, r\, dr\, d\theta \qquad (A.21)$$

where $\bar{N}_i(r) = N_i(r,H)$. It should be noted that $\bar{N}_i(r)$ vanish if nodes i are not on the free surface, i.e. $F_{ij}^S = 0$ if either nodes i or j are not on the free surface.

Coefficients F_{ij}^S can be expressed as a summation of F_{ij}^{Ce}, contributions of elements containing nodes i and j, i.e.

$$F_{ij}^S = \sum_e F_{ij}^{Se}$$

where

$$F_{ij}^{Se} = \int_0^{2\pi}\int_{re} \frac{1}{g} \bar{N}_i \bar{N}_j \Theta^2(\theta)\, r\, dr\, d\theta \qquad (A.22)$$

The Gauss quadrature may be used to evaluate Eq. A.22. However, for a four node quadrilateral element or a three node triangular element, Eq. A.22 can be integrated explicitly.

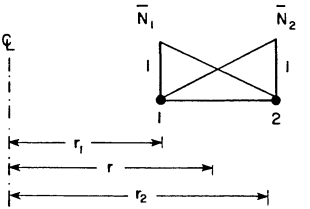

The interpolation functions for the figure shown above are

Reproduced with permission of the copyright owner. Further reproduction prohibited without permission.

$$\left.\begin{aligned} \bar{N}_1(r) &= \frac{r-r_2}{r_1-r_2} \\ \bar{N}_2(r) &= \frac{r-r_1}{r_2-r_1} \end{aligned}\right\} \qquad (A.23)$$

Upon substituting Eq. A.23 into Eq. A.22, one obtains, for the horizontal and the rotational excitation cases,

$$\left.\begin{aligned} F_{11}^{Se} &= \frac{\pi}{g}\frac{1}{(r_1-r_2)^2}\left[\frac{1}{4}(r_2^4-r_1^4)-\frac{2}{3}(r_2^3-r_1^3)r_2+\frac{1}{2}(r_2^2-r_1^2)r_2^2\right] \\ F_{12}^{Se} = F_{21}^{Se} &= -\frac{\pi}{g}\frac{1}{(r_1-r_2)^2}\left[\frac{1}{4}(r_2^4-r_1^4)-\frac{1}{3}(r_2^3-r_1^3)(r_2+r_1)+\frac{1}{2}(r_2^2-r_1^2)r_1r_2\right] \\ F_{22}^{Se} &= \frac{\pi}{g}\frac{1}{(r_1-r_2)^2}\left[\frac{1}{4}(r_2^4-r_1^4)-\frac{2}{3}(r_2^3-r_1^3)r_1+\frac{1}{2}(r_2^2-r_1^2)r_1^2\right] \end{aligned}\right\} \qquad (A.24)$$

For the vertical excitation case, the right hand sides of Eqs. A.24 are multiplied by two.

A.5 Formulation of $\{\bar{D}\}$

Components $\bar{D}_i(\omega)$ of $\{\bar{D}\}$ have been defined as

$$\bar{D}_i(\omega) = \int_{IF} -\frac{w}{g} N_i^G \bar{a}_n \, dS \qquad (A.25)$$

where $\bar{a}_n(r,\theta,z,\omega)$ is the acceleration function of fluid particles in the outward normal direction to fluid surface. This function $\bar{a}_n$ is given by

$$\bar{a}_n(r,\theta,z,\omega) = \bar{a}_r(r,\theta,z,\omega)n_r + \bar{a}_z(r,\theta,z,\omega)n_z \qquad (A.26)$$

Reproduced with permission of the copyright owner. Further reproduction prohibited without permission.

where $\bar{a}_r$ and $\bar{a}_z$ are the accelerations of the body in the r and z directions at the interface. The direction cosines n_r and n_z are those of the outward normal vector of fluid surface.

Substituting Eqs. A.3 and A.26 into Eq. A.25, and noting that

$$\left.\begin{aligned} n_r ds &= \frac{n_r}{|n_r|}\, r\, d\theta\, dz \\ n_z ds &= \frac{n_z}{|n_z|}\, r\, d\theta\, dr \end{aligned}\right\} \qquad (A.27)$$

one obtains

$$\bar{D}_i(\omega) = \int_{IF} -\frac{w}{g} N_i \Theta \bar{a}_r \frac{n_r}{|n_r|}\, r\, d\theta\, dz + \int_{IF} -\frac{w}{g} N_i \Theta \bar{a}_z \frac{n_z}{|n_z|}\, r\, d\theta\, dr \qquad (A.28)$$

Equation A.28 is evaluated over the interface; thus, the interpolation functions $N_i(r,z)$ in the first and the second term of the right hand side of Eq. A.28 may be written as $\hat{N}_i(z)$ and $\bar{N}_i(r)$, respectively.

The acceleration functions $\bar{a}_r$ and $\bar{a}_z$ are different for each of the excitation cases. For the horizontal motion case, these functions are

$$\bar{a}_r(r,\theta,z,\omega) = \bar{a}_H(\omega) \cos\theta$$

$$\bar{a}_z(r,\theta,z,\omega) = 0$$

where $\bar{a}_H(\omega)$ is the acceleration of the rigid body in the horizontal direction. For the vertical motion case, they are

$$\bar{a}_r(r,\theta,z,\omega) = 0$$

Reproduced with permission of the copyright owner. Further reproduction prohibited without permission.

$$\bar{a}_z(r,\theta,z,\omega) = \bar{a}_v(\omega)$$

where $\bar{a}_v(\omega)$ is the acceleration of the rigid body in the vertical direction. For the rotational motion case (see Fig. 4.3), they are

$$\bar{a}_r(r,\theta,z,\omega) = -\bar{a}_\phi(\omega)\ (z-\bar{z})\ \cos\theta$$

$$\bar{a}_z(r,\theta,z,\omega) = \bar{a}_\phi(\omega)\ r\ \cos\theta$$

where $\bar{a}_\phi(\omega)$ is the angular acceleration about the center of gravity of the rigid body.

Upon substituting appropriate $\bar{a}_r$ and $\bar{a}_z$ into Eq. A.28, one obtains vector $\{\bar{D}\}$ for the horizontal, vertical, and rotational motion cases as

$$\{\bar{D}\} = \frac{w}{g}\,\pi\,\bar{a}_H(\omega)\{D_0^H\}$$

$$\{\bar{D}\} = 2\,\frac{w}{g}\,\pi\,\bar{a}_v(\omega)\{D_0^V\}$$

$$\{\bar{D}\} = \frac{w}{g}\,\pi\,\bar{a}_\phi(\omega)\,(\bar{z}\{D_0^H\} - \{D_0^z\} + \{D_0^r\})$$

respectively, where

$$\{D_0^H\} = -\int_0^{H_S} \frac{n_r}{|n_r|} \langle\hat{N}(z)\rangle^T\, r\, dz$$

$$\{D_0^V\} = -\int_0^{r_0} \frac{n_z}{|n_z|} \langle\bar{N}(r)\rangle^T\, r\, dr \qquad \text{(A.29)}$$

$$\{D_0^r\} = -\int_0^{r_0} \frac{n_z}{|n_z|} \langle\bar{N}(r)\rangle^T\, r^2\, dr$$

$$\{D_0^z\} = -\int_0^{H_S} \frac{n_r}{|n_r|} \langle\hat{N}(z)\rangle^T\, z\, r\, dz$$

Vector $\{\bar{D}\}$ is an nxl column matrix, where n is the total number of nodes. Elements $\bar{D}_i(\omega)$ vanish if nodes i are not on the interface.

Reproduced with permission of the copyright owner. Further reproduction prohibited without permission.

These $\bar{D}_i(\omega)$ are evaluated for individual elements and the contributions of all elements containing nodes i are assembled; thus

$$\bar{D}_i(\omega) = \sum_e \bar{D}_i^e(\omega)$$

The formulation for vectors in Eqs. A.29 are presented for three-node triangular and four-node quadrilateral elements.

A.5.1 Formulation of $\{D_0^H\}$

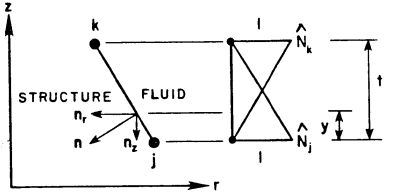

The i^{th} elements D_{0i}^H of $\{D_0^H\}$ can be written as

$$D_{0i}^H = \sum_e D_{0i}^{He}$$

where

$$D_{0i}^{He} = -\int_{z^e} \frac{n_r}{|n_r|} \hat{N}_i(z)\, r\, dz \qquad \text{(A.30)}$$

For the figure shown above,

$$\hat{N}_j(y) = y/t$$

$$\hat{N}_k(y) = 1-y/t$$

$$r(y) = r_j+(r_k-r_j)\, y/t$$

Reproduced with permission of the copyright owner. Further reproduction prohibited without permission.

$$\frac{n_r}{|n_r|} = -1$$

where y is a dummy variable and $t = z_k - z_j$. Using the last two relations, Eq. A.30 becomes

$$D_{0i}^{He} = \int_0^t \hat{N}_i(y)\, r(y)\, dy$$

Upon evaluating this equation for nodes j and k as shown in the figure above, one obtains

$$D_{0j}^{He} = \frac{1}{6} t\,(2r_j + r_k)$$

$$D_{0k}^{He} = \frac{1}{6} t\,(2r_k + r_j)$$

A.5.2 Formulation of $\{D_0^v\}$

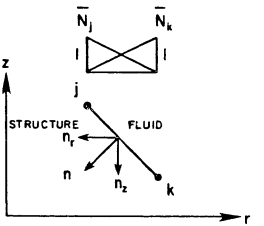

Elements D_{0i}^v of D_0^v are given by

$$D_{0i}^v = \sum_e D_{0i}^{ve}$$

where

$$D_{0i}^{ve} = -\int_{r_e} \frac{n_z}{|n_z|} \bar{N}_i(r)\, r\, dr \qquad \text{(A.31)}$$

Reproduced with permission of the copyright owner. Further reproduction prohibited without permission.

For the figure shown above,

$$\bar{N}_j(r) = \frac{r-r_k}{r_j-r_k}$$

$$\bar{N}_k(r) = \frac{r-r_j}{r_k-r_j}$$

$$\frac{n_z}{|n_z|} = -1$$

Evaluating Eq. A.31 for nodes j and k, gives

$$D_{0j}^{ve} = \frac{1}{r_j-r_k}\left(\frac{1}{3}\left|r_k^3-r_j^3\right| - \frac{1}{2}\, r_k\left|r_j^2-r_k^2\right|\right)$$

$$D_{0k}^{ve} = \frac{1}{r_k-r_j}\left(\frac{1}{3}\left|r_k^3-r_j^3\right| - \frac{1}{2}\, r_j\left|r_j^2-r_k^2\right|\right)$$

A.5.3 Formulation of $\{D_0^z\}$

Elements D_{0i}^z of $\{D_0^z\}$ are given by

$$D_{0i}^z = \sum_e D_{0i}^{ze}$$

where

$$D_{0i}^{ze} = -\int_{z^e} \frac{n_r}{|n_r|}\, \hat{N}_i(z)\; z\; r\; dz \qquad \text{(A.32)}$$

Referring to the figure in Appendix A.5.1, one has

$$\hat{N}_j(z) = \frac{z_k-z}{z_k-z_j}$$

$$\hat{N}_k(z) = \frac{z-z_j}{z_k-z_j}$$

Reproduced with permission of the copyright owner. Further reproduction prohibited without permission.

$$r(z) = r_j + \frac{r_k - r_j}{z_k - z_j}(z - z_j)$$

$$\frac{n_r}{|n_r|} = -1$$

Substituting the last two relations into Eq. A.32, yields

$$D_{0i}^{ze} = \int_{z^e} \hat{N}_i(z)\, z\, r\, dz \qquad (A.33)$$

Evaluating Eq. A.33 for nodes j and k, one obtains

$$D_{0j}^{ze} = \frac{1}{(\Delta z)^2}\left[(z_k r_j - z_j r_k)\left(\frac{1}{2} z_k \left|\Delta^2 z\right| - \frac{1}{3}\left|\Delta^3 z\right|\right) + (r_k - r_j)\left(\frac{1}{3} z_k \left|\Delta^3 z\right| - \frac{1}{4}\left|\Delta^4 z\right|\right)\right]$$

$$D_{0k}^{ze} = \frac{1}{(\Delta z)^2}\left[(z_j r_k - z_k r_j)\left(\frac{1}{2} z_j \left|\Delta^2 z\right| - \frac{1}{3}\left|\Delta^3 z\right|\right) + (r_j - r_k)\left(\frac{1}{3} z_j \left|\Delta^3 z\right| - \frac{1}{4}\left|\Delta^4 z\right|\right)\right]$$

where

$$\Delta^n z = z_k^n - z_j^n \quad , \qquad n = 1,2,3,4$$

A.5.4 Formulation of $\{D_0^r\}$

Elements D_{0i}^r of $\{D_0^r\}$ are given by

$$D_{0i}^r = \sum_e D_{0i}^{re}$$

where

$$D_{0i}^{re} = -\int_{r^e} \frac{n_z}{|n_z|} \bar{N}_i(r)\, r^2\, dr \qquad (A.34)$$

Referring to the figure and the interpolation functions in Appendix A.5.2, one obtains, after evaluating Eq. A.34 for nodes j and k,

$$D_{0j}^{re} = \frac{1}{r_k - r_j}\left(\frac{1}{3} r_k \left|r_k^3 - r_j^3\right| - \frac{1}{4}\left|r_k^4 - r_j^4\right|\right)$$

Reproduced with permission of the copyright owner. Further reproduction prohibited without permission.

$$D_{0k}^{re} = \frac{1}{r_j - r_k}\left(\frac{1}{3} r_j \left| r_k^3 - r_j^3 \right| - \frac{1}{4}\left| r_k^4 - r_j^4 \right|\right)$$

A.6 Formulation of [P] and [Q]

Coefficients P_{ij} and Q_{ij} of matrices [P] and [Q] have been defined as

$$P_{ij} = \int_0^H \hat{N}_i'(z)\, \hat{N}_j'(z)\, dz$$

$$Q_{ij} = \int_0^H \hat{N}_i(z)\, \hat{N}_j(z)\, dz$$

These coefficients are evaluated for individual elements containing nodes i and j, i.e.

$$P_{ij} = \sum_e P_{ij}^e$$

$$Q_{ij} = \sum_e Q_{ij}^e$$

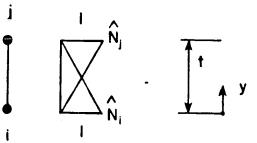

For the figure shown above,

$$\hat{N}_i(y) = 1 - y/t \quad , \quad \hat{N}_i'(y) = -1/t$$

$$\hat{N}_j(y) = y/t \quad , \quad \hat{N}_j'(y) = 1/t$$

where y is a dummy variable. Using this dummy variable, P_{ij}^e and Q_{ij}^e are given by

Reproduced with permission of the copyright owner. Further reproduction prohibited without permission.

$$P^e_{ij} = \int_0^t \hat{N}_i'(y)\, \hat{N}_j'(y)\, dy$$

$$Q^e_{ij} = \int_0^t \hat{N}_i(y)\, \hat{N}_j(y)\, dy$$

After evaluating these equations, one obtains

$$[P^e] = \begin{bmatrix} 1/t & -1/t \\ -1/t & 1/t \end{bmatrix}$$

$$[Q^e] = \frac{1}{6} \begin{bmatrix} 2t & t \\ t & 2t \end{bmatrix}$$

Reproduced with permission of the copyright owner. Further reproduction prohibited without permission.

APPENDIX B

COMPUTER PROGRAM USER'S GUIDE

B.1 Identification

HYPAM - Hydrodynamic Pressure and Added Mass for Axisymmetric Bodies

B.2 Purpose

The purpose of this computer program is to determine hydrodynamic pressure distributions and added masses for rigid bodies axisymmetric about vertical axis. The boides can be totally or partially submerged in an inviscid fluid extending to infinity in the horizontal directions but having finite depth in the vertical direction. The program gives hydrodynamic pressure distributions and added masses for horizontal, vertical, and rotational harmonic oscillations (including the coupled horizontal-rotational added mass). There are options in the program for either including or neglecting the fluid compressibility and surface waves generated by the bodies.

In order to define the computer input, the fluid domain must be idealized as an assemblage of quadrilateral (in the rz-plane) or triangular elements. To reduce the computational effort, the outer boundary of the discretized fluid domain or the transmitting boundary is placed as close as possible to the body provided that the fluid depth outside the boundary is constant.

B.3 Input Data

The following sequence of punched cards numerically define the axisymmetric system to be analyzed.

Reproduced with permission of the copyright owner. Further reproduction prohibited without permission.

B.3.1 Title Card (20A4)

Columns 1-80: Contain information to be printed with results.

B.3.2 Control Cards

There are two control cards.

B.3.2.1 First Control Card (10I5)

Columns 1-5 NUMFN: Number of total fluid nodes.

6-10 NUMFE: Number of total fluid elements.

11-15 NE: Number of nodes per element (4 for both four-node quadrilateral and three-node triangular elements).

16-20 NFNIF: Number of nodes on the interface between the body and the fluid.

21-25 NFNFS: Number of nodes on the free surface.

26-30 NFNTB: Number of nodes on the transmitting boundary.

31-35 MODTB: Number of nodes to be used in the transmidding boundary representation (MODTB $\leq$ NFNTB).

36-40 NTYPE: Number of types of oscillation of the body (NTYPE $\leq$ 3).

41-45 IWAVE: $\leq$ 0, surface waves are neglected.
$\geq$ 1, surface waves are included.

46-50 KOMP: = 0, fluid compressibility is neglected.
= 1, fluid compressibility is included.

Reproduced with permission of the copyright owner. Further reproduction prohibited without permission.

B.3.2.2 Second Control Card (6F10.0)

Columns 1-10 DFTB: Depth of fluid outside the transmitting boundary.

11-20 RTB: Radius of the transmitting boundary (r_b).

21-30 W: Weight per unit volume of fluid.

31-40 G: Gravitational acceleration.

41-50 ZCG: Height of the center of gravity of the body (= $\bar{z}$ of Fig. 4.3).

51-60 C: Velocity of sound in fluid. This can be left blank if KOMP = 0.

The quantity ZCG is defined such that the rotational and the coupled added masses are associated with the moment about the center of gravity of the body. One may define this quantity differently such that the added masses are associated with the overturning moment about the base of the body. This quantity is not needed in the vertical oscillation case; thus, it may be left blank if only the vertical oscillation is interested.

B.3.3 Fluid Nodal Cards (I5,2F10.0,I5)

Columns 1-5 NFN: Fluid nodal number.

6-15 R: r-ordinate.

16-25 Z: z-ordinate.

26-30 KN: Generating code.

Nodal cards need not be in numerical sequence. However, the last node 'NUMFN' must be supplied as the last nodal card.

If node numbers of a nodal group to be generated are N, N+KN, N+2*KN,.....,M, the nodal cards of nodes N and M must be supplied. The integer value of KN must be specified on the nodal card of node N;

Reproduced with permission of the copyright owner. Further reproduction prohibited without permission.

and integer (M-N) must be a multiple of KN. The coordinates of nodes N+KN, N+2*KN,.....,M-KN are generated at equal intervals from the coordinates of nodes N and M. If there is no nodal generation, columns 26-30 for the generating code is left blank.

When numbering the fluid nodes, the nodes on the transmitting boundary must be numbered last by starting from the node on the free surface as node number 'NUMFN-NFNTB+1' and ending with the node on the ground as node number 'NUMFN'.

B.3.4 Fluid Element Cards (6I5)

Columns 1-5 NFE: Fluid element number.

6-10 I: Node I.

11-15 J: Node J.

16-20 K: Node K.

21-25 L: Node L.

26-30 KE: Generating Code.

Element cards must be in element number sequence starting from one. The last element 'NUMFE' must be supplied as the last element card. If element cards are omitted, the program automatically generates the omitted information by incrementing the preceeding node numbers I, J, K, and L by KE which is specified on the first card of a generating element group.

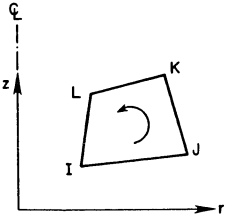

Reproduced with permission of the copyright owner. Further reproduction prohibited without permission.

For a right-hand coordinate system, the node numbers I, J, K, and L must be in sequence in a counter-clockwise direction around the element. Triangular elements are identified by repeating the last node number, e.g. I, J, K, K.

B.3.5 Interface Nodal Cards (16I5)

Columns 1-5, 6-10, 11-15, etc. Fluid node numbers on the interface between the body and the fluid. They must be in order either as n_1, n_2, n_3....., n_N or as n_N, n_{N-1},.....n_2, n_1 as shown in the figure below, where N=NFNIF.

If node numbers n_i, where $3 \leq i \leq N$, are omitted, the program generates the omitted information by setting

$$n_i = n_{i-1} + (n_{i-1} - n_{i-2})$$

$$= 2n_{i-1} - n_{i-2}$$

B.3.6 Free Surface Nodal Cards (16I5)

Columns 1-5, 6-10, 11-15, etc. Fluid node numbers on the fluid free surface. They must be in order either as m_1, m_2..... ....m_M or as m_M, m_{M-1},....., m_2, m_1 as shown in the figure below, where M=NFNFS.

If node numbers m_i, where $3 \leq i \leq M$, are omitted, the program generates the omitted information by setting

$$m_i = 2m_{i-1} - m_{i-2}$$

Reproduced with permission of the copyright owner. Further reproduction prohibited without permission.

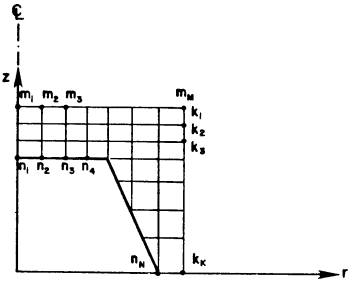

B.3.7 Transmitting Boundary Nodal Cards (16I5)

Columns 1-5, 6-10, etc. Fluid node numbers on the transmitting boundary. They must be in numerical sequence as k_1, k_2,.... ...k_K, K=NFNTB, starting from node k_1 on the free surface where k_1=NUMFN-NFNTB+1 and k_K= NUMFN.

If node numbers k_i, where $3 \leq i \leq K$, are omitted, the program generates the omitted information by setting

$$k_i = 2k_{i-1} - k_{i-2}$$

B.3.8 Type and Frequency Cards

The maximum number of types (NTYPE) of oscillation of the body is three. There are three sets of cards per type of oscillation.

B.3.8.1 Type of Oscillation Card (A4)

Columns 1-4 TYPE: Punch 'HORI' or 'VERT' or 'ROTA' starting with column one for horizontal or vertical or rotational oscillation, respectively.

Reproduced with permission of the copyright owner. Further reproduction prohibited without permission.

B.3.8.2 Number of Frequencies Card (I5)

Columns 1-5 NFREQ: Number of frequencies in Hz. to be analyzed for the type of oscillation in B.3.8.1.

B.3.8.3 Frequency Cards (8F10.0)

Columns 1-10, 11-20, etc. } Frequencies of the oscillation type (in Hz.) to be analyzed.

The next oscillation type card, if there is any, follows the last frequency card of the previous oscillation type. A set of data cards of a next problem, if there is any, follows the last card of the previous problem. Two blank cards must be supplied following the last card of the last problem.

B.4 Output

Beside the input and generated data, the values of hydrodynamic pressure amplitudes at nodes on the interfaces (at θ=0) and the added masses of the specified oscillation frequencies are printed as an output. These pressure amplitudes and added masses are separated into real and imaginary parts. The imaginary part of the added mass is associated with the hydrodynamic damping (= $\bar{f}^{I}_{ij}(\omega)$ of Eq. 2.10) while the real part is the added mass (= $\bar{f}^{R}_{ij}(\omega)$ of Eq. 2.9). The units of the hydrodynamic pressure amplitude and of the added mass are consistent with the input data. For example, if the input data are in ft, lb, and sec, the hydrodynamic pressure and the added mass are in lb/sq. ft and lb-sec^2/ft, respectively.

Reproduced with permission of the copyright owner. Further reproduction prohibited without permission.

B.5 Limitations and Requirements

The computer program is written in FORTRAN IV and was developed on a CDC 6400 computer at the University of California, Berkeley. It can be executed on other computers with minimum changes.

The core storage requirements of the program can be changed depending on the size of the problem to be solved. This is done by changing two FORTRAN statements at the beginning of the program:

```
COMMON A(N)

MSTOR = N
```

The value specified for N is given by

```
N = 5 * NUMFN + 4 * NUMFE + 4 * NFNIF + NFNFS * (1 + NFNFS) +
    NFNTB * (2 + 5 * NFNTB) + 3 * LA
```

where all quantities except LA are defined in Section B.3.2.1. Quantity LA is determined by the program in subroutine EDATA and it is always less than or equal to $\frac{1}{2}(n^2+n)$ and is always less than nx(m+1), where n=NUMFN and m is the maximum difference between node numbers of individual elements. Since the value of LA must be specified beforehand, one may assume the lesser between $\frac{1}{2}(n^2+n)$ and nx(m+1) as its value.

The other changeable storage requirements are for array FREQ(L) in the DIMENSION statement of the main program and arrays RR(M) and RI(M) in the DIMENSION statement of subroutine TBOUN. The values of L and M must be equal to or greater than the maximum number of frequencies and number of nodes on the transmitting boundary, respectively.

Reproduced with permission of the copyright owner. Further reproduction prohibited without permission.

APPENDIX C

COMPUTER PROGRAM LISTING

Reproduced with permission of the copyright owner. Further reproduction prohibited without permission.

```
      PROGRAM HYPAN(INPUT,OUTPUT,TAPE5=INPUT,TAPE6=OUTPUT)
C*****************************************************************************
C
C     A PROGRAM FOR COMPUTING HYDRODYNAMIC PRESSURES AND ADDED MASSES
C      FOR A RIGID AXISYMMETRIC BODY SUBMERGED IN A COMPRESSIBLE FLUID
C      AND SUBJECTED TO HORIZONTAL, VERTICAL, AND ROTATIONAL HARMONIC
C      OSCILLATIONS
C
C*****************************************************************************
      DIMENSION HED(20),FREQ(40),TYPE(3),ITYPE(3)
      COMMON/TAPES/IIN,IOUT
      COMMON/NN/N7,N12,N13,N14
      COMMON/WG/W,G
      COMMON/PI/PI
      COMMON/LA/LA
      COMMON/COMP/KOMP
      COMMON/FREQS/FREQS,C
      DATA HEX,VEX,REX/3HHOR,3HVER,3HROT/
C
C     THE FOLLOWING TWO CARDS ARE FOR BLANK COMMON STORAGE
C
      COMMON A(16000)
      NSTOR=16000
C
C     THE FOLLOWING SCRATH FILES ARE USED
C     IIN =INPUT TAPE
C     IOUT=OUTPUT TAPE
C
      IIN =5
      IOUT=6
C - - - - - - - - - - - - - - - - - - - - - - - - - - - - - - - - - - - - - -
C
C     INPUT PHASE
C
C - - - - - - - - - - - - - - - - - - - - - - - - - - - - - - - - - - - - - -
      PI=4.*ATAN(1.)
C
C     READ AND PRINT CONTROL INFORMATION
C
   10 READ(IIN,1000) HED,NUMFN,NUMFE,NE,NFNIF,NFAFS,NFNTB,MODTB,NTYPE,
     1                IWAVE,KOMP,DFTB,RTB,W,G,ZCG,C
      IF(NUMFN.EQ.0) STOP
      IF(MODTB.EQ.0) MODTB=NFNTB
      IF(NTYPE.EQ.0) NTYPE=1
      WRITE(IOUT,2000) HED,NUMFN,NUMFE,NE,NFNIF,NFAFS,NFNTB,MODTB,NTYPE,
     1                 DFTB,RTB,W,G,ZCG
      IF(KOMP.GE.1) WRITE(IOUT,2040)
      IF(KOMP.EQ.1) WRITE(IOUT,2030) C
      IF(KOMP.EQ.0) WRITE(IOUT,2050)
      IF(IWAVE.LE.0) WRITE(IOUT,2080)
      IF(IWAVE.GT.0) WRITE(IOUT,2090)
C
      N1=1
      N2=N1+NUMFN
      N3=N2+NUMFN
      N4=N3+NE*NUMFE
      N5=N4+NFNIF
      N6=N5+NFNFS
      N7=N6+NFNTB
      N8=N7+NFNTR
      N9=N8+NFNIF
```

Reproduced with permission of the copyright owner. Further reproduction prohibited without permission.

```
      N10=N9+NFNFS*NFNFS
      N11=N10+NFNTB*NFNTB
      N12=N11+NFNTB*NFNTB
      N13=N12+NFNTB*NFNTB
      N14=N13+NFNTB*NFNTB
      N15=N14+NFNTB*NFNTB
      N16=N15+2*NUMFN
      N17=N16+NUMFN
      N19=N17+NFNIF
      N19=N18+NFNIF
      N20=N19+NUMFE
      N21=N20+NFNTB*NFNTB
      IF(KOMP.NE.2) N21=N19
      IF(N21.LT.NSTOR) GO TO 20
      NSTOR=N21-NSTOR
      WRITE(IOUT,2010) NSTOR
      STOP
C
C     READ AND PRINT NODES AND THIER COORDINATES
C
   20 CALL NDATA(A(N1),A(N2),NUMFN)
C
C     READ AND PRINT ELEMENT NUMBERS AND THIER NODE NUMBERS
C      DETERMINE PROFILE
C
      CALL EDATA(A(N3),A(N19),A(N15),A(N16),NE,NUMFE,NUMFN)
      N22=N21+LA
      N23=N22+2*LA
      NTOT=N23-1
      IF(KOMP.GE.1) NTOT=NTOT+LA
      IF(NTOT.LE.NSTOR) GO TO 30
      NSTOR=NTOT-NSTOR
      WRITE(IOUT,2010) NSTOR
      STOP
C
C     READ AND PRINT INTERFACE NODE NUMBERS
C
   30 CALL INTER(A(N4),NFNIF,NUMFN)
C
C     READ AND PRINT FREE SURFACE NODE NUMBERS
C
      CALL FREE(A(N5),NFNFS,NUMFN)
C
C     READ TRANSMITTING BOUNDARY NODES AND FORM THICNESS ARRAY
C
      CALL BOUND(A(N2),A(N6),A(N7),NFNTB,NUMFN)
      IF(KOMP.EQ.2) CALL CTB(A(N15),NFNTB,NE)
C - - - - - - - - - - - - - - - - - - - - - - - - - - - - - - - - - -
C
C     FORMING MATRICES PHASE
C
C - - - - - - - - - - - - - - - - - - - - - - - - - - - - - - - - - -
C
C     FORM P,Q
C
      CALL FORM(A(N7),A(N10),A(N11),NFNTB,NE)
      P11=A(N10)
      IF(KOMP.EQ.2) CALL FORMOC(A(N7),A(N15),A(N20),NFNTB,NE)
C
C     FORM MATRIX FS
C
```

Reproduced with permission of the copyright owner. Further reproduction prohibited without permission.

```
      IF(IWAVE.LE.0) GO TO 35
      CALL FORMC(A(N1),A(N5),A(N9),NE,NFNFS)
C
C     FORM MATRIX FC
C
   35 IF(KOMP.GE.1) CALL FORMF(A(N1),A(N2),A(N3),A(N16),A(N19),A(N21),
     1 NE,NUMFE,NUMFN,ITYPE(K),2)
      CALL FORMDR(A(N1),A(N17),A(N4),NFNIF)
      CALL FORMDZ(A(N1),A(N2),A(N18),A(N4),NFNIF)
      DO 100 K=1,NTYPE
      READ(IIN,1030) TYPE(K)
      IF(TYPE(K).EQ.HEX) ITYPE(K)=1
      IF(TYPE(K).EQ.VEX) ITYPE(K)=2
      IF(TYPE(K).EQ.REX) ITYPE(K)=3
C
C     FORM FLUID ELEMENT MATRIX FE AND ASSEMBLE GLOBAL MATRIX F
C
      CALL FORMF(A(N1),A(N2),A(N3),A(N16),A(N19),A(N21),NE,NUMFE,NUMFN,
     1           ITYPE(K),1)
C
C     FORM VECTOR D
C
      CALL FORMD(A(N1),A(N2),A(N4),A(N8),A(N17),A(N18),ZCG,NE,NFNIF,
     1           NUMFN,ITYPE(K))
C
C     READ EXCITATION FREQUENCIES
C
      IF(ITYPE(K).EQ.1) WRITE(IOUT,2060)
      IF(ITYPE(K).EQ.2) WRITE(IOUT,2070)
      IF(ITYPE(K).EQ.3) WRITE(IOUT,2100)
      READ(IIN,1010) NFREQ
      READ(IIN,1020) (FREQ(I),I=1,NFREQ)
      WRITE(IOUT,2020) NFREQ,(FREQ(I),I=1,NFREQ)
      DO 100 I=1,NFREQ
      FRQ=2.*PI*FREQ(I)
      FRQS=FRQ*FRQ
      IF(IWAVE.LE.0) GO TO 40
      FG=FRQS/G
      CALL COPYPQ(A(N10),A(N11),A(N13),A(N14),NFNTB)
      A(N13)=P11-FG
      NNN=NFNTB
      GO TO 50
   40 NNN=NFNTB-1
      FG=0.
      CALL COPQ2(A(N10),A(N11),A(N13),A(N14),NFNTB,NNN)
C
C     SOLVE EIGENVALUE PROBLEM AT THE TRANSMITTING BOUNDARY
C
   50 IF(KOMP.EQ.2) CALL FORMPC(A(N13),A(N20),NFNTB,NNN)
      CALL JACOBI(A(N13),A(N14),A(N12),A(N7),NNN,5,10)
C
C     FORM MATRIX FB
C
      IF(FG.EQ.0.) CALL COPQ2(A(N10),A(N11),A(N13),A(N14),NFNTB,NNN)
      IF(FG.NE.0.) CALL COPYPQ(A(N10),A(N11),A(N13),A(N14),NFNTB)
      IF(MODTB.GT.NNN) MODTB=NNN
      CALL TRDUN(NTB,MODTB,NNN,ITYPE(K))
C - - - - - - - - - - - - - - - - - - - - - - - - - - - - - - - - - - - -
C
C     SOLUTION PHASE
```

Reproduced with permission of the copyright owner. Further reproduction prohibited without permission.

```
C - - - - - - - - - - - - - - - - - - - - - - - - - - - - - - - - - - - - - - -
C
C     FORM SF=F-FB-FC-FS WHERE SF AND FB ARE COMPLEX
C
      CALL SUMF(A(N5),A(N6),A(N9),A(N12),A(N14),A(N16),A(N21),A(N22),FG,
     1          NFNFS,NFNFB,NUMFN,NNN)
      IF(KOMP.GE.1) CALL SUMF2(A(N22),A(N23))
C
C     SOLVE FOR HYDRODYNAMIC PRESSURE
C
      CALL COPYD(A(N8),A(N15),A(N4),NFNIF,NUMFN)
      IF(FG.NE.0.) GO TO 60
      CALL IMPOSE(A(N3),A(N15),A(N16),A(N22),NFNFS,NUMFN)
   60 CALL ACTCOL(A(N22),A(N15),A(N16),NUMFN,.TRUE.,.TRUE.)
      CALL OUTP(A(N4),A(N15),NFNIF,FREQ(I))
      CALL AMASSI(A(N4),A(N8),A(N15),A(N17),A(N18),ZCG,NFNIF,ITYPE(K),
     1            FREQ(I))
  100 CONTINUE
      GO TO 10
 1000 FORMAT(20A4/10I5/6F10.0)
 1010 FORMAT(15)
 1020 FORMAT(8F10.0)
 1030 FORMAT(A3)
 2000 FORMAT(1H1,20A4///
     1//38H C O N T R O L  I N F O R M A T I O N /
     2//55H NUMBER OF TOTAL FLUID NODAL CIRCLES . . . . . I5
     3//55H NUMBER OF TOTAL FLUID ELEMENTS  . . . . . I5
     4//55H NUMBER OF NODES PER ELEMENT . . . . . I5
     5//55H NUMBER OF FLUID NODAL CIRCLES ON THE INTERFACE. . . I5
     6//55H NUMBER OF FLUID NODAL CIRCLES ON THE FREE SURFACE . . I5
     7//55H NUMBER OF FLUID NODAL CIRCLES ON THE TRANSMITTING
     8/ 55H                                BOUNDARY . . I5
     9//55H NUMBER OF MODES TO BE USED ON TRANSMITTING BOUNDARY . I5
     0//55H NUMBER OF TYPES OF EXCITATION . . . . . I5
     A//55H DEPTH OF FLUID AT THE TRANSMITTING BOUNDARY . . . . . F10.3
     B//55H RADIUS OF THE TRANSMITTING BOUNDARY . . . . . F10.3
     C//55H WEIGHT PER UNIT VOLUME OF FLUID . . . . . F10.3
     D//55H GRAVITY CONSTANT . . . . . F10.3
     E//55H CENTER OF GRAVITY OF THE TANK (ZCG) . . . . . F10.3)
 2010 FORMAT(23HOSTORAGE IS EXCEEDED BY ,I6)
 2020 FORMAT(///37H NUMBER OF EXCITATION FREQUENCIES   =,I5//
     1       30H EXCITATION FREQUENCIES IN CPS/(12F10.2))
 2030 FORMAT(
     1   55H  VELOCITY OF SOUND IN FLUID . . . . . F10.3)
 2040 FORMAT(//40H COMPRESSIBILITY OF FLUID IS INCLUDED   )
 2050 FORMAT(//39H COMPRESSIBILITY OF FLUID IS NEGLECTED )
 2060 FORMAT(41H1H O R I Z O N T A L  E X C I T A T I O N )
 2070 FORMAT(37H1V E R T I C A L  E X C I T A T I O N )
 2080 FORMAT(/28H SURFACE WAVES ARE NEGLECTED )
 2090 FORMAT(/27H SURFACE WAVES ARE INCLUDED )
 2100 FORMAT(42H1R O T A T I O N A L  E X C I T A T I O N )
      END
      SUBROUTINE ACTCOL(A,B,LDIAG,NEQ,AFAC,BACK)
C*********************************************************************
C
C     ACTIVE COLUMN PROFILE SYMMETRIC EQUATION SOLVER
C       A(1) A(4) . . . . . .
C            A(3) A(5) . . . . . .
C                 A(6) . . . . . .
C
C*********************************************************************
```

Reproduced with permission of the copyright owner. Further reproduction prohibited without permission.

```
      DIMENSION A(1),B(1),LDIAG(1)
      LOGICAL AFAC,BACK
      COMPLEX A,B,D,DOT
C
C     FACTOR A TO UT*D*U,REDUCE B
C
      JP=0
      DO 600 J=1,NEQ
      JD=LDIAG(J)
      JH=JD-JP
      IS=J-JH+2
      IF(JH-2) 600,300,100
  100 IF(.NOT.AFAC) GO TO 500
      IE=J-1
      K=JP+2
      ID=LDIAG(IS-1)
C     REDUCE ALL EQUATIONS EXCEPT DIAGONAL
      DO 200 I=IS,IE
      IR=ID
      ID=LDIAG(I)
      IM=MINO(ID-IR-1,I-IS+1)
      IF(IM.GT.0) A(K)=A(K)-DOT(A(K-IM),A(ID-IM),IM)
  200 K=K+1
C     REDUCE DIAGONAL TERM
  300 IF(.NOT.AFAC) GO TO 500
      IR=JP+1
      IE=JD-1
      K=J-JD
      DO 400 I=IR,IE
      ID=LDIAG(K+I)
      IF(A(ID).EQ.(0.,0.)) GO TO 400
      D=A(I)
      A(I)=A(I)/A(ID)
      A(JD)=A(JD)-D*A(I)
  400 CONTINUE
C     REDUCE RHS
  500 IF(BACK) B(J)=B(J)-DOT(A(JP+1),B(IS-1),JH-1)
  600 JP=JD
      IF(.NOT.BACK) RETURN
C     DIVIDE BY DIAGONAL PIVOTS
      DO 700 I=1,NEQ
      ID=LDIAG(I)
      IF(A(ID).NE.(0.,0.)) B(I)=B(I)/A(ID)
  700 CONTINUE
C
C     BACKSUBSTITUTE
C
      J=NEQ
      JD=LDIAG(J)
  800 D=B(J)
      J=J-1
      IF(J.LE.0) RETURN
      JR=LDIAG(J)
      IF(JD-JP.LE.1) GO TO 1000
      IS=J-JD+JR+2
      K=JP-IS+1
      DO 900 I=IS,J
  900 B(I)=B(I)-A(I+K)*D
 1000 JD=JR
      GO TO 800
      END
```

Reproduced with permission of the copyright owner. Further reproduction prohibited without permission.

```
      SUBROUTINE AMASS1(NIF,D,P,DR,DZ,ZCG,NFNIF,ITYPE,FREQ)
C
C     COMPUTE ADDED MASSES
C
      DIMENSION NIF(1),D(1),DR(1),DZ(1)
      COMPLEX P(1),AMRR,AMOR
      COMMON/TAPES/ITN,IOUT
      COMMON/PI/PI
C
C     HORIZONTAL ADDED MASS
      AMRR=(0.,0.)
      DO 40 I=1,NFNIF
      N=NIF(I)
   40 AMRR=AMRR+P(N)*D(I)
      AMRR=AMRR*PI
      IF(ITYPE.NE.2) GO TO 60
C     VERTICAL ADDED MASS
      AMRR=AMRR*2.
      WRITE(IOUT,2200) AMRR
      RETURN
C     COUPLED ADDED MASS
   60 AMOR=(0.,0.)
      DO 80 I=1,NFNIF
      N=NIF(I)
   80 AMOR=AMOR+P(N)*(DR(I)-DZ(I))
      IF(ITYPE.EQ.3) GO TO 100
      AMOR=AMOR*PI+ZCG*AMRR
      WRITE(IOUT,2000) AMRR
      WRITE(IOUT,2100) AMOR
      RETURN
  100 AMOR=(AMRR-AMOR*PI)/ZCG
      WRITE(IOUT,2300) AMRR
      WRITE(IOUT,2100) AMOR
      RETURN
 2000 FORMAT(////22H HORIZONTAL ADDED MASS/6X,4HREAL,5X,9HIMAGINARY/1X,
     1       2E12.5)
 2100 FORMAT(//41H COUPLED HORIZONTAL-ROTATIONAL ADDED MASS /6X,4HREAL,
     1       5X,9HIMAGINARY/1X,2E12.5)
 2200 FORMAT(////20H VERTICAL ADDED MASS /6X,4HREAL,5X,9HIMAGINARY/1X,
     1       2E12.5)
 2300 FORMAT(///22H ROTATIONAL ADDED MASS /6X,4HREAL,5X,9HIMAGINARY/1X,
     1       2E12.5)
      END
      SUBROUTINE BESSEL(LM,RO,RR,PI,ICODE,ITYPE)
C*********************************************************************
C
C     BESSEL FUNCTIONS
C
C*********************************************************************
      COMMON/PI/PI
      REAL JO,J1,JY1,KO,KT,KY1,LM
C
      RL=RO*LM
      IF(ICODE.EQ.1) GO TO 300
      X=RL/3.
      X2=X*X
      X3=X*X2
      X4=X*X3
      X5=X*X4
      X6=X*X5
      X8=X4*X4
```

Reproduced with permission of the copyright owner. Further reproduction prohibited without permission.

```
      X10=X5*X5
      X12=X6*X6
      IF(RL.GT.3.) GO TO 80
      JO=1.-2.2499997*X2+1.2656208*X4-.3163866*X6+.0444479*X8-.0039444*X
     110+.0002100*X12
      YO=2.*ALOG(RL/2.)*JO/PI+.36746691+.60559366*X2-.7478038*X4+
     1.2535011?*X6-.4261214*X8+.00427916*X10-.00024846*X12
      JI=RL*(.5-.5624985*X2+.2109373?*X4-.0395428?*X6+.0044331?*X8-
     1.0003176?*X10+.0000109?*X12)
      YI=(2.*PL*ALOG(RL*.5)*JI/PI-.6366198+.2212091*X2+2.168279?*X4-
     11.3164827*X6+.3123951*X8-.0400576*X10+.0027873*X12)/RL
      GO TO 90
   80 FO=.7978?8456-.00000077/X-.00552740/X2-.00009512/X3+.00137237/X4-
     1 .0007?805/X5+.00014476/X6
      THETA=RL-.7853?816-.04166397/X-.00003954/X2+.00?62573/X3-.00054125
     1/X4-.0002?333/X5+.00013558/X6
      SRL=SQRT(RL)
      JO=FO*COS(THETA)/SRL
      YO=FO*SIN(THETA)/SRL
      FI=.7978?8456+.00000156/X+.01659667/X2+.00017105/X3-.00249511/X4+
     1.00113653/X5-.00020033/X6
      THETA=RL-2.3561?A49+.12499612/X+.00005650/X2-.00637879/X3+
     1.0007A3A?/X4+.00079824/X5-.00029166/X6
      JI=FI*COS(THETA)/SRL
      YI=FI*SIN(THETA)/SRL
   90 IF(ITYPE.EQ.2) GO TO 100
      JII=JI*2./RL-JO
      YII=YI*2./RL-YO
C
      DOS=(JI*JI+YI*YI)/((JO-JII)*(JO-JII)+(YO-YII)*(YO-YII))
      DO=SQRT(DOS)
      ER1=ATAN2(-YI,JI)
      ER2=ATAN2(-YO+YII,JO-JII)
      ER=ER1-ER2
      RR= .5?LM*COS(ER)/DO
      RI=-.5?LM*SIN(ER)/DO
      RETURN
  100 DOS=(JO*JO+YO*YO)/(JI*JI+YI*YI)
      DO=SQRT(DOS)
      ER1=ATAN2(-YO,JO)
      ER2=ATAN2(-YI,JI)
      ER=ER1-ER2
      RR=-LM*COS(ER)/DO
      RI= LM*SIN(ER)/DO
      RETURN
C
C     MODIFIED BESSEL FUNCTIONS
  300 RI=0.
      RR=-LM
      IF(RL.GT.170.) RETURN
      X=2./RL
      X2=X*X
      X3=X*X2
      X4=X*X3
      X5=X*X4
      X6=X*X5
      IF(RL.LE.2.) GO TO 310
      KO=(1.25331414-.07A3235A*X+.02199568*X2-.0106?446*X3+.005A7872*X4-
     1 .002?1540*X5+.00053208*X6)/(SQRT(RL)*EXP(RL))
      KI=(1.25331414+.23498619?X-.036?5620*X2+.01504268*X3-.007A0353*X4+
     1.00325614*X5-.00068245*X6)/(SQRT(RL)*EXP(RL))
```

Reproduced with permission of the copyright owner. Further reproduction prohibited without permission.

```
      GO TO 320
  310 T2=(RL/3.75)*(RL/3.75)
      T4=T2*T2
      T6=T4*T2
      T8=T4*T4
      T10=T8*T2
      T12=T6*T6
      KO=1.+3.5156229*T2+3.0899424*T4+1.2067492*T6+.2659732*T8+.0360768*
     1T10+.0045813*T12
      KI=RL*(.5+.87890594*T2+.51498869*T4+.15084934*T6+.02658733*T8+
     1.00301532*T10+.00032411*T12)
      KO=-ALOG(1./X)*KO+.57721566+.42278420/X2+.23069756/X4+.0348859D/X6
     1+.00262698/(X6*X2)+.00010750/(X5*X5)+.0000074D/(X6*X6)
      KI=(RL*ALOG(1./X)*KI+1.+.15443144/X2-.67278579/X4+.18156897/X6-
     1.01919402/(X6*X2)+.00110404/(X5*X5)+.00004686/(X6*X6))/RL
  320 IF(ITYPE.EQ.2) GO TO 350
      KT=KO+2.*KI/RL
      EM=KI/(KO*KI)
      RR=-.5*LM/EM
      RETURN
  350 RR=-LM*K1/KO
      RETURN
      END
      SUBROUTINE BOUND(Z,NTB,T,NFNTB,NUMFN)
C*************************************************************************
C
C     READ NODE NUMBERS ON TRANSMITTING BOUNDARY
C      FORM LAYER THICKNESS ARRAY
C
C*************************************************************************
      DIMENSION NTB(1),T(1),Z(1)
      COMMON/TAPES/IIN,IOUT
C
C     READ NODE NUMBERS ON THE TRANSMITTING BOUNDARY
C
      READ(IIN,1000) (NTB(I),I=1,NFNTB)
      IF(NFNTB.LT.3) GO TO 15
      DO 10 I=3,NFNTB
      IF(NTB(I).LE.0) NTB(I)=NTB(I-1)*2-NTB(I-2)
      IF(NTB(I).LE.0.OR.NTB(I).GT.NUMFN) GO TO 100
   10 CONTINUE
C
C     PRINT TRANSMITTING BOUNDARY NODE NUMBERS
C
   15 WRITE(IOUT,2000)
      WRITE(IOUT,2010) (NTB(I),I=1,NFNTB)
C
C     ARRAY OF LAYER THICKNESSES AT TRANSMITTING BOUNDARY
C
      NT=NFNTB-1
      K=NTB(1)
      DO 20 I=1,NT
      KK=NTB(I+1)
      T(I)=ABS(Z(K)-Z(KK))
   20 K=KK
      RETURN
  100 WRITE(IOUT,2100)
      STOP
 1000 FORMAT(16I5)
 2000 FORMAT(///105H NODE NUMBERS ON THE TRANSMITTING BOUNDARY(IN ORDER
     1FROM THE NODE ON THE FREE SURFACE TO THE BOTTOM NODE) //)
```

Reproduced with permission of the copyright owner. Further reproduction prohibited without permission.

```
 2010 FORMAT(2A1S)
 2100 FORMAT(//90H *****ERROR***** NODE NUMBER ON TRANSMITTING BOUNDARY
     1IS GREATER THAN NUMFN OR LESS THAN 1    )
      END
      SUBROUTINE CB(S,WT,R,C)
C*************************************************************************
C
C     AXISYMMETRIC 3-NODE LINE ELEMENT
C
C*************************************************************************
      DIMENSION R(3),C(3,3),H(3),HS(3)
C
C     INTERPOLATION FUNCTIONS
      H(1)=.5*S*(1.-S)-(1.-S*S)
      H(2)=1.-S*S
      H(3)=.5*S*((1.+S)-(1.-S*S))
C     DERIVATIVES
      HS(1)=-.5+S
      HS(2)=-2.*S
      HS(3)= .5+S
C     RADIUS AND JACOBIAN
      RR=H(1)*R(1)+H(2)*R(2)+H(3)*R(3)
      XJ=HS(1)*R(1)+HS(2)*R(2)+HS(3)*R(3)
      RJ=RR*XJ
C     FORM C(3,3) (CONTRIBUTION OF PT S)
      DO 10 I=1,3
      DO 10 J=1,3
   10 C(I,J)=WT*H(I)*H(J)*RJ
      RETURN
      END
      SUBROUTINE COPO2(P,Q,PP,QQ,NFNTB,N)
C
C     COPY MATRICES P,Q WHEN SURFACE WAVES ARE NEGLECTED
C
      DIMENSION P(NFNTB,1),Q(NFNTB,1),PP(N,1),QQ(N,1)
C
      DO 10 I=1,N
      DO 10 J=1,N
      PP(I,J)=P(I+1,J+1)
   10 QQ(I,J)=Q(I+1,J+1)
      RETURN
      END
      SUBROUTINE COPYD(D,DD,NIF,NFNIF,NUMFN)
C*************************************************************************
C
C     COPY REAL ARRAY D INTO COMPLEX ARRAY DD
C
C*************************************************************************
      DIMENSION D(1),NIF(1)
      COMPLEX DD(1)
      COMMON/WG/W,G
C
      DO 10 I=1,NUMFN
   10 DD(I)=(0.,0.)
      DO 20 I=1,NFNIF
      J=NIF(I)
   20 DD(J)=CMPLX(D(I),0.)*W/G
      RETURN
      END
      SUBROUTINE COPYPQ(P,Q,PP,QQ,NFNTB)
```

Reproduced with permission of the copyright owner. Further reproduction prohibited without permission.

```
C     COPY MATRICES P,Q
C
      DIMENSION P(NFNTB,1),Q(NFNTB,1),PP(NFNTB,1),QQ(NFNTB,1)
C
      DO 10 I=1,NFNTB
      DO 10 J=1,NFNTB
      PP(I,J)=P(I,J)
   10 QQ(I,J)=Q(I,J)
      RETURN
      END
      SUBROUTINE CTB(C,NFNTB,NE)
C
C     READ ARRAY C (VELOCITIES OF SOUND IN LAYEPS AT TRANSMITTING
C      BOUNDARY)
C
      DIMENSION C(1)
      COMMON/TAPES/IIN,IOUT
C
      N=NFNTB-1
      IF(NE.EQ.8) N=N/2
      READ(IIN,1000) (C(I),I=1,N)
      WRITE(IOUT,2000)
      DO 10 I=1,N
   10 WRITE(IOUT,2010) I,C(I)
      RETURN
 1000 FORMAT(8F10.0)
 2000 FORMAT(//61H VELOCITY OF SOUND IN EACH LAYER AT THE TRANSMITTING B
     1OUNDARY(FROM TOP TO BOTTOM)
     2       /10H LAYER NO.,5X,17HVELOCITY OF SOUND)
 2010 FORMAT(17,10X,F10.1)
      END
      SUBROUTINE DMULT(A,B,D,M,N,RTB)
C*****************************************************************************
C
C     A(N,N)=B(N,M)*D(M,M)*BT(M,N)*RTB
C      WHERE D=DIAGONAL MATRIX
C
C*****************************************************************************
      DIMENSION A(N,N),D(M),B(N,M)
      COMMON/PI/PI
C
      DO 10 I=1,N
      DO 10 J=1,N
   10 A(I,J)=0.
      DO 20 I=1,N
      DO 20 J=I,N
      DO 20 K=1,M
      IF(D(K).EQ.0.) GO TO 20
      A(I,J)=A(I,J)+B(I,K)*D(K)*B(J,K)
   20 CONTINUE
      DO 30 I=1,N
      DO 30 J=I,N
      A(I,J)=A(I,J)*RTB
   30 A(J,I)=A(I,J)
      RETURN
      END
      COMPLEX FUNCTION DOT(A,B,N)
C
C     VECTOR DOT PRODUCT
C
      COMPLEX A(1),B(1)
```

Reproduced with permission of the copyright owner. Further reproduction prohibited without permission.

```
      DOT=(0.,0.)
      DO 10 I=1,N
   10 DOT=DOT+A(I)*B(I)
      RETURN
      END
      SUBROUTINE EDATA(NODE,C,MHT,LDIAG,NE,NUMFE,NUMFN)
C*****************************************************************************
C
C     READ, GENERATE AND PRINT ELEMENT NODE NUMBERS
C      AND DETERMINE PROFILE
C
C*****************************************************************************
      DIMENSION NODE(NUMFE,I),LDIAG(1),MHT(1),C(1)
      COMMON/TAPES/IIN,IOUT
      COMMON/LA/LA
      COMMON/COMP/KOMP
C
C     READ, GENERATE AND PRINT NODES OF ELEMENTS
C
      WRITE(IOUT,2000)
      WRITE(IOUT,2010)
      DO 5 I=1,NUMFN
    5 MHT(I)=0
      M=0
      KN=0
   10 KNOLD=KN
      IF(KOMP-1) 11,11,13
   11 READ(IIN,1000) N,(NODE(N,I),I=1,NE),KN
      GO TO 20
   13 IF(NE.EQ.4) READ(IIN,1010) N,(NODE(N,I),I=1,NE),KN,C(N)
      IF(NE.EQ.8) READ(IIN,1020) N,(NODE(N,I),I=1,NE),KN,C(N)
      NC=0
   20 M=M+1
      IF(M.EQ.N) GO TO 40
      IF(KN.EQ.0) KN=1
      IF(KOMP.NE.2) GO TO 25
      IF(NC.EQ.0) CC=(C(N)-C(M-1))/FLOAT(IABS(N-M+1))
      C(M)=C(M-1)+CC
      NC=NC+1
   25 DO 30 I=1,NE
   30 NODE(M,I)=NODE(M-1,I)+KNOLD
   40 IF(KOMP.NE.2) WRITE(IOUT,2020) M,(NODE(M,I),I=1,NE)
      IF((KOMP.EQ.2).AND.(NE.EQ.4)) WRITE(IOUT,2030) M,
     1 (NODE(M,I),I=1,NE),C(M)
      IF((KOMP.EQ.2).AND.(NE.EQ.8)) WRITE(IOUT,2040) M,
     1 (NODE(M,I),I=1,NE),C(M)
      IF(M.NE.N) GO TO 70
C
C     DETERMINE PROFILE
C
C     DETERMINE SMALLEST NODE NUMBER OF THE ELEMENT
      NS=100000
      DO 50 I=1,NE
      IF(NODE(M,I).LT.NS) NS=NODE(M,I)
   50 CONTINUE
C     DETERMINE COLUMN HEIGHT ABOVE DIAGONAL
      DO 60 I=1,NE
      II=NODE(M,I)
      IHT=II-NS
      IF(IHT.GT.MHT(II)) MHT(II)=IHT
   60 CONTINUE
```

Reproduced with permission of the copyright owner. Further reproduction prohibited without permission.

```
   70 IF(M.EQ.NUMFE) GO TO 90
      IF(M.EQ.N) GO TO 10
      DO 80 I=1,NE
      II=NODE(M,I)
      JJ=NODE(M-1,I)
      IF(MHT(II).LT.MHT(JJ)) MHT(II)=MHT(JJ)
   80 CONTINUE
   10 GO TO 20
C     LOCATION ARRAY OF DIAGONALS
   90 LDIAG(1)=1
      DO 100 I=2,NUMFN
  100 LDIAG(I)=LDIAG(I-1)+MHT(I)+1
      LA=LDIAG(NUMFN)
      RETURN
 1000 FORMAT(1015)
 1010 FORMAT(615,F10.0)
 1020 FORMAT(1015,F10.0)
 2000 FORMAT(1H1,34HF L U I D  E L E M E N T  D A T A //)
 2010 FORMAT(14H FLUID ELEMENT,40X,5HNODES,37X,8HVELOCITY/
     1         4X,6HNUMBER,11X,1HI,9X,1HJ,9X,1HK,9X,1HL,8X,2HIJ,8X,2HJK,
     2         8X,2HKL,8X,2HLI,4X,8HOF SOUND //)
 2020 FORMAT(3X,15,4X,8(5X,I5))
 2030 FORMAT(3X,15,4X,4(5X,I5),4X,F10.1)
 2040 FORMAT(3X,15,4X,8(5X,I5),11X,F10.1)
      END
      SUBROUTINE FORM(T,P,Q,N,NE)
C*********************************************************************
C
C     FORM MATRICES P,Q
C
C*********************************************************************
      DIMENSION P(N,1),Q(N,1),T(1)
      DO 20 I=1,N
      DO 20 J=1,N
      P(I,J)=0.
   20 Q(I,J)=0.
      NN=N-1
      IF(NE.EQ.8) GO TO 50
      P(1,1)=1./T(1)
      P(1,2)=-P(1,1)
      Q(1,1)=T(1)/3.
      Q(1,2)=T(1)/6.
      P(N,N)=1./T(NN)
      P(N,N-1)=-P(N,N)
      Q(N,N)=T(NN)/3.
      Q(N,N-1)=T(NN)/6.
      DO 40 I=2,NN
      P(I,I)=1./T(I-1)+1./T(I)
      P(I,I-1)=-1./T(I-1)
      P(I,I+1)=-1./T(I)
      Q(I,I)=(T(I-1)+T(I))/3.
      Q(I,I-1)=T(I-1)/6.
   40 Q(I,I+1)=T(I)/6.
      RETURN
   50 M=NN/2
      DO 70 L=1,M
      I=2*L-1
      IF(T(I).EQ.T(I+1)) GO TO 60
      A=T(I)
      B=T(I+1)
      D=A+B
```

Reproduced with permission of the copyright owner. Further reproduction prohibited without permission.

```
      A2=A*A
      B2=B*B
      D2=D*D
      D3=D*D2
      P(I,I)     =P(I,I)+(82*D+4.*D3/3.-2.*B*D2)/(D2*A2)
      P(I,I+1)   =-D2/(3.*A2*B)
      P(I,I+2)   =(D2/3.-A*B)/(D*A*B)
      P(I+1,I+1)=D3/(3.*A2*B2)
      P(I+1,I+2)=-D2/(3.*A*B2)
      P(I+2,I+2)=(4.*D2/3.-A*(D+B))/(D*B2)
      Q(I,I)     =Q(I,I)+D*(82/3.+D2/5.-B*D/2.)/A2
      Q(I,I+1)   =D3*(5.*A-2.*D)/(60.*A2*B)
      Q(I,I+2)   =D*(-10.*B2+10.*D*B-3.*D2)/(60.*A*B)
      Q(I+1,I+1)=D3*D2/(30.*A2*B2)
      Q(I+1,I+2)=D3*(5.*B-2.*D)/(60.*A*B2)
      Q(I+2,I+2)=D*(D2-5.*D*B+10.*B2)/(30.*B2)
      GO TO 70
   60 D=T(I)+T(I+1)
      DP=D*3.
      DD=D/30.
      P(I,I)     =P(I,I)+7./DP
      P(I,I+1)   =-8./DP
      P(I,I+2)   =1./DP
      P(I+1,I+1)=16./DP
      P(I+1,I+2)=-8./DP
      P(I+2,I+2)=7./DP
      Q(I,I)     =Q(I,I)+4.*DD
      Q(I,I+1)   =2.*DD
      Q(I,I+2)   =-DD
      Q(I+1,I+1)=16.*DD
      Q(I+1,I+2)=2.*DD
      Q(I+2,I+2)=4.*DD
   70 CONTINUE
      DO 80 I=1,N
      DO 80 J=I,N
      P(J,I)=P(I,J)
   80 Q(J,I)=Q(I,J)
      RETURN
      END
      SUBROUTINE FORM4(S,T,R,Z,HH,NE,ITYPE,III)
C*****************************************************************************
C
C     AXISYMMETRIC 4 OR 8-NODE QUADRILATERAL TOROID ELEMENT OF FLUID
C
C*****************************************************************************
      DIMENSION H(8),HS(8),HT(8),R(1),Z(1),HR(8),HZ(8),HH(8,1)
      COMMON/TAPES/IIN,IOUT
      COMMON/NEL/NEL
C
      SM=1.-S
      SP=1.+S
      TM=1.-T
      TP=1.+T
C
C     INTERPOLATION FUNCTIONS
C
      H(1)=SM*TM/4.
      H(2)=SP*TM/4.
      H(3)=SP*TP/4.
      H(4)=SM*TP/4.
```

Reproduced with permission of the copyright owner. Further reproduction prohibited without permission.

```
C     NATURAL COORDINATE DERIVATIVES OF INTERPOLATION FUNCTIONS
C
      HS(1)=-TM/4.
      HS(2)=-HS(1)
      HS(3)= TP/4.
      HS(4)=-HS(3)
      HT(1)=-SM/4.
      HT(2)=-SP/4.
      HT(3)=-HT(2)
      HT(4)=-HT(1)
C
C     8-NODE ELEMENT
C
      IF(NE.LE.4) GO TO 20
      H(5)=SM*SP*TM/2.
      H(6)=SP*TP*TM/2.
      H(7)=SP*SM*TP/2.
      H(8)=SM*TP*TM/2.
C
      HS(5)=-S*TM
      HS(6)= TM*TP/2.
      HS(7)=-S*TP
      HS(8)=-HS(6)
      HT(5)=-SM*SP/2.
      HT(6)=-T*SP
      HT(7)=-HT(5)
      HT(8)=-T*SM
C
      H(1) =H(1) -(H(5)+H(8))/2.
      HS(1)=HS(1)-(HS(5)+HS(8))/2.
      HT(1)=HT(1)-(HT(5)+HT(8))/2.
      DO 10 I=2,4
      H(I) =H(I) -(H(I+3) +H(I+4) )/2.
      HS(I)=HS(I)-(HS(I+3)+HS(I+4))/2.
   10 HT(I)=HT(I)-(HT(I+3)+HT(I+4))/2.
C
C     JACOBIAN AT POINT (S,T)
C
   20 RS=0.
      RT=0.
      ZS=0.
      ZT=0.
      DO 30 I=1,NE
      RS=RS+HS(I)*R(I)
      RT=RT+HT(I)*R(I)
      ZS=ZS+HS(I)*Z(I)
   30 ZT=ZT+HT(I)*Z(I)
      XJ=RS*ZT-RT*ZS
      IF(XJ.GT.0.00000001) GO TO 40
      WRITE(IOUT,2000) NEL
      STOP
C
C     RADIUS AT POINT (S,T)
C
   40 RR=0.
      DO 50 I=1,NE
   50 RR=RR+H(I)*R(I)
C
C     R-Z COORDINATE DERIVATIVES OF INTERPOLATION FUNCTIONS
C
      DO 60 I=1,NE
```

Reproduced with permission of the copyright owner. Further reproduction prohibited without permission.

```
      HR(I)=(HS(I)*ZT-HT(I)*ZS)/XJ
   60 HZ(I)=(-HS(I)*RT+HT(I)*RS)/XJ
C
C     FORM MATRIX HH AT POINT (S,T)
C
      IF(III.EQ.2) GO TO 90
      DO 70 I=1,NE
      DO 70 J=I,NE
      HH(I,J)=(HR(I)*HR(J)+HZ(I)*HZ(J))*RR*XJ
   70 HH(J,I)=HH(I,J)
      IF(ITYPE.EQ.2) RETURN
      DO 80 I=1,NE
      DO 80 J=I,NE
      HH(I,J)=HH(I,J)+H(I)*H(J)*XJ/RR
   80 HH(J,I)=HH(I,J)
      RETURN
   90 DO 100 I=1,NE
      DO 100 J=I,NE
      HH(I,J)=H(I)*H(J)*RR*XJ
  100 HH(J,I)=HH(I,J)
      RETURN
 2000 FORMAT(18H ***** ERROR *****,
     1       38H ZERO OR NEGATIVE JACOBIAN FOR ELEMENT,I5)
      END
      SUBROUTINE FORMC(R,NFS,C,NE,NFNFS)
C*********************************************************************
C
C     FORM MATRIX FS
C
C*********************************************************************
      DIMENSION C(NFNFS,1),NFS(1),R(1)
      DIMENSION GP(4),WT(4),PR(3),CC(2,2),CCC(3,3),CP(3,3)
      DATA GP/-.8611363115940S,-.3399810435848S,.33998104358486,.86113631159405/
     1       ,-.86113631159405/
      DATA WT/.34785484513745,.65214515486255,.65214515486255
     1       ,.34785484513745/
C
      DO 10 I=1,NFNFS
      DO 10 J=1,NFNFS
   10 C(I,J)=0.
C
      NN=NFNFS-1
      IF(NE.EQ.8) GO TO 30
      DO 20 N=1,NN
      I=NFS(N)
      J=NFS(N+1)
      RI=R(I)
      RJ=R(J)
      RI2=RI*RI
      RJ2=RJ*RJ
      DRS=(RJ-RI)*(RJ-RI)
      DR2=ABS(RJ-RI2)
      DR3=ABS(RJ2*RJ-RI2*RI)
      DR4=ABS(RJ2*RJ2-RI2*RI2)
C
      CC(1,1)=(.25*DR4-2.*DR3*RJ/3.+.5*DR2*RJ2)/DRS
      CC(2,2)=(.25*DR4-2.*DR3*RI/3.+.5*DR2*RI2)/DRS
      CC(1,2)=(-.25*DR4+DR3*(RJ+RI)/3.-.5*DR2*RJ*RI)/DRS
      CC(2,1)=CC(1,2)
C
      C(N,N)=C(N,N)+CC(1,1)
```

Reproduced with permission of the copyright owner. Further reproduction prohibited without permission.

```
      C(N,N+1)=C(N,N+1)+CC(1,2)
      C(N+1,N)=C(N+1,N)+CC(2,1)
      C(N+1,N+1)=C(N+1,N+1)+CC(2,2)
   20 CONTINUE
      RETURN
   30 NN=NN/2
      DO 90 N=1,NN
C     RADIUS OF NODE
      DO 40 J=1,3
      JJ=2*N-2+J
      I=NFS(JJ)
   40 RR(J)=R(I)
C
C     FORM CCC(3,3)
C
      DO 50 I=1,3
      DO 50 J=1,3
   50 CCC(I,J)=0.
C     CONTRIBUTION FROM EACH GAUSS POINT
      DO 70 II=1,4
      CALL CR(GP(II),WT(II),RR,CP)
      DO 60 I=1,3
      DO 60 J=1,3
   60 CCC(I,J)=CCC(I,J)+CP(I,J)
   70 CONTINUE
C
C     ASSEMBLE C(NFNFS,NFNFS)
C
      K=2*N-1
      DO 80 I=1,3
      L=K-1+I
      DO 80 J=1,3
      M=K-1+J
   80 C(L,M)=C(L,M)+CCC(I,J)
   90 CONTINUE
      RETURN
      END
      SUBROUTINE FORMD(R,Z,NIF,D,DDR,DDZ,ZCG,NE,NFNIF,NUMFN,ITYPE)
C*********************************************************************
C
C     FORM VECTOR D ALONG NODES ON THE INTERFACE
C
C*********************************************************************
      DIMENSION D(1),R(1),Z(1),NIF(1),DD(3,3)
      DIMENSION DDR(1),DDZ(1)
C
      DO 10 I=1,NFNIF
   10 D(I)=0.
C
      NL=NFNIF-1
      IF(ITYPE.EQ.2) GO TO 70
C
C     FOR HORIZONTAL EXCITATION
C
      IF(NE.EQ.8) GO TO 30
C     FOR LINEAR ELEMENTS
      DO 20 N=1,NL
      I=NIF(N)
      J=NIF(N+1)
      DZ=ABS(Z(J)-Z(I))
      IF(DZ.EQ.0.) GO TO 20
```

Reproduced with permission of the copyright owner. Further reproduction prohibited without permission.

```
      D(N)=D(N)+DZ*(2.*R(I)+R(J))/6.
      D(N+1)=D(N+1)+DZ*(2.*R(J)+R(I))/6.
   20 CONTINUE
      IF(ITYPE.EQ.3) GO TO 110
      RETURN
C     FOR QUADRATIC ELEMENTS
   30 NL=NL/2
      DO 60 N=1,NL
      M=2*N-1
      I=NIF(M)
      J=NIF(M+1)
      K=NIF(M+2)
      IF(Z(I).EQ.Z(K)) GO TO 60
      DR=ABS(R(I)-R(J))
      DZ=ABS(Z(I)-Z(J))
      A=SQRT(DR*DR+DZ*DZ)
      DR=ABS(R(J)-R(K))
      DZ=ABS(Z(J)-Z(K))
      B=SQRT(DR*DR+DZ*DZ)
      T=A+B
      IF(A.EQ.B) GO TO 40
      A2=A*A
      B2=B*B
      T2=T*T
      T3=T*T2
      DD(1,1)=T*(B2/3.+T2/5.-B*T/2.)/A2
      DD(1,2)=T3*(5.*A-2.*T)/(60.*A2*B)
      DD(1,3)=T*(10.*A*B-3.*T2)/(60.*A*B)
      DD(2,2)=T3*T2/(30.*A2*B2)
      DD(2,3)=T3*(5.*B-2.*T)/(60.*A*B2)
      DD(3,3)=T*(T2-5.*T*B+10.*B2)/(30.*B2)
      GO TO 50
   40 TT=T/30.
      DD(1,1)=4.*TT
      DD(1,2)=2.*TT
      DD(1,3)=-TT
      DD(2,2)=16.*TT
      DD(2,3)=2.*TT
      DD(3,3)=4.*TT
   50 COSB=ABS(Z(I)-Z(K))/T
      D(M)=D(M)+COSB*(DD(1,1)*R(I)+DD(1,2)*R(J)+DD(1,3)*R(K))
      D(M+1)=D(M+1)+COSB*(DD(1,2)*R(I)+DD(2,2)*R(J)+DD(2,3)*R(K))
      D(M+2)=D(M+2)+COSB*(DD(1,3)*R(I)+DD(2,3)*R(J)+DD(3,3)*R(K))
   60 CONTINUE
      IF(ITYPE.EQ.3) GO TO 110
      RETURN
C
C     FOR VERTICAL EXCITATION
C
   70 IF(NE.EQ.4) GO TO 90
C     FOR LINEAR ELEMENTS
      DO 80 N=1,NL
      I=NIF(N)
      J=NIF(N+1)
      DR=R(J)-R(I)
      IF(DR.EQ.0.) GO TO 80
      DR2=ABS(R(J)*R(J)-R(I)*R(I))
      DR3=ABS(R(J)*R(J)-R(I)*R(I)*R(I)*R(I))
      D(N)=D(N)+(DR3/3.-R(J)*DR2/2.)/DR
      D(N+1)=D(N+1)+(DR3/3.-R(I)*DR2/2.)/DR
   80 CONTINUE
```

Reproduced with permission of the copyright owner. Further reproduction prohibited without permission.

```
      RETURN
C     FOR QUADRATIC ELEMENTS
   90 NL=NL/2
      DO 100 N=1,NL
      M=2*N-1
      I=NIF(M)
      J=NIF(M+1)
      K=NIF(M+2)
      A=ABS(R(I)-R(J))
      B=ABS(R(J)-R(K))
      T=A+B
      IF(T.EQ.0.) GO TO 100
      IF(A.EQ.B) GO TO 95
      T2=T*T
      D(M)=D(M)+T2*(2.*A-T)/(12.*(R(J)-R(I)))+T*R(I)*(3.*A-T)/(6.*A)
      D(M+1)=D(M+1)+T2*T*(B-A)/(12.*(R(J)-R(I))*B)+T2*T*R(J)/(6.*A*B)
      D(M+2)=D(M+2)+T2*(T-2.*B)/(12.*(R(K)-R(J)))+T*R(K)*(3.*B-T)/(6.*B)
      GO TO 100
   95 D(M)=D(M)+T*R(I)/6.
      D(M+1)=D(M+1)+T*(R(K)+R(I))/3.
      D(M+2)=D(M+2)+T*R(K)/6.
  100 CONTINUE
      RETURN
  110 DO 120 N=1,NFNIF
  120 D(N)=D(N)*ZCG-DDZ(N)+DDR(N)
      RETURN
      END
      SUBROUTINE FORMDR(R,DR,NIF,NFNIF)
C
C     FORM VECTOR DR
C
      DIMENSION R(1),DR(1),NIF(1)
C     FOR LINEAR ELEMENTS
      N=NFNIF-1
      DO 10 I=1,NFNIF
   10 DR(I)=0.
      DO 20 K=1,N
      I=NIF(K)
      J=NIF(K+1)
      IF(R(I).EQ.R(J)) GO TO 20
      R3=ABS(R(J)*R(J)-R(I)*R(I))*R(I)*R(I)
      R4=ABS(R(J)*R(J)*R(J)*R(J)-R(I)*R(I)*R(I)*R(I))
      DR(K)=DR(K)+(R(J)*R3/3.-R4/4.)/(R(J)-R(I))
      DR(K+1)=DR(K+1)+(R4/4.-R(I)*R3/3.)/(R(J)-R(I))
   20 CONTINUE
      RETURN
      END
      SUBROUTINE FORMDZ(R,Z,DZ,NIF,NFNIF)
C
C     FORM VECTOR DZ
C
      DIMENSION R(1),Z(1),DZ(1),NIF(1)
C     FOR LINEAR ELEMENTS
      N=NFNIF-1
      DO 10 I=1,NFNIF
   10 DZ(I)=0.
      DO 20 K=1,N
      I=NIF(K)
      J=NIF(K+1)
      IF(Z(I).EQ.Z(J)) GO TO 20
      ZI2=Z(I)*Z(I)
```

Reproduced with permission of the copyright owner. Further reproduction prohibited without permission.

```
      ZT3=ZT2*Z(I)
      ZT4=ZT3*Z(I)
      ZJ2=Z(J)*Z(J)
      ZJ3=ZJ2*Z(J)
      ZJ4=ZJ3*Z(J)
      Z2=ABS(ZJ2-ZT2)
      Z3=ABS(ZJ3-ZT3)
      Z4=ABS(ZJ4-ZT4)
      DZ(K)=DZ(K)+((Z(J)*R(I)-Z(I)*R(J))*(Z(J)*Z2/2.-Z3/3.)
     1 +(R(J)-R(I))*(Z(J)*Z3/3.-Z4/4.))/((Z(J)-Z(I))*(Z(J)-Z(I)))
      DZ(K+1)=DZ(K+1)+((Z(J)*R(I)-Z(I)*R(J))*(Z3/3.-Z(I)*Z2/2.)
     1 +(R(J)-R(I))*(Z4/4.-Z(I)*Z3/3.))/((Z(J)-Z(I))*(Z(J)-Z(I)))
   20 CONTINUE
      RETURN
      END
      SUBROUTINE FORMF(P,Z,NODE,LDIAG,C,F,NE,NUMFE,NUMFN,ITYPE,III)
C*********************************************************************
C
C     FORM FLUID ELEMENT MATRIX FE USING 2-POINT GAUSS QUADRATURE AND
C      ASSEMBLE GLOBAL MATRIX F
C
C*********************************************************************
      DIMENSION R(1),Z(1),NODE(NUMFE,1),F(1),LDIAG(1),C(1)
      DIMENSION GP(2),RR(8),ZZ(8),FE(8,8),H(8,8)
      COMMON/NEL/N
      COMMON/COMP/KOMP
      DATA GP/-.577350269189&3,.577350269189&3/
C
      LL=LDIAG(NUMFN)
      DO 5 I=1,LL
    5 F(I)=0.
C
      DO 100 N=1,NUMFE
C     COORDINATES OF NODES OF ELEMENT N
      DO 10 I=1,NE
      II=NODE(N,I)
      RR(I)=R(II)
   10 ZZ(I)=Z(II)
C
C     FORM ELEMENT MATRIX FE
C
      DO 20 I=1,NE
      DO 20 J=1,NE
   20 FE(I,J)=0.
C     CONTRIBUTION FROM EACH GAUSS POINT
      DO 40 II=1,2
      DO 40 JJ=1,2
      CALL FORM4(GP(II),GP(JJ),RR,ZZ,H,NE,ITYPE,III)
      DO 30 I=1,NE
      DO 30 J=1,NE
      FE(I,J)=FE(I,J)+H(I,J)
   30 CONTINUE
   40 CONTINUE
      DO 45 I=1,NE
      DO 45 J=1,NE
      IF((KOMP.EQ.2).AND.(III.EQ.2)) FE(I,J)=FE(I,J)/(C(N)*C(N))
   45 FE(J,I)=FE(I,J)
C
C     ASSEMBLE GLOBAL MATRIX F
C
      DO 50 I=1,NE
```

Reproduced with permission of the copyright owner. Further reproduction prohibited without permission.

```
      II=NODE(N,I)
      L=LDIAG(II)-II
      DO 50 J=1,NE
      JJ=NODE(N,J)
      IF(JJ.GT.II) GO TO 50
      JJ=L+JJ
      F(JJ)=F(JJ)+FE(J,I)
   50 CONTINUE
  100 CONTINUE
      RETURN
      END
      SUBROUTINE FORMPC(P,QC,NFNTB,NNN)
C
C     PC=PP-QC
C
      DIMENSION P(NNN,1),QC(NFNTB,1)
      COMMON/FREQS/FROS,C
C
      K=0
      IF(NNN.NE.NFNTB) K=1
      DO 10 I=1,NNN
      DO 10 J=I,NNN
      II=I+K
      JJ=J+K
      IF(P(I,J).EQ.0.) GO TO 10
      P(I,J)=P(I,J)-FROS*QC(II,JJ)
      P(J,I)=P(I,J)
   10 CONTINUE
      RETURN
      END
      SUBROUTINE FORMQC(T,C,QC,N,NE)
C
C     FORM MATRIX QC
C
      DIMENSION QC(N,1),T(1),C(1)
      DO 20 I=1,N
      DO 20 J=1,N
   20 QC(I,J)=0.
      NN=N-1
      IF(NE.EQ.8) GO TO 50
      QC(1,1)=T(1)/(3.*C(1)*C(1))
      QC(1,2)=T(1)/(6.*C(1)*C(1))
      QC(N,N)=T(NN)/(3.*C(NN)*C(NN))
      QC(N,N-1)=T(NN)/(6.*C(NN)*C(NN))
      DO 40 I=2,NN
      QC(I,I)=(T(I-1)/(C(I-1)*C(I-1))+T(I)/(C(I)*C(I)))/3.
      QC(I,I-1)=T(I-1)/(6.*C(I-1)*C(I-1))
   40 QC(I,I+1)=T(I)/(6.*C(I)*C(I))
      RETURN
   50 M=NN/2
      DO 70 L=1,M
      CC=C(L)*C(L)
      I=2*L-1
      IF(T(I).EQ.T(I+1)) GO TO 60
      A=T(I)
      B=T(I+1)
      D=A+B
      A2=A*A
      B2=B*B
      D2=D*D
      D3=D*D2
```

Reproduced with permission of the copyright owner. Further reproduction prohibited without permission.

```
      QC(I,I)    =QC(I,I)+D*(B2/3.+D2/5.-B*D/2.)/(A2*CC)
      QC(I,I+1)  =D3*(5.*A-2.*D)/(60.*A2*B*CC)
      QC(I,I+2)  =D*(-10.*B2+10.*D*B-3.*D2)/(60.*A*B*CC)
      QC(I+1,I+1)=D3*D2/(30.*A2*B2*CC)
      QC(I+1,I+2)=D3*(5.*B-2.*D)/(60.*A*B2*CC)
      QC(I+2,I+2)=D*(D2-5.*D*B*10.*B2)/(30.*B2*CC)
      GO TO 70
   60 D=T(I)+T(I+1)
      DP=D*3.
      DQ=D/30.
      QC(I,I)    =QC(I,I)+4.*DQ/CC
      QC(I,I+1)  =2.*DQ/CC
      QC(I,I+2)  =-DQ/CC
      QC(I+1,I+1)=16.*DQ/CC
      QC(I+1,I+2)=2.*DQ/CC
      QC(I+2,I+2)=4.*DQ/CC
   70 CONTINUE
      DO 80 I=1,N
      DO 80 J=I,N
   80 QC(J,I)=QC(I,J)
      RETURN
      END
      SUBROUTINE FREE(NFS,NFNFS,NUMFN)
C*************************************************************************
C
C     READ AND PRINT FREE SURFACE NODE NUMBERS
C
C*************************************************************************
      DIMENSION NFS(1)
      COMMON/TAPES/IIN,IOUT
C
C     READ FREE SURFACE NODE NUMBERS
C
      READ(IIN,1000) (NFS(I),I=1,NFNFS)
      IF(NFNFS.LT.3) GO TO 20
      DO 10 I=3,NFNFS
      IF(NFS(I).LE.0) NFS(I)=2*NFS(I-1)-NFS(I-2)
      IF(NFS(I).LE.0.OR.NFS(I).GT.NUMFN) GO TO 100
   10 CONTINUE
C
C     PRINT FREE SURFACE NODE NUMBERS
C
   20 WRITE(IOUT,2000)
      WRITE(IOUT,2010) (NFS(I),I=1,NFNFS)
      RETURN
  100 WRITE(IOUT,2100)
      STOP
 1000 FORMAT(16I5)
 2000 FORMAT(///43H NODE NUMBERS ON THE FREE SURFACE(IN ORDER)  //)
 2010 FORMAT(24I5)
 2100 FORMAT(//85H *****EPROP***** NODE NUMBER ON THE FREE SURFACE IS GR
     1EATER THAN NUMFN OR LESS THAN 1 )
      END
      SUBROUTINE IMPOSE(NFS,DD,LDIAG,SF,NFNFS,NUMFN)
C
C     IMPOSE BOUNDARY CONDITION THAT HYDRODYNAMIC PRESSURE AT FREE
C      SURFACE IS ZERO
C
      DIMENSION NFS(1),DD(1),LDIAG(1),SF(1)
      COMPLEX DD,SF
```

Reproduced with permission of the copyright owner. Further reproduction prohibited without permission.

```
      DO 100 I=1,NFNES
      J=NFS(I)
      DD(J)=(0.,0.)
      K=LDIAG(J)
      IF(J.EQ.1) GO TO 20
C     COLUMN J
      L=LDIAG(J-1)+1
      IF(K.EQ.L) GO TO 20
      KK=K-1
      DO 10 M=L,KK
   10 SF(M)=(0.,0.)
   20 SF(K)=(1.,0.)
C     ROW J
      JJ=J+1
      KK=0
      DO 50 M=JJ,NUMFN
      KK=KK+1
      L=LDIAG(M-1)
      N=LDIAG(M)
      IF(N-L.LE.KK) GO TO 50
      SF(N-KK)=(0.,0.)
   50 CONTINUE
  100 CONTINUE
      RETURN
      END
      SUBROUTINE INTER(NIF,NFNIF,NUMFN)
C*********************************************************************
C
C     READ AND PRINT INTERFACE NODE NUMBERS
C
C*********************************************************************
      DIMENSION NIF(1)
      COMMON/TAPES/IIN,IOUT
C
C     READ INETRFACE NODE NUMBERS
C
      READ(IIN,1000) (NIF(I),I=1,NFNIF)
      IF(NFNIF.LT.3) GO TO 20
      DO 10 I=3,NFNIF
      IF(NIF(I).LE.0) NIF(I)=2*NIF(I-1)-NIF(I-2)
      IF(NIF(I).LE.0.OR.NIF(I).GT.NUMFN) GO TO 100
   10 CONTINUE
C
C     PRINT INTERFACE NODE NUMBERS
C
   20 WRITE(IOUT,2000)
      WRITE(IOUT,2010) (NIF(I),I=1,NFNIF)
      RETURN
  100 WRITE(IOUT,2100)
      STOP
 1000 FORMAT(16I5)
 2000 FORMAT(40H1NODE NUMBERS ON THE INTERFACE(IN ORDER) //)
 2010 FORMAT(2415)
 2100 FORMAT(//85H *****ERROR****** NODE NUMBER ON THE INTERFACE IS GREAT
     1ER THAN NUMFN OR LESS THAN 1    )
      END
      SUBROUTINE JACOBI (A,B,X,E,N,NFIG,NSMAX)
C-----------------------------------------------------------------------
C  AN EIGENVALUE SOLUTION AFTER E.L. WILSON (1977)
C     SUBROUTINE SOLVES EIGENVALUE PROBLEM  AX = BXE  WHERE
C     A AND B ARE N X N SYMMETRIC MATPICES
```

Reproduced with permission of the copyright owner. Further reproduction prohibited without permission.

```
C      E IS A DIAGONAL MATRIX OF EIGENVALUES STORED AS A ROW ARRAY
C      X IS A N X N MATRIX OF EIGENVECTORS
C      NSMAX IS THE MAXIMUM NUMBER OF SWEEPS TO BE PERFORMED
C      NFIG IS THE NUMBER OF SIGNIFICANT FIGURES TO BE OBTAINED
C-------------------------------------------------------------------
       DIMENSION A(N,N),B(N,N),X(N,N),E(N)
C------INITIALIZATION-----------------------------------
       NT=0
       NN=N-1
       RTOL=0.1**(2*NFIG)
       EPS=0.01
       DO 30 I=1,N
       DO 20 J=1,N
    20 X(I,J)=0.
    30 X(I,I)=1.
       IF(N.EQ.1) GO TO 820
C------SWEEP OFF-DIAGONAL TERMS FOR POSSIBLE REDUCTION-------
       DO 800 M=1,NSMAX
       YMAX=0.0
       DO 700 J=1,NN
       JJ=J+1
       DO 700 K=JJ,N
C------COMPARE WITH THRESHOLD VALUE---------------------
       EA=ABS((A(J,K)*A(J,K))/(A(J,J)*A(K,K)))
       EB=ABS((B(J,K)*B(J,K))/(B(J,J)*B(K,K)))
       YME=EA+EB
       IF(Y.GT.YMAX) YMAX=Y
       IF(Y.LT.EPS) GO TO 700
C------CALCULATE TRANSFORMATIONS TERMS------------------
       Y=A(J,J)*B(K,K)-A(K,K)*B(J,J)
       AK=A(K,K)*B(J,K)-B(K,K)*A(J,K)
       AJ=A(J,J)*B(J,K)-B(J,J)*A(J,K)
       D1=Y/2.
       D2=Y**2+4.*AK*AJ
       IF(D2.LT.0.0) PRINT 4000,J,K
 4000 FORMAT(20H OFF DIANGONAL TERM  2I5)
       IF(D2.LT.0.0) GO TO 700
       D2=SQRT(D2)/2.
       Z=D1+D2
       IF(D1.LT.0.0) Z=D1-D2
       IF(Z) 80,70,80
    70 CA=0.0
       CG=-A(J,K)/A(K,K)
       GO TO 90
    80 CA=AK/Z
       CG=-AJ/Z
C------ZERO TERMS A(J,K) AND B(J,K)---------------------
    90 DO 100 I=1,N
       IF(I.EQ.J.OR.I.EQ.K) GO TO 100
       A(J,I)=A(I,J)+CG*A(I,K)
       A(K,I)=A(I,K)+CA*A(I,J)
       A(I,J)=A(J,I)
       A(I,K)=A(K,I)
       B(J,I)=B(I,J)+CG*B(I,K)
       B(K,I)=B(I,K)+CA*B(I,J)
       B(I,J)=B(J,I)
       B(I,K)=B(K,I)
  100 CONTINUE
       AK=A(K,K)
       BK=B(K,K)
       A(K,K)=AK+CA*(A(J,K)+A(J,K)+CA*A(J,J))
```

Reproduced with permission of the copyright owner. Further reproduction prohibited without permission.

```
      B(K,K)=BK+CA*(B(J,K)+B(J,K)+CA*B(J,J))
      A(J,J)=A(J,J)+CG*(A(J,K)+A(J,K)+CG*AK)
      B(J,J)=B(J,J)+CG*(B(J,K)+B(J,K)+CG*BK)
      A(J,K)=0.
      B(J,K)=0.
      A(K,J)=0.0
      B(K,J)=0.0
C-----TRANSFORM EIGENVECTORS-----------------------
      DO 200 I=1,N
      XJ=X(I,J)
      XK=X(I,K)
      X(I,J)=XJ+CG*XK
  200 X(I,K)=XK+CA*XJ
      NT=NT+1
  700 CONTINUE
      IF(YMAX.LT.RTOL) GO TO 820
      EPS=.01*(YMAX)**2
      IF(YMAX.GT.1.0) EPS=0.01
  800 CONTINUE
C-----SCALE EIGEN VECTORS
  820 DO 840 J=1,N
      E(J)=A(J,J)/B(J,J)
      BB=SQRT(B(J,J))
      DO 840 K=1,N
  840 X(K,J)=X(K,J)/BB
      IF(NN.EQ.0) RETURN
C-----ORDER EIGENVALUES AND EIGENVECTORS ----------
      DO 900 I=1,NN
      JL=I+1
      HT=E(I)
      IM=I
      DO 850 J=JL,N
      IF(HT.LT.E(J)) GO TO 850
      HT=E(J)
      IM=J
  850 CONTINUE
      E(IM)=E(I)
      E(I)=HT
      DO 900 J=1,N
      HT=X(J,I)
      X(J,I)=X(J,IM)
  900 X(J,IM)=HT
      RETURN
C-------------------------------------------------------------------------
      END
      SUBROUTINE MULT(A,B,C,M,N)
C**************************************************************************
C
C     MATRIX MULTIPLICATION     C(N,M)=A(N,N)*B(N,M)
C
C**************************************************************************
      DIMENSION A(N,N),B(N,M),C(N,M)
C
      DO 10 I=1,N
      DO 10 J=1,M
   10 C(I,J)=0.
      DO 20 I=1,N
      DO 20 J=1,M
      DO 20 K=1,N
      IF(A(I,K).EQ.0.) GO TO 20
      C(I,J)=C(I,J)+A(I,K)*B(K,J)
```

Reproduced with permission of the copyright owner. Further reproduction prohibited without permission.

```
   20 CONTINUE
      RETURN
      END
      SUBROUTINE NDATA(R,Z,NUMFN)
C*************************************************************************
C
C     READ AND GENERATE NODAL DATA
C
C*************************************************************************
      DIMENSION R(1),Z(1)
      COMMON/TAPES/IIN,IOUT
C
      NOLD =0
      KNOLD=0
      WRITE(IOUT,2000)
      WRITE(IOUT,2010)
      WRITE(IOUT,2020)
C
C     READ AND GENERATE NODAL DATA
C
   10 READ(IIN,1000) N,R(N),Z(N),KN
      IF(N.GT.NUMFN) GO TO 50
      WRITE(IOUT,2030) N,R(N),Z(N),KN
      IF(KNOLD.EQ.0) GO TO 30
      NDIV=(N-NOLD)/KNOLD
      NGEN=NDIV-1
      IF(NGEN.LT.1) GO TO 30
      DR=(R(N)-R(NOLD))/FLOAT(NDIV)
      DZ=(Z(N)-Z(NOLD))/FLOAT(NDIV)
      NG=NOLD
      DO 20 NN=1,NGEN
      NN=NN
      NG=NG+KNOLD
      IF(NG.GE.NUMFN) GO TO 60
      IF(NG.LE.0)     GO TO 60
      R(NG)=R(NN)+DR
   20 Z(NG)=Z(NN)+DZ
C
   30 NOLD=N
      KNOLD=KN
      IF(N.NE.NUMFN) GO TO 10
C
C     PRINT COMPLETE NODAL DATA
C
      WRITE(IOUT,2040)
      WRITE(IOUT,2020)
      DO 40 N=1,NUMFN
   40 WRITE(IOUT,2030) N,R(N),Z(N)
      RETURN
   50 WRITE(IOUT,2050) N,NUMFN
      STOP
   60 WRITE(IOUT,2060) NOLD
      STOP
 1000 FORMAT(I5,2F10.0,I5)
 2000 FORMAT(1H1,44HF L U I D  N O D A L  C O O R D I N A T E S //)
 2010 FORMAT(17H INPUT NODAL DATA //)
 2020 FORMAT( 6H  NODE,5X,17HNODAL COORDINATES,4X,10HGENERATING/
     1       7H NUMBER,6X,2HR-,9X,2HZ-,9X,4HCODE/)
 2030 FORMAT(I5,4X,F10.3,1X,F10.3,3X,I5)
 2040 FORMAT(///21H GENERATED NODAL DATA  //)
 2050 FORMAT(// 12H NODE NUMBER I5,21H EXCEEDS TOTAL NODES I5)
```

Reproduced with permission of the copyright owner. Further reproduction prohibited without permission.

```
 2060 FORMAT(// 42H ERROR IN NODE GENERATION CONSTANT OF NODE ,I5)
      END
      SUBROUTINE OUTP(NIF,P,NFNIF,FREQ)
C*****************************************************************************
C
C     PRINT OUTPUT
C
C*****************************************************************************
      DIMENSION P(1),NIF(1)
      COMMON/TAPES/IIN,IOUT
      COMPLEX P
C
      WRITE(IOUT,2000) FREQ
      WRITE(IOUT,2020)
      DO 30 I=1,NFNIF
      N=NIF(I)
      AP=CABS(P(N))
      WRITE(IOUT,2030) N,P(N),AP
   30 CONTINUE
      RETURN
 2000 FORMAT(///
     1       27H FREQUENCY OF EXCITATION  =,F6.2,4H CPS//
     2       45H HYDRODYNAMIC PRESSURE ON THE INTERFACE NODES /)
 2020 FORMAT(6H  NODE,16X,21HHYDRODYNAMIC PRESSURE /
     1       7H NUMBER,9X,4HREAL,8X,9HIMAGINARY,7X,8HABSOLUTE /)
 2030 FORMAT(I5,2X,3E15.5)
      END
      SUBROUTINE SUMF(NFS,NTB,C,F1R,F1I,LDIAG,F,SF,FG,NFNFS,NFNTB,NUMFN,
     1                NNN)
C*****************************************************************************
C
C     SF=F-FB-FS
C
C*****************************************************************************
      DIMENSION NTB(1),NFS(1),F(1),SF(1),F1R(NNN,1),F1I(NNN,1)
      DIMENSION C(NFNFS,1),LDIAG(1)
      COMPLEX SF
C
      LL=LDIAG(NUMFN)
      DO 10 I=1,LL
   10 SF(I)=CMPLX(F(I),0.)
C
C     F=FB
C
      K=1
      IF(FG.EQ.0.) K=2
      DO 20 I=K,NFNTB
      II=I-K+1
      N=NTB(I)
      L=LDIAG(N)-N
      DO 20 J=K,NFNTB
      JJ=J-K+1
      M=NTB(J)
      IF(M.GT.N) GO TO 20
      M=L+M
      SF(M)=SF(M)-CMPLX(F1R(JJ,II),F1I(JJ,II))
   20 CONTINUE
C
C     F=FB-FS
C
      IF(FG.EQ.0.) RETURN
```

Reproduced with permission of the copyright owner. Further reproduction prohibited without permission.

```
      DO 30 I=1,NFNFS
      M=NFS(I)
      L=LDIAG(N)-N
      DO 30 J=1,NFNFS
      M=NFS(J)
      IF(M.GT.N) GO TO 30
      M=L+M
      SF(N)=SF(N)-FG*C(J,I)
   30 CONTINUE
      RETURN
      END
      SUBROUTINE SUMF2(SF,FC)
C
C     SF=(W2/C2)*FC
C
      DIMENSION FC(1)
      COMPLEX SF(1)
      COMMON/LA/LA
      COMMON/COMP/KOMP
      COMMON/FREQS/FROS,C
C
      IF(KOMP.EQ.1) FFQS=FROS/(C*C)
      DO 10 I=1,LA
   10 SF(I)=SF(I)-FFQS*FC(I)
      RETURN
      END
      SUBROUTINE TBOUN(RTA,MODTB,NFNTB,ITYPE)
C*********************************************************************
C
C     FORM MATRIX FB REPRESENTING TRANSMITTING BOUNDARY
C
C*********************************************************************
      DIMENSION RR(30),RI(30)
      COMMON/NN/N7,N12,N13,N14
      COMMON/COMP/KOMP
      COMMON/FREQS/FROS,C
      COMMON A(1)
C
C     TO IS THE NUMBER OF THE FIRST TERM THAT IS IN THE FORM OF MODIFIED
C      BESSEL FUNCTION
      TO=0
      IF(KOMP.EQ.1) FSC=FROS/(C*C)
      DO 10 I=1,NFNTB
      J=N7+1-I
      A(J)=-A(J)
      IF(KOMP.EQ.1) A(J)=A(J)*FSC
      IF(TO.NE.0) GO TO 10
      IF(A(J).LT.0.) TO=I
   10 A(J)=SQRT(ABS(A(J)))
      IF(TO.EQ.0) TO=NFNTB+100
C
C     FORM DIAGONAL MATRICES RR,RI
C
      ICODE=0
      DO 20 I=1,MODTB
      J=N7+1-I
      IF(A(J).NE.0.) GO TO 15
      IF(ITYPE.NE.2) RR(I)=-1./RTB
      IF(ITYPE.EQ.2) RR(I)=0.
      RI(I)=0.
      GO TO 20
```

Reproduced with permission of the copyright owner. Further reproduction prohibited without permission.

```
   15 IF(I.GE.ID) ICODE=1
      CALL RESSEL(A(J),RTB,RR(I),RI(I),ICODE,ITYPE)
   20 CONTINUE
C
C     QE=Q*E
C
      CALL MULT(A(N14),A(N12),A(N13),MODTB,NFNTB)
C
C     F1=RTB*Q*E*R*ET*Q
C
      CALL DMULT(A(N12),A(N13),RR,MODTB,NFNTB,RTB)
      CALL DMULT(A(N14),A(N13),RI,MODTB,NFNTB,RTB)
      RETURN
      END
```

Reproduced with permission of the copyright owner. Further reproduction prohibited without permission.